

UCSF

UC San Francisco Electronic Theses and Dissertations

Title

The SAD-1 kinase regulates presynaptic development in *C. elegans*

Permalink

<https://escholarship.org/uc/item/0vx3g3j1>

Author

Crump, Justin Gage

Publication Date

2000

Peer reviewed|Thesis/dissertation

The SAD-1 Kinase Regulates Presynaptic Development in *C. elegans*

by

Justin Gage Crump

DISSERTATION

Submitted in partial satisfaction of the requirements for the degree of

DOCTOR OF PHILOSOPHY

in

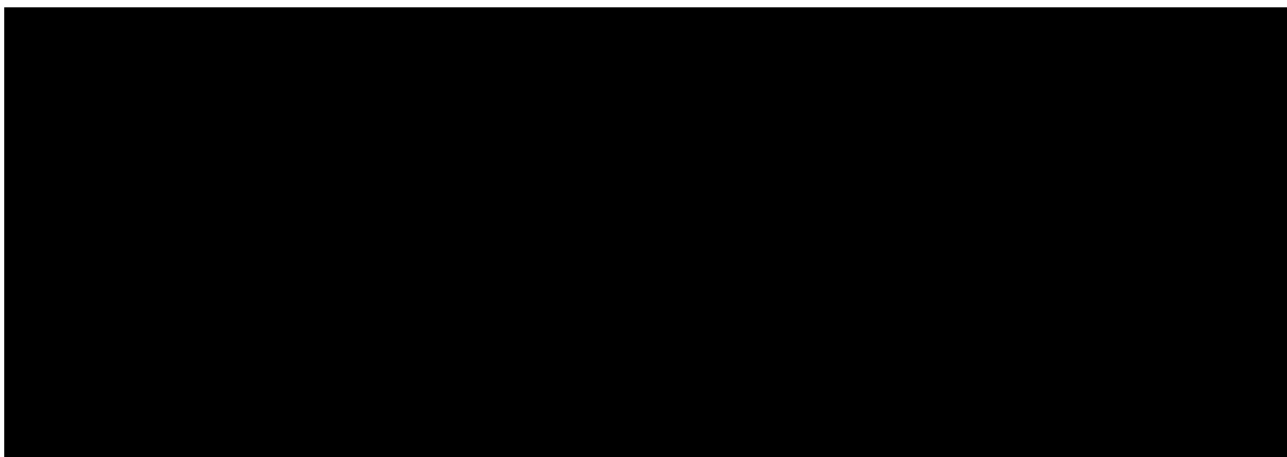
Biochemistry

in the

GRADUATE DIVISION

of the

UNIVERSITY OF CALIFORNIA SAN FRANCISCO



Date

University Librarian

Degree Conferred:

copyright (2000)
by
Justin Gage Crump

this thesis is dedicated to Shau Lon

Acknowledgements

I thank people for different things. I could not imagine a better mentor than Cori Bargmann. She was wonderful to talk with and always full of too many ideas. I am constantly amazed by her intellectual energy. I am grateful for the creative freedom she allowed me in the course of my experiments. Despite being extremely intense she exhibits a great amount of interest in and compassion for students. Though she remains a great mystery for me, I am blessed to have spent nearly six years in her lab.

People in the lab: it was like being in a spaceship on the way to Mars, knowing that the red dust surface laid several years ahead and you were trapped with these other people. That being said I love these fellow trapped human beings. I am most thankful that no religiophilosophical argument ever came to physical violence, though there were a few close calls with Erik Lundquist and Alvaro Sagasti. These were people who never left an idea alone, though some of them like Mario DeBono and Zemer Gitai had sex always on the mind. If Jesus is reborn a second time I hope he comes to the lab because that would make Noelle L'Etoile very happy. Actually, I'm convinced that her baby-to-be is the reincarnation of Jesus. No, seriously, I really believe this. Really. Maria and men, hmmm. Many thanks to Carrie Adler for bringing some acoustical aesthetics to the lab. To counteract the salsa and Alice of David Tobin. Also, hello to those people on the other side of the ocean and in Antarctica.

Thanks to Sophia Ng for keeping me stirred up inside. She introduced a combination of steady beauty and intense chaos in my life. I never knew life could be so unpredictable. To which Justin Keisel helped greatly. The bizarre is always around the corner. And Hien Tran for sneaking off with me to dark clubs for shoegaze. Also I must thank my wonderful padre, who could only give the Y, and madre, who learned to cope with the Y. I thank my brother Derek for giving me my sense of competition and my brother Travis for being the first subject case of endless teasing. I deeply bow to my grandmother Esther, whose famous aphorism, "If you're going to do something, you might as well do it well", mutated to my mantra, "If you're going to do something, you should do it to the extreme".

I was very fortunate to have collaborated with Mei Zhen and Yishi Jin on the *sad-1* work. Their knowledge and technical expertise were invaluable to the project, and their friendliness made the collaboration blissful. I thank my thesis committee members, Marc Tessier-Lavigne and Reg Kelly, for their helpful advice and for their understanding in the light of the rushed ending to this thesis. I thank the UCSF community for the fervor and buzzing going on within the walls of "The Castle", and especially the organizers of the Biochemistry and Neuroscience seminars who ensured a constant fix for the thinking habit. That's it: if I forgot to mention you, that means I don't like you.

Enish, Meredith

From: Gage Crump [gage@itsa.ucsf.edu]
Sent: Monday, May 22, 2000 5:44 PM
To: neuron@cell.com

Monday May 22, 2000

Neuron
Cell Press
1050 Massachusetts Avenue
Cambridge, Massachusetts 02138

To whom it may concern:

I would like to request permission to include in my thesis dissertation a copy of the paper cited below:

Roayaie K, Crump JG, Sagasti A, Bargmann CI. The G alpha protein ODR-3 mediates nociceptive function and controls cilium morphogenesis in *C. elegans* olfactory neurons. *Neuron*. 1998 Jan;20(1):55-67.

The dissertation will be microfilmed by University Microfilms Incorporated and they request permission to supply single copies upon demand. Since I must submit my thesis by May 26, I would greatly appreciate it if you could respond within the next week by fax to (415) 476-3493

Thank you very much.

Sincerely,


Justin Gage Crump
UC San Francisco

"PERMISSION GRANTED SUBJECT TO CITATION OF THE ORIGINAL MANUSCRIPT AND NOTATION THAT COPYRIGHT IS HELD BY CELL PRESS. (OUR PERMISSION IS CONTINGENT ON PERMISSION OF THE AUTHOR.)"

Advisor Statement

The work in Chapter 2 was previously published as *Neuron*, Vol. 20., No. 1, pp. 55-67, 1998. The authors Kayvan Roayaie and Gage Crump made similar contributions to this work. Gage did the cloning of *odr-3*, the characterization of dominant negative and gain of function ODR-3, and the analysis of cilia morphology. Kayvan did the molecular characterization of *odr-3*, the ODR-3 overexpression studies, and the ODR-3 expression analysis.

Chapter 4 was done in collaboration with Mei Zhen and Yishi Jin from UC Santa Cruz. Mei contributed the characterization of *sad-1* neuromuscular junction defects, neuron-specific rescue experiments, and SAD-1 and SNT-1 colocalization data. All other experiments were performed by Gage Crump.

A handwritten signature in black ink that reads "Cori Bargmann". The signature is fluid and cursive, with a long horizontal line extending from the end of the name.

Cori Bargmann, Ph.D.

Associate Professor

HHMI, Department of Anatomy UCSF

The SAD-1 Kinase Regulates Presynaptic Development in *C. elegans*

Justin Gage Crump

Abstract

The development of a functioning nervous system requires the precise wiring of its component neurons. The formation of synapses between neurons involves the postsynaptic concentration of neurotransmitter receptors and the presynaptic clustering of neurotransmitter-filled vesicles and release machinery. The mechanisms that govern synapse formation between neurons are largely unknown. The nematode *C. elegans* has a relatively simple and highly defined nervous system that consists of 302 neurons and about 7000 synapses. In order to identify molecules involved in neuron to neuron synapse formation we conducted a genetic analysis of synapse formation in *C. elegans*.

In a screen for mutants that disrupted presynaptic vesicle clusters in sensory neurons we isolated six major complementation groups. Mutations in three genes, *unc-104*, *unc-11*, and *unc-51*, affected the transport and biogenesis of synaptic vesicles. Three new mutants, *sad-1*, *sad-2*, and *sad-3*, had defects in the organization of synaptic vesicle clusters. In addition, we found that *eat-7(ad450)* mutants have defects in the shape of vesicle clusters. Together, these mutants describe a pathway in which synaptic vesicles are generated, localized, and organized at the synapse.

In order to understand how presynaptic development is coordinated, we further analyzed *sad-1* mutants. *sad-1* encodes a novel predicted serine/threonine kinase. SAD-1 is expressed in the nervous system and localizes to synapse-rich regions of axons. In *sad-1* mutants vesicle clusters were disorganized but an active zone protein was localized normally. In addition, sensory axons failed to properly terminate. Overexpression of SAD-1 caused vesicle clusters to form ectopically and disrupted axon outgrowth. These results reveal a function for SAD-1 in organizing vesicle clusters at the synapse and

suggest a model in which SAD-1 couples the end of axon outgrowth with the beginning of presynaptic differentiation. SAD-1 has homology with PAR-1, a kinase involved in generating polarity in embryonic and epithelial cells. We speculate that the localization of proteins and organelles to synapses within neurons is mechanistically related to the processes that generate polarity in many cell types.

R. B. Kelly

TABLE OF CONTENTS

Dedication	iii
Acknowledgements	iv
Advisor Statement	vii
Abstract	viii
List of Tables and Figures	xii
CHAPTER ONE	1
Introduction: Mechanisms of synapse formation	
Overview	2
Polarity	2
Adhesion and Specificity	4
Postsynaptic Development	8
Presynaptic Development	13
<i>C. elegans</i> Synapses	19
References	23
CHAPTER TWO	38
The G alpha protein ODR-3 mediates olfactory and nociceptive function and controls cilium morphogenesis in <i>C. elegans</i> olfactory neurons	
Summary	39
Introduction	39
Results	40
Discussion	46
Experimental Procedures	48
References	49
CHAPTER THREE	52
Isolation of mutations that disrupt presynaptic vesicle clustering or trafficking in <i>C. elegans</i>	

Summary	53
Introduction	53
Results	55
Discussion	67
Experimental Procedures	77
References	80

CHAPTER FOUR **85**

The SAD-1 Kinase Organizes Presynaptic Vesicle Clusters and Arrests Axon Outgrowth in *C. elegans*

Summary	86
Introduction	86
Results	88
Discussion	115
Experimental Procedures	120
References	124

CHAPTER FIVE **133**

Model for SAD-1 Function and Future Directions

The Model	134
Future Directions	136

LIST OF TABLES AND FIGURES

CHAPTER TWO

Figure 1: Morphologies of Sensory Cilia	40
Figure 2: <i>odr-3</i> Encodes a G Protein α Subunit	41
Figure 3: Behavioral Phenotypes of <i>odr-3</i> Mutants and Rescued Strains	42
Figure 4: Expression of Endogenous ODR-3 Protein and <i>odr-3</i> Fusion Genes	43
Figure 5: Behavioral Phenotypes of <i>odr-3</i> Overexpression and of <i>odr-3</i> Point Mutants	45
Figure 6: Cilium Morphology in Wild-Type and <i>odr-3</i> Mutant Animals	46
Figure 7: Summary of G α Function in Different Chemosensory Neurons	47

CHAPTER THREE

Table 1: Complete Summary of Screen for SNB-1::GFP Fffects in the ASI Neurons	57
Figure 1: $p_{str.3}$ SNB-1::GFP Phenotypes of <i>unc-104</i> , <i>unc-11</i> , <i>unc-51</i> , and <i>sad</i> Mutants	59
Figure 2: In <i>eat-7(ad450)</i> Animals Vesicle Clusters are Less Discrete	66
Figure 3: Mutations that define a pathway from vesicle biogenesis to mature synaptic vesicle clusters	69
Figure 4: Genetic model for <i>sad-1</i> and <i>sad-2</i> interaction	73

CHAPTER FOUR

Figure 1: $p_{str.3}$ SNB-1::GFP Labels Presynaptic Vesicle Clusters in the ASI Chemosensory Neurons	90
Table 1: Summary of Screen for SNB-1::GFP Clustering Defects in the ASI Neurons	92
Figure 2: In <i>sad-1</i> Mutants SNB-1::GFP Clusters are Disorganized and More Diffuse in the ASI neurons	95
Figure 3: SNB-1::GFP Clusters, but not SYD-2 Localization, are Disrupted at the NMJ of <i>sad-1</i> Mutants	98
Figure 4: SAD-1 Protein is a Novel Serine/Threonine Kinase	101
Figure 5: SAD-1 Expression and Protein Localization	107
Figure 6: SAD-1 Overexpression Promotes the Formation of Vesicle Clusters	111

Figure 7: Reciprocal Axon Phenotypes in *sad-1* Mutants and SAD-1 Overexpressing Animals 114

CHAPTER FIVE

Figure 1: Model for SAD-1 Function 135

Chapter 1

Introduction:

Mechanisms of synapse formation

Overview

The pattern of neuronal connectivity determines the behavior and cognition of an animal. The development of neuronal connectivity can be broken down into five major steps: 1.) the acquisition of neuron- and neuron subtype-specific fates, 2.) the migration of neurons, 3.) the directed outgrowth of axonal and dendritic processes, 4.) the establishment of synaptic connections, and 5.) the activity-dependent modification, elimination and growth of synaptic connections. The focus of this thesis was to analyze the molecular and cellular mechanisms governing the formation of synaptic connections. Chemical synapses are intercellular adhesion junctions that have become specialized for asymmetric release of, and response to, modulators of electrical excitability. A synapse consists of the following structural elements: cell-cell adhesion, postsynaptic clusters of neurotransmitter receptors and regulatory molecules, presynaptic clusters of neurotransmitter-filled vesicles and exocytotic and endocytic machinery, and a specialized cytoskeleton. This chapter reviews the concepts behind synapse formation by comparing work on vertebrate, *Drosophila*, and *C. elegans* neuromuscular junctions (NMJs); vertebrate central nervous system (CNS) synapses; and structures in non-neuronal cells that share common properties with synapses. The issues addressed in this discussion include how the specificity of synaptic connections are generated, how proteins and organelles are targeted to different synaptic regions, and how the events of synapse formation are coordinated. Signaling between the pre- and post-synaptic cells seems to be important for synaptic development, though pre- and post-synaptic structures can form in isolation. In neurons cell-cell interactions may organize pre- and post-synaptic structures by mechanisms general to many polarized cells.

Neurons are polarized cells

Polarized cells can spatially segregate intracellular functions and [to] interact asymmetrically with other cells in a tissue. Common features of polarized cells include the asymmetric localization of proteins, RNAs, and

organelles, usually in association with the cell cortex; a functionally specialized cytoskeleton; and intercellular signaling systems. However, the functional role of polarization varies from cell to cell. Asymmetrically dividing cells localize determinants differentially such that the resultant daughter cells acquire separate fates. In yeast the localization of vesicles and exocytotic machinery to a region of the cell cortex promotes bud formation. Polarity has been extensively studied in epithelial cells, where it plays roles both in organ function, such as the asymmetric flow of salts through the intestinal wall, and the development of tissues. For example, in the developing vulva of *C. elegans* the polarization of the vulval precursor cell P6.p allows it to respond to fate-inducing signals from the anchor cell (reviewed in Kim, 1997). Epithelial polarization also seems to be important for convergent extension cell movements during gastrulation (Heisenberg et al., 2000; Wallingford et al., 2000).

In neurons polarization allows electrical information to be transferred asymmetrically through a circuit of interconnected cells. Information from the environment or another neuron is received in the dendrite and then transmitted via the axon to the dendrite of another neuron or to muscle. For example, in excitatory synaptic transmission the release of neurotransmitter from the presynaptic axon activates neurotransmitter receptors on the postsynaptic dendrite; receptor activation in the dendrite generates an action potential that stimulates neurotransmitter release in the downstream axon, thus continuing the cycle. Modulatory information is also transmitted asymmetrically between the axon and dendrite.

It is useful to think of neurons as having two superimposed layers of polarity. On a first level, neurons are polarized in that they have functionally different processes, dendrites and axons. In addition to polarity on the level of dendrites versus axons, regions within the dendrite and axon are spatially and functionally segregated. In a sensory neuron signal transduction machinery required for detecting environmental stimuli is concentrated in specialized endings of the dendrite. In other neuron types postsynaptic regions are specified within the dendrite. Similarly, within the axon certain regions are specified to be presynaptic. The specification of regions to be synaptic or non-synaptic is analogous to other forms of polarity in that it involves the segregation of

proteins, RNAs, organelles, and specialized cytoskeletons to discrete regions of the cell. The division of the axon and dendrite into discrete units, or synapses, allows a neuron to selectively alter its interactions with different neurons. Indeed, neurons have been shown to independently modulate the efficacy of individual synapses in response to activity (Casadio et al., 1999).

There is increasing evidence that the mechanisms that generate polarity in different cell types share not only a common logic but some of the same regulatory molecules (Rongo et al., 1998). Thus, it will be useful to contrast how neurons establish different compartments (dendrites versus axons) and sub-compartments (synaptic versus non-synaptic regions) with how polarity in non-neuronal cells is generated. In the discussion of synapse formation that follows specific examples of such parallels will be given when appropriate.

Adhesion and synaptic specificity

Adhesion between the pre- and post- synaptic cells seems to be an early event in synaptic development. At the *Drosophila* NMJ adhesion can be observed before other morphological features (Suzuki, 2000). Synaptic adhesion serves at least two purposes. First, it structurally supports the synapse. This is especially important at the NMJ where the forces exerted during muscle contraction could dislodge the much smaller innervating motor neuron. Second, it helps to align the pre- and post- synaptic structures by providing intracellular anchor points that are intercellularly linked. For example, the neurexin-neurologin adhesion complex has been shown to bind protein complexes on both the pre- and post-synaptic sides of a synapse (Butz et al., 1998; Song et al., 1999).

Two different types of adhesion are seen at synapses. At the vertebrate NMJ adhesion between the motor neuron and muscle occurs indirectly through a specialized extracellular matrix, or basal lamina, that occupies the synaptic cleft. The muscle interacts with the basal lamina at least in part through the dystrophin-associated glycoprotein complex (DGC); the DGC contains α and β dystroglycan and other proteins and is linked intracellularly to a specialized actin cytoskeleton containing syntrophin and dystrophin (reviewed in Carbonetto and Lindenbaum, 1995). Motor neurons interact with a synapse-specific isoform of laminin, laminin β 2 (Hunter et al., 1989). At CNS synapses

and some invertebrate NMJs the pre- and post- synaptic membranes are closely apposed, within about 200Å. An iterated pattern of electron dense material is often seen between the apposed membranes (Fannon and Colman, 1996). This has led to the idea that transmembrane proteins on either side of the synapse are directly interacting across the extracellular space to promote adhesion. Transmembrane cell adhesion proteins implicated at the synapse include homophilic molecules such as cadherins (Fannon and Colman, 1996) and immunoglobulin-superfamily members (e.g. NCAM/FasII) (Thomas et al., 1997) and heterophilic molecules such as neuexins and neuroligins (Butz et al., 1998; Song et al., 1999).

An outstanding problem in synapse formation is how neurons choose the correct synaptic partner. Even when its axon runs close to several potential postsynaptic partners, a neuron makes highly specific choices in selecting a postsynaptic neuron or muscle. For example, in *C. elegans* a neuron on average makes synapses with only one out of six of its neighbors (White et al., 1986). In the adhesive code model, cell adhesion molecules themselves determine the specificity of synaptic connections. This model postulates that each pre- and post- synaptic neuron has a unique collection of cell adhesion molecules; those neurons that share interacting cell adhesion molecules would be able to make synapses with each other. Due to the high complexity of neuronal connectivity, especially in the CNS, this model requires a large number of unique cell adhesion molecules.

The diversity of the cadherin family suggests that they may provide synaptic specificity in the CNS (Fannon and Colman, 1996). Cadherins are transmembrane proteins that intracellularly couple to the actin cytoskeleton via a complex containing α and β catenins (reviewed in Kemler, 1993). Extracellularly, cadherins from apposing membranes bind each other in a calcium-dependent manner using the first of several repeated domains (Tomschy et al., 1996); crystallographic studies suggest that cadherins act as physical zippers to bring membranes together (Shapiro et al., 1995). Transfected cells expressing different isoforms of cadherins reassociated into different cellular aggregates in culture, suggesting that cadherins provide differential adhesive forces important for selective cell-cell interactions (Nose et al., 1988). In addition to N-, E-, and R-

classical cadherins, there is a large family of cadherin-related (CNR) proteins expressed in neurons (Kohmura et al., 1998). The genomic organization of the CNR genes allows multiple exons encoding extracellular domains to be spliced to a common exon encoding the intracellular domain. In humans this generates 52 different CNR genes that have unique extracellular binding domains yet share 3 common intracellular domains (Wu and Maniatis, 1999). This organization has been proposed to allow neurons to make diverse cell-cell interactions while maintaining common intracellular interactions required for assembling a synapse. However, the functions of the CNR proteins in the brain has yet to be tested.

Another diverse class of proteins that could mediate neuronal recognition are the neuroligins. Neuroligins are presynaptic transmembrane proteins that are one of two receptors for α -latrotoxin, a black widow spider toxin that stimulates calcium-independent exocytosis (Sugita et al., 1999). Neuroligins bind neuroligins, a class of postsynaptic transmembrane proteins (Ichtchenko et al., 1995). Alternative splicing of three neuroligin loci could generate more than a thousand different neuroligin isoforms (Ullrich et al., 1995). No function has been identified for neuroligin-neuroligin complexes in synaptic specification. However, mutations in a *Drosophila* neuroligin IV protein lead to defects in glial adhesion, suggesting that other neuroligins may have roles in cell-cell interactions at the synapse (Baumgartner 1996).

A variation of the adhesive code model of synaptic specification is the combinatorial code model. In this model the precise levels of receptors that either promote or inhibit adhesion impart to a neuron its unique pattern of connectivity. The best support for this model is at the *Drosophila* NMJ. The homophilic cell adhesion molecules FasII (Schuster et al., 1996A) and FasIII (Kose et al., 1997); the leucine-rich repeat protein CAPRICIOUS (Shishido et al., 1998); and the ligand-receptor systems Netrin A-Frazzled and Netrin B-Frazzled can promote recognition between a motor neuron and a muscle (Winberg et al., 1998). Conversely, the Toll transmembrane receptor (Rose et al., 1997) and the extracellular ligands Netrin B (Winberg et al., 1998) and Semaphorin II (Matthes et al., 1995) inhibit motor neuron-muscle recognition. Different muscles and motor neurons express different complements of these proteins. Moreover,

whereas loss or overexpression of an attractive or inhibitory molecule caused defects in the pattern of muscle innervation, compensatory changes in molecules of opposite sign often restored proper innervation. For example, decreasing Semaphorin II levels increased innervation of muscles 6 and 7 by the RP3 motor neuron, whereas decreasing Netrin B levels decreased innervation. However, simultaneously decreasing Semaphorin II and Netrin B levels caused little effect. Similarly, whereas overexpression of Semaphorin II or Netrin B alone altered innervation, simultaneous overexpression of Semaphorin II and Netrin B had little effect (Winberg et al., 1998). Similar effects were seen with FasII versus Semaphorin II (Winberg et al., 1998) and FasIII versus Toll (Rose and Chiba, 1999). These data support the model that the relative levels of attractive versus inhibitory proteins and not particular individual proteins determine the specificity of innervation at the *Drosophila* NMJ. However, one caveat to these experiments is that what is being affected may be short range axon guidance and not the sort of synaptic specification seen in the CNS. Indeed, the majority of the molecules in the above study more generally affect axon guidance. In addition, in manipulations that inhibit innervation (such as ectopically expressing Toll at high levels in the muscle) motor neurons no longer extend processes over the target muscle. In these cases it is not clear whether the defect is in axon targeting or in selective synapse formation. Thus, it remains to be seen whether similar mechanisms occur in the CNS where axons must choose between multiple dendrites that are in close approximation.

Synaptic adhesion is dynamically controlled during development. In the CNS N-cadherin localizes throughout synaptic regions early in development but becomes perisynaptic later when the presynaptic active zone and postsynaptic density form (Uchida et al., 1996). Similarly, during T cell activation adhesion between the T cell and B cell, the “immunological synapse”, is dynamically controlled (Grakoui et al., 1999). At the “immunological synapse” heterophilic adhesion occurs through the immunoglobulin superfamily transmembrane proteins LFA-1 (T cell) and ICAM (B cell). Initially, LFA-1 – ICAM interactions occur at the center of the “immunological synapse”. Subsequently, LFA-1 and ICAM proteins become localized peripherally in a ring and T cell receptors and B cell MHC molecules occupy the central core. What might be the purpose for the

dynamic localization of adhesion molecules? In early stages, cell adhesion molecules may need to be locally concentrated in order to initiate membrane adhesion. Once initiated, the transition of adhesion from a central core to the periphery could theoretically serve two purposes. One function could be to locally concentrate signaling molecules, such as T cell receptors and synaptogenic factors, in the core, thus facilitating their activation (Monks et al., 1998). Another possibility is that a ring of adhesion may regulate the size of the synapse, either by acting as a physical barrier or by recruiting proteins that downregulate synaptogenic signaling.

During later development the levels of adhesion function to control synaptic growth. At the *Drosophila* NMJ the levels of FasII protein regulate the stabilization and growth of new synapses. In animals with greatly reduced levels of FasII synapses form but are not maintained (Schuster et al., 1996A). However, in animals with intermediate levels of FasII the addition of new synapses is accelerated (Schuster et al., 1996B). This result suggests that too much or too little adhesion is restrictive for synaptic growth. This property has been suggested to provide a mechanism in which the modification of adhesion may in part underlie the experience-dependent regulation of synaptic strength associated with learning and memory.

Postsynaptic development

Once formed, synaptic adhesion likely functions to organize intracellular structures on both sides of the synapse. The postsynaptic specialization is defined electron microscopically as an electron-dense region adjacent to the membrane and functionally as the site of receptors that respond to the presynaptic release of the corresponding neurotransmitter. Molecules that localize and regulate receptors and modify neurotransmission are found at the postsynaptic density (PSD). The PSD is often associated with a specialized cytoskeleton and polyribosomes. Postsynaptic structures differ morphologically from synapse to synapse. At the vertebrate NMJ numerous membrane invaginations create junctional folds that maximize the surface area available for neurotransmitter receptors. At some CNS synapses actin-rich dendritic spines project from the dendritic shaft to presynaptic axons, and the PSD localizes to the

tip of the dendritic spine. Other CNS synapses are made in passing; in these cases the PSD is located within the dendritic shaft and there are no actin-rich membrane protrusions. Perhaps, the localization of a PSD to a dendritic spine allows a synapse to be more independently regulated.

The molecular mechanisms controlling postsynaptic development have been best worked out at the vertebrate NMJ. Signaling from the presynaptic neuron to the postsynaptic muscle appears to organize the PSD. Prior to innervation acetylcholine receptors (AChRs) are diffusely distributed throughout the plasma membrane of the muscle. Upon arrival at a muscle the motor neuron sends a signal to the muscle that causes the redistribution and concentration of AChRs to synaptic sites. Early experiments, in which a deinnervated muscle was partially destroyed and allowed to regrow within a shell of remaining extracellular matrix, indicated that the neuron-derived AChR clustering factor was a component of the synaptic basal lamina. These types of experiments led to the identification of agrin, a component of the basal lamina that when added to cultured muscles induces the clustering of AChRs (Nitkin et al., 1987). Agrin is made by both neurons and muscle, however neurons secrete an isoform of agrin that is 1000 fold more potent at inducing AChR clusters than the muscle isoform (Burgess et al., 1999). Agrin activates the muscle-specific tyrosine kinase (MuSK) receptor, probably through interactions with an unidentified MuSK coreceptor (Glass et al., 1996). Rapsyn is an intracellular protein implicated in clustering AChRs. Coexpression of rapsyn and AChRs in heterologous cells leads to the formation of AChR clusters (Froehner et al., 1990), and mice deficient in rapsyn, agrin, or MuSK fail to cluster AChRs (Gautam et al., 1995; Gautam et al., 1996; DeChiara et al., 1996). It is unclear how kinase signaling downstream of MuSK organizes AChR clusters. MuSK signaling seems to be upstream of rapsyn; agrin induces synaptic clusters of MuSK in rapsyn null mice (Apel et al., 1997). MuSK activation leads to AChR phosphorylation, but this phosphorylation is not required for AChR clustering (Glass et al., 1997). Additionally, ectopic laminin can induce AChR clusters in muscles from MuSK null mice but not in muscles from rapsyn null mice (Sugiyama et al., 1997). This result suggests that pathways in addition to MuSK converge on rapsyn to induce AChR clustering.

In addition to the redistribution of AchRs, local transcription increases the concentration of AchRs at synaptic zones. Muscles are multinucleated syncytial cells. Signaling from the presynaptic neuron selectively induces the transcription of AchRs from the closest nucleus. The secreted factor, neuregulin, can stimulate AchR transcription when added to cultured muscles (Jo et al., 1995). Mice heterozygous for neuregulin have reduced AchR levels (Sandrock et al., 1997). The receptors for neuregulin are the ErbB family of transmembrane tyrosine kinases (Altiok et al., 1995). However, mouse knockouts of ErbB family members cause early embryonic lethality, precluding an analysis of their requirement for postsynaptic development (Lee et al., 1995; Gassmann et al., 1995). Nonetheless, the early embryonic phenotypes suggest that this signaling system may influence transcription in neurons. Thus, at the NMJ tyrosine kinase signaling serves to increase the local concentration of neurotransmitter receptors by two mechanisms: the redistribution of preexisting AchR proteins and the local transcription and translation of new AchR proteins.

Although many of the same principles governing postsynaptic development at the NMJ probably apply to neuron to neuron synaptogenesis, much less is known about the molecular pathways that regulate postsynaptic development in the CNS. Though expressed in the CNS, agrin does not seem to play a major role in CNS postsynaptic development (Serpinskaya et al., 1999). There may be tyrosine kinase signaling pathways analogous to agrin-MuSK in the CNS, or cell adhesion molecules may play a more direct role in organizing the PSD. Furthermore, it is unclear to what extent the presynaptic neuron is required for postsynaptic differentiation in the CNS.

What is clear is that there are protein families in the CNS that function like rapsyn to organize neurotransmitter receptors at the PSD. Indeed, much of our understanding of CNS synaptogenesis has come from the biochemical identification of proteins that localize to the PSD and interact with postsynaptic neurotransmitter receptors. These include gephyrin for glycine receptors; gephyrin and GABARAP for GABA receptors; Homer for group I metabotropic glutamate receptors (mGluRs); GRIP, ABP, and PICK1 for AMPA-type glutamate receptors; and PSD-95/SAP-90 for NMDA-type glutamate receptors (reviewed in Lee and Sheng, 2000). While these interacting proteins are cytoplasmic, an

extracellular protein, Narp, also has been implicated in the clustering of AMPA receptors (O'Brien et al., 1999).

Homer, GRIP and PSD-95 are representative of an increasing number of synaptic proteins which contain one or more PDZ domains. PDZ domains are protein-protein interaction motifs that have been shown to bind the carboxy terminal tails of neurotransmitter receptors and to the internal surfaces of signaling molecules such as neuronal nitric oxide synthase (reviewed in Craven and Bredt, 1998). Furthermore, the characterization of additional proteins that contain or interact with PDZ domains suggests that a complex multiprotein web functions to link neurotransmitter clusters with regulatory molecules, the cytoskeleton, and the presynaptic density. For example, Shank can interact with PSD-95 and NMDA receptors through the GKAP protein, mGluRs through Homer, and the actin cytoskeleton through cortactin (Naisbitt et al., 1999; Tu et al., 1999). Neuroligin, a postsynaptic transmembrane protein, interacts with both PSD-95 and its presynaptic receptor, neurexin (Irie et al., 1997).

The *in vivo* functional significance of only a few of these biochemically defined protein-protein interactions have been studied. In gephyrin knockout mice glycine receptor localization was defective (Feng et al., 1998). In *C.elegans* the PDZ domain-containing protein LIN-10 is required for the clustering of an AMPA-related receptor, GLR-1 (Rongo et al., 1998). Interestingly, LIN-10 is also required for the apical localization of the LET-23 tyrosine kinase receptor in epithelia cells (Kaech et al., 1998), suggesting that sorting to postsynaptic sites within dendrites and sorting to epithelial apical domains share common proteins and mechanisms. In contrast, glutamate receptors cluster normally in a mouse knockout of PSD-95 (Migaud et al., 1998), showing that not all biochemically defined receptor interacting-proteins are required for *in vivo* receptor clustering.

What is the mechanism by which these interacting proteins concentrate receptors at the PSD? An emerging view is that proteins such as PSD-95 and GRIP serve to anchor preformed clusters of receptors at the PSD rather than cluster receptors *per se*. Studies in neuronal cell culture show that AMPA and NMDA receptors can form clusters in the absence of GRIP and PSD-95, but these clusters are not localized to synapses (Rao et al., 1998). Clusters of GRIP or PSD-95 but not receptors are first seen at sites of newly forming synapses.

Subsequently, clusters of AMPA or NMDA receptors are recruited to the synaptic site. Other evidence suggests that PSD-95 stabilizes receptors at the synapse but is not the primary signal for the synaptic targeting of receptors. Localization of PSD-95 to synapses requires its first two PDZ domains, which bind things like NMDA receptors, suggesting that the receptors recruit PSD-95 rather than vice versa (Craven et al., 1999).

How are receptor-interacting proteins localized? Gephyrin has been shown to interact with microtubules (Kirsch and Betz, 1995) and GABARAP has homology to microtubule associated proteins (Wang et al., 1999), suggesting that anchoring to microtubules may be important for their synaptic targeting. A few molecules have been identified that biochemically interact with receptor-interacting proteins. PSD-95 interacts with synGAP (Kim et al., 1998), whereas gephyrin interacts with collybistin, a guanine nucleotide exchange factor (GEF) for small GTPases (Kins et al., 2000). GTPase activating proteins (GAPs) increase the intrinsic rate of GTP hydrolysis of small GTPases, whereas GEFs promote the exchange of GDP for GTP; small GTPases interact with different sets of proteins depending on whether they are complexed with GTP or GDP. Rho GTPase family members modulate the actin cytoskeleton (reviewed in Tapon and Hall, 1997). The control of rho activity could regulate PSD-95 and gephyrin localization through the synapse-specific modification of the actin cytoskeleton. Lastly, cypin, a cytoplasmic protein that binds PSD-95, can negatively regulate PSD-95 clustering. Cotransfection of cypin and PSD-95 in hippocampal neurons leads to a decrease in the number of PSD-95 clusters compared to transfection of PSD-95 alone (Firestein et al., 1999). Thus, a balance of positive and negative forces may control the localization of receptor-interacting proteins and perhaps the receptors themselves.

Individual neurons are able to regulate the composition of different postsynaptic sites. Excitatory and inhibitory synapses are spatially segregated (Craig et al., 1994), and among excitatory synapses some have NMDA and AMPA receptors and others have NMDA receptors only (Rao et al., 1998). The mechanisms that determine synaptic composition are largely unknown. One potential way to segregate excitatory and inhibitory receptors is to couple receptor localization to neurotransmission. If receptor activity were required for

localization, it would ensure that postsynaptic sites containing a class of neurotransmitter receptor apposed presynaptic vesicle clusters containing the appropriate neurotransmitter. However, the initial stages of synaptic development seem to be largely activity-independent. In Munc13 knockout mice little or no spontaneous or evoked neurotransmitter release was observed, yet glutamatergic synapses formed normally (Augustin et al., 1999). At excitatory synapses, inhibition of AMPA or NMDA receptor activity does not disrupt their targeting and in the case of NMDA receptors actually increases their synaptic levels (Rao and Craig, 1997). One exception is the glycine receptor, where inhibition by strychnine disrupts its localization (Kirsch and Betz, 1998). Nonetheless, it appears that for most receptors localization is controlled by distinct signal transduction pathways and not receptor activity. Thus, an understanding of how neurons sort neurotransmitter receptors to different postsynaptic sites will require the identification of the upstream signal transduction machinery required for postsynaptic development.

Presynaptic development

Even less is known about the structural and regulatory molecules controlling presynaptic development. The presynaptic specialization is characterized by an electron-dense region of the membrane known as the active zone, tightly clustered vesicles filled with neurotransmitter, and mitochondria. The active zone contains proteins that regulate vesicle exocytosis. Synaptic vesicles exist in two pools: a readily releasable pool that consists of vesicles docked at the presynaptic membrane and a reserve pool that consists of vesicles associated with the underlying actin cytoskeleton. Presynaptic structures are morphologically varied. The majority of synapses have an active zone that lies parallel to the plasma membrane and have both readily releasable and reserve pools of vesicles. However, retinal neurons, which have a high rate of neurotransmission, have specialized ribbon synapses that consist of active zones perpendicular to the membrane and docked vesicles only.

Work at the vertebrate NMJ has shown evidence for a retrograde signal from the postsynaptic muscle that induces presynaptic differentiation. As an axon navigates its surroundings, vesicles are diffusely distributed and numerous

membranous structures, called filopodia and lamellipodia, are being extended and retracted within the growth cone. Upon contact with the muscle a dramatic reorganization of the growth cone ensues. Vesicles become clustered, an active zone forms, and the dynamic extension of filopodia and lamellipodia ceases. In agrin- and MuSK- deficient mice presynaptic vesicles fail to cluster and axons grow past their target (Gautam et al., 1996; DeChiara et al., 1996). However, these defects are the indirect consequence of postsynaptic developmental defects; MuSK signaling is required in the muscle for the generation of a retrograde signal that induces presynaptic differentiation in the neuron. A clue to the nature of the retrograde signal came from early deinnervation studies. When a neuron is allowed to extend processes back to a deinnervated muscle, synapses form at the exact sites of previous innervation. This occurs even when all that remains of the muscle is the basal lamina, suggesting that a factor associated with the basal lamina functions to induce presynaptic differentiation (Glicksman and Sanes, 1983). A strong candidate for such a factor is laminin β 2, previously called s-laminin, a synapse specific isoform of laminin consisting of α 5, β 2, and γ 1 subunits. When added to cultured neurons, laminin β 2 induces vesicle clustering and causes axons to stop growing (Porter et al., 1995). In mice lacking laminin β 2 vesicle clustering and active zone formation are impaired (Noakes et al., 1995). However, some presynaptic development occurs even in the absence of laminin β 2, suggesting that other molecules cooperate with laminin β 2 to promote presynaptic differentiation. The receptor for laminin β 2 is unknown, though biochemical interactions with SV2, a synaptic vesicle protein, have been observed (Son et al., 2000). It is unclear how a synaptic vesicle protein could interact with a component of the extracellular matrix. At the *Drosophila* NMJ, a presynaptic tetraspanin protein, encoded by *late bloomer*, is a candidate receptor for a retrograde signal; in *late bloomer* mutant animals presynaptic differentiation is delayed (Kopczynski et al., 1996).

In the vertebrate CNS homologs of proteins involved in wingless signaling have been implicated in the control of presynaptic development. Addition of the secreted wingless homolog Wnt7A causes axonal remodeling and the accumulation of presynaptic proteins in cultured cerebellar neurons

(Lucas and Salinas, 1997). In *Wnt7A* mutants the presynaptic differentiation of mossy fiber to granule cell synapses is delayed (Hall et al., 2000). A dominant negative version of frizzled, the wingless receptor, blocks the effect of *Wnt7A*, and downstream components of wingless signaling, such as β -catenin (Uchida et al., 1996) and APC (Matsumine et al., 1996), localize to presynaptic regions. Wingless signaling controls cell polarity in many different cell types through transcription-dependent and independent pathways (reviewed in Bejsovec, 1999). At the synapse *Wnt7A* may promote presynaptic development by upregulating the transcription of presynaptic structural components. Alternatively, *Wnt7A* signaling may serve to recruit synaptic proteins or modify the underlying synaptic cytoskeleton. Interestingly, β -catenin is involved in both wingless signaling and cadherin adhesion. Although experiments in other cell types have demonstrated independent pools of β -catenin that participate in wingless signaling and cadherin interaction (Sanson et al., 1996), it is possible that at the synapse wingless signaling modifies cadherin adhesion by acting on β -catenin.

The intracellular pathways regulating presynaptic structure at NMJ and CNS synapses are probably similar as many of the molecules associated with the active zone and synaptic vesicles are found at both types of synapses. Synaptic vesicle (SV) proteins are first trafficked to the axon in immature vesicles. After immature vesicles deliver SV proteins to the plasma membrane, SV proteins are endocytosed and delivered to the endosome. It is from the endosome that some mature synaptic vesicles are generated, though other vesicles directly shuttle between endocytosis and exocytosis cycles (Kuromi and Kidokoro, 1998). It is not known how synaptic vesicles are targeted to presynaptic sites. Proteins involved in membrane fusion, such as the SNARE complex, are not required for synaptic targeting (Broadie et al., 1995). In yeast, the Sec6/Sec8 exocyst complex is required early for the targeting of vesicles to the future site of bud formation (TerBush et al., 1996). A neuronal Sec6/Sec8 complex is found at presynaptic sites, however there is no evidence that it is required for synaptic vesicle targeting (Hazuka et al., 1999). Vesicles are transported along microtubules. One mechanism for targeting vesicles to particular sites within the axon is to

create local disturbances of the microtubule network; these disturbances would then cause vesicles to be disengaged from microtubules and deposited at synaptic sites. Microtubule associated proteins (MAPs) can influence both microtubule stability and the transport of organelles along microtubules (Bulinski et al., 1997; Drewes et al., 1997). One hypothesis is that the local regulation of MAPs within axons marks sites for vesicle deposition (Sato-Harada et al., 1996).

One candidate for a protein that clusters synaptic vesicles is synapsin. Synapsin binds lipids and associates with synaptic vesicles *in vivo* (Lu et al., 1992). A mouse synapsin I/synapsin II double knockout has a 50% reduction in the number of clustered synaptic vesicles (Rosahl et al., 1995). Additionally, the clustering of vesicles by synapsin may be regulated. Phosphorylation of synapsin by protein kinase A (PKA) decreases its affinity for synaptic vesicles (Hosaka et al., 1999), and phosphorylation by calcium/calmodulin-dependent protein kinase II (CaMKII) decreases its affinity for actin (Goold et al., 1995). The regulation of synapsin by PKA may control the size of the reserve pool, whereas CaMKII regulation may allow some vesicles to transition from the reserve to the readily releasable pool in response to calcium signaling.

Active zone formation involves many of the same principles of protein localization and clustering encountered at the PSD. In fact, some of the same anchoring proteins regulate protein targeting on both sides of the synapse. Discs-large is required for the presynaptic clustering of FasII (Thomas et al., 1997), whereas it is required for Shaker K⁺ channel localization postsynaptically (Tejedor et al., 1997). A complex of vertebrate LIN-2, LIN-7, and LIN-10 associates with neurexin presynaptically (Butz et al., 1998), whereas *C.elegans* LIN-10 is required for postsynaptic glutamate receptor clustering (Rongo et al., 1998).

As with the PSD, active zones are subdivided into different microdomains. Proteins involved in endocytosis are found at the perimeter of active zones, whereas machinery for exocytosis is concentrated in the center (Roos and Kelly, 1999). Additionally, regulatory molecules can be sorted to different presynaptic zones within a single neuron. For example, the mGluR7 metabotropic glutamate receptor is segregated to different presynaptic sites

(Shigemoto et al., 1996). How presynaptic proteins are targeted to a particular microdomain within a particular type of synapse is completely unknown.

Likewise, it is not known how active zone formation and vesicle clustering are coordinated or what roles active zones and vesicle clusters play in their mutual development. As already discussed, studies of the vertebrate NMJ suggest that signals from the postsynaptic cell induce the formation of active zones and vesicle clusters. However, work at the *Drosophila* NMJ and in cultured neurons suggests that many aspects of presynaptic development can occur independently of the postsynaptic cell. In *Drosophila twist* mutants, in which muscles are absent, units of active zones and vesicle clusters still form; in the absence of the normal postsynaptic muscle, active zones and vesicle clusters are in apposition with neurons and the extracellular matrix (Prokop et al., 1996). Furthermore, the visualization of synaptic vesicles in cultured neurons has revealed that vesicles are transported as preformed clusters within the axon (Ahmari et al., 2000). Preformed vesicle clusters were seen to move along the axon until they were “captured” and stabilized by a postsynaptic dendrite. Most surprisingly, by electron microscopic analysis these preformed vesicle clusters were associated with active zone proteins contained in tubular membrane structures. This suggests that whole presynaptic structures may be preformed and then transported to the site of synaptic contact. Thus, the postsynaptic cell may be more an organizer than an inducer, whose function is to align the presynaptic structure with the postsynaptic density.

Presynaptic structures are also regulated in terms of number, size, and spacing. In general, synapses of a certain type are uniform in size and regularly spaced along the axon (Meinertzhagen et al., 1998). The compartmentalization of regulatory machinery at the level of individual synapses requires that synaptic areas are sharply defined and well-separated from each other. In *C. elegans syd-2* mutant animals active zones and vesicle clusters are expanded in size (Zhen and Jin, 1999). SYD-2 protein localizes to active zones and has homology to liprins; vertebrate liprins interact with tyrosine phosphatase receptors (Serra-Pagés et al., 1998). This suggests that tyrosine kinase signaling is involved in demarcating the boundaries of synaptic regions. In one model tyrosine kinase signaling promotes the accumulation of active zone proteins and clustered vesicles. If there were a

gradient of kinase signaling with its highest point at the middle of the future synaptic site, synapse-promoting kinase activity would decrease shallowly as the distance from the synaptic site increased. However, the superposition of an opposing gradient of kinase-antagonizing phosphatase activity would sharpen the gradient of kinase activity, thus allowing for a sharper demarcation of synaptic boundaries. The identification of tyrosine kinase(s) and phosphatase(s) that function presynaptically will allow for the testing of this model.

Three very large proteins, Bassoon, Piccolo (Fenster et al., 2000), and RPM-1/Highwire, localize at or near presynaptic specializations. Mutations in *C. elegans rpm-1* (Zhen et al., 2000; Schaeffer et al., 2000) and its *Drosophila* homolog *Highwire* (Wan et al., 2000) lead to a variety of presynaptic structural phenotypes depending on the type of synapse studied; these include reductions in and a disorganization of presynaptic structures in *C. elegans* and a hyperproliferation of synapses in *Drosophila*. In particular, at the NMJ of *rpm-1* mutants the regular spacing of presynaptic structures is disrupted; "fused" synapses are seen in which expanded vesicle clusters are associated with multiple active zones. This suggests that RPM-1 protein is required for synapses to maintain an appropriate distance from each other. How could a neuron ensure the regular spacing of synapses? One model is that there are molecular rulers that measure synaptic width and intersynaptic distance. In muscle development two exceptionally large proteins, titin and nebulin, have been implicated in measuring sarcomere length (Labeit et al., 1991; reviewed in Trinick and Tskhovrebova, 1999). In fact, a single molecule of titin spans half a sarcomere, a distance of over 1 μm , and as such could function as a scaffold for the assembly of a sarcomere of defined length. Similarly, the differential splicing of the nebulin gene to create proteins of different lengths suggests a molecular mechanism by which sarcomere size is differentially regulated between muscles (Labeit and Kolmerer, 1995). By analogy to the roles of titin and nebulin in sarcomere development, RPM-1/Highwire could physically measure out the distance between synapses. Intriguingly, RPM-1/Highwire is also very large and localizes to regions adjacent to active zones. Similarly, Piccolo and Bassoon, which localize to active zones, could measure synaptic width. An alternative model for controlling synaptic spacing is that signaling from the synapse could prevent other synapses

from forming within a certain distance. Once a synapse begins to form it could prevent other synapses from initiating in the immediate vicinity while remaining refractory to the inhibitory signal it generates. This logic is seen in the S-phase of the cell cycle, in which the triggering of DNA replication prevents subsequent rounds of DNA replication before the next mitosis. RPM-1/Highwire may signal through its GEF domain. Interestingly, the *Drosophila* Still-life protein also has a GEF domain and localizes adjacent to active zones (Sone et al., 1997).

Introduction of a dominant negative Still-life protein results in a reduction in the number of synapses at the NMJ. The expression of Still-life in human KB cells promotes actin-based structures such as membrane ruffles; this suggests that Still-life may promote synapse formation through the modification of the actin cytoskeleton, perhaps by activating rho family GTPases. Furthermore, the identification of GAP and GEF proteins on both sides of the synapse suggests that small GTPases play an important role in synaptic organization.

***C. elegans* as a model system for studying the development of neuronal connectivity**

Between 1962 and 1963, Sydney Brenner wrote: "We must move on to other problems of biology which are new, mysterious and exciting. Broadly speaking, the fields which we should now enter are development and the nervous system. . . Part of the success of molecular genetics was due to the use of extremely simple organisms which could be handled in large numbers: bacteria and bacterial viruses. . . We should like to attack the problem of cellular development in a similar fashion, choosing the simplest possible differentiated organism and subjecting it to the analytical methods of microbial genetics. . . We think we have a good candidate in the form of a small nematode worm, *Caenorhabditis briggsae*." (Wood et al., 1988). In fact, Sydney Brenner ended up choosing a related nematode species, *Caenorhabditis elegans*, as a model system for studying "development and the nervous system". In particular, *C. elegans* has proved to be a powerful genetic system for identifying proteins involved in axon pathfinding. Parallel studies in *Drosophila* and vertebrates have shown that many of the proteins required for axon development in *C. elegans* have conserved functions throughout the animal kingdom. For example, the secreted factor

UNC-6/Netrin was identified genetically in *C. elegans* as being required for dorsoventral axon guidance (Ishii et al., 1992; Hedgecock et al., 1990), and biochemical studies in vertebrates identified UNC-6/Netrin as a chemoattractant for explanted dorsal root spinal cord axons (Kennedy et al., 1994). In addition, mutations that affect the development of neuronal connectivity have been identified at all steps: cell fate (e.g. *unc-86*, *lim-4*), cell migration (e.g. *vab-8*, *mig-13*), axon outgrowth and guidance (e.g. *unc-6*, *sax-3*, *unc-33*), synapse formation (e.g. *syd-2*, *lin-10*), and synaptic growth (e.g. *unc-43*). Thus, it is conceivable that a complete understanding of the development of the comparatively simpler nervous system of *C. elegans* could be achieved.

In *C. elegans*, the complete cell lineage of about thousand cells has been determined (Sulston et al., 1983). Additionally, the complete connectivity of the *C. elegans* nervous system, which consists of 302 neurons and about 7000 synapses, has been reconstructed from serial section electron micrographs (White et al., 1986). Cell lineage and to a certain extent synaptic connectivity occur in stereotyped patterns from animal to animal. Combined with the rapid lifecycle, small size, and transparency of *C. elegans*, this reproducibility allows the consistent identification of neuronal structures, such as individual synapses, in large populations of wild-type or mutants animals.

C. elegans synapses have typical synaptic elements such as presynaptic active zones and vesicle clusters and postsynaptic densities, though PSDs are often difficult to see in electron micrographs (White et al., 1986). Most neuromuscular junctions differ from NMJs of vertebrates and *Drosophila* in that, instead of the neuron projecting to the muscle, the muscle extends an "arm" to the neuron. The majority of connections between chemosensory neurons, interneurons, and motor neurons are made either in the anterior neuropil, a structure of densely packed processes located between the first and second pharyngeal bulbs, or along the ventral nerve cord. Neuron to neuron synapses are made in passing, sometimes in association with swellings in the axon. In addition, many interneurons have only one process which serves as both axon and dendrite. Thus, postsynaptic and presynaptic sites must be sorted within the same process. Synaptic output is sometimes diadic, i.e. presynaptic varicosities are seen in apposition to two postsynaptic processes. The stereotyped pattern of

synapses suggests a hard-wired program of development. However, some synaptic remodelling occurs during larval development, such as in the GABAergic motor neuron circuit. In the first larval stage (L1) the GABAergic DD motor neurons make synaptic connections exclusively onto ventral muscle. However, at the end of L1, DD motor neurons eliminate ventral synapses and establish connectivity with dorsal muscle; at the same time the VD motor neurons are born and begin to innervate ventral muscle (White et al., 1978).

Recently, several labs have begun to address the problem of synapse formation genetically in *C. elegans*. This is an especially appropriate time for a genetic analysis of synapse formation as many of the key players, particularly in the CNS, have yet to be identified. The expression of fusions between green fluorescent protein (GFP) and proteins that localize to synapses has allowed the visualization of synaptic structures in live animals (Nonet, 1999). During the course of this work the labs of Yishi Jin, Mike Nonet, and Joshua Kaplan have reported the identification of two molecules required for presynaptic development (*syd-2* and *rpm-1*) (Zhen and Jin, 1999; Zhen et al., 2000; Schaeffer et al., 2000) and one required for postsynaptic development (*lin-10*) (Rongo et al., 1998) in *C. elegans*. It is the hope that the combined efforts of our labs will begin to shed light on the regulatory pathways controlling synapse development. As such, the purpose of this thesis was to identify and characterize proteins important for synapse formation in *C. elegans*.

Chapter 2 of this thesis recounts "presynaptic" work, done in collaboration with Kayvan Roayaie, that characterized the G_α protein ODR-3. Chemosensation in *C. elegans* is mediated by sensory neurons, such as AWC and ASI, whose dendrites end in specialized cilia in the amphid pore. Sensory signal transduction machinery is localized to the cilia and serves to convert environmental stimuli into electrical excitability of the neuron. In *odr-3* mutants olfaction and osmosensation are defective. This chapter describes the identification of *odr-3* as a divergent G_ω protein, providing the first evidence that chemosensation in *C. elegans* uses seven transmembrane receptors. Since the time that this work was initiated, the sensory signal transduction pathways have been more fully characterized. A large family of seven transmembrane receptors have been identified and shown to be expressed in subsets of chemosensory

neurons (Troemel et al., 1995). Some of these receptors localize to sensory cilia, and mutations in the ODR-10 receptor cause specific defects in diacetyl sensation (Sengupta et al., 1996). These results suggest that some of these seven transmembrane receptors function to detect odorants. In the AWC neurons ODR-3 signals to the TAX-2/TAX-4 cyclic nucleotide gated channel (Coburn and Barmann, 1996; Komatsu et al., 1996) in a cGMP-dependent pathway that involves the ODR-1 guanylyl cyclase (L'Etoile and Bargmann, 2000). In the chemosensory AWA and osmosensory ASH neurons ODR-3 signaling couples to the capsaicin receptor-related OSM-9 channel (Colbert et al., 1997). Separable from its role in primary signal transduction, ODR-3 was found to control the morphology of sensory cilia. The cilia of AWC neurons are flat and wing-shaped, whereas AWA cilia are thin and highly branched. In *odr-3* mutants AWC cilia became thin like AWA cilia, and ODR-3 overexpression transformed AWA cilia into a flat AWC-like morphology. These results demonstrate that ODR-3 is necessary and sufficient to promote the characteristic morphology of AWC cilia, revealing a role for G_{α} proteins in cell shape generation. In conclusion, this work showed that ODR-3 plays a direct role in both the function and development of olfactory cilia.

Chapter 3 details a genetic screen that identified mutants that disrupt the presynaptic development of chemosensory neurons. Chapter 4 describes the cloning and characterization of one of these mutants, *sad-1*. This work shows that SAD-1 is a novel serine/threonine kinase that organizes and shapes presynaptic vesicle clusters but not active zones and controls axon outgrowth. Signaling through SAD-1 may provide a mechanism by which the neuron couples the end of axon outgrowth with aspects of presynaptic development such as vesicle clustering. SAD-1 may define a new signal transduction pathway in the presynaptic neuron that is downstream of postsynaptic signals. In addition, SAD-1 is related to PAR-1, a kinase involved in regulating polarity in both embryonic and epithelial cells. This result suggests that the mechanisms that organize and target vesicle clusters to presynaptic specializations are similar to those that control asymmetric protein and organelle localization in many polarized cells.

References

Ahmari, S.E., Buchanan, J., and Smith, S.J. (2000). Assembly of presynaptic active zones from cytoplasmic transport packets. *Nat. Neurosci.* 3, 445-451.

Altiok, N., Bessereau, J.L, and Changeux, J.P. (1995). ErbB3 and ErbB2/neu mediate the effect of heregulin on acetylcholine receptor gene expression in muscle: differential expression at the endplate. *EMBO J.* 14, 4258-4266.

Apel, E.D., Glass, D.J., Moscoso, L.M., Yancopoulos, G.D., and Sanes, J.R. (1997). Rapsyn is required for MuSK signaling and recruits synaptic components to a MuSK-containing scaffold. *Neuron* 18, 623-635.

Augustin, I., Rosenmund, C., Sudhof, T.C., and Brose, N. (1999). Munc13-1 is essential for fusion competence of glutamatergic synaptic vesicles. *Nature* 400, 457-461.

Baumgartner, S., Littleton, J.T., Broadie, K., Bhat, M.A., Harbecke, R., Lengyel, J.A., Chiquet-Ehrismann, R., Prokop, A., and Bellen, H.J. (1996). A *Drosophila* neurexin is required for septate junction and blood-nerve barrier formation and function. *Cell* 87, 1059-1068.

Bejsovec, A. (1999). Wnt signalling shows its versatility. *Curr. Biol.* 9 684-687.

Broadie, K., Prokop, A., Bellen, H.J., O'Kane, C.J., Schulze, K.L., and Sweeney, S.T. (1995). Syntaxin and synaptobrevin function downstream of vesicle docking in *Drosophila*. *Neuron* 15, 663-673.

Bulinski, J.C., McGraw, T.E., Gruber, D., Nguyen, H.L., and Sheetz, M.P. (1997). Overexpression of MAP4 inhibits organelle motility and trafficking in vivo. *J. Cell Sci.* 110, 3055-3064.

Burgess, R.W., Nguyen, Q.T., Son, Y.J., Lichtman, J.W., and Sanes, J.R. (1999). Alternatively spliced isoforms of nerve- and muscle-derived agrin: their roles at the neuromuscular junction. *Neuron* 23, 33-44.

Butz, S., Okamoto, M., and Sudhof, T.C. (1998). A tripartite protein complex with the potential to couple synaptic vesicle exocytosis to cell adhesion in brain. *Cell* 94, 773-782.

Carbonetto, S., and Lindenbaum, M. (1995). The basement membrane at the neuromuscular junction: a synaptic mediatrix. *Curr. Opin. Neurobiol.* 5, 596-605.

Casadio, A., Martin, K.C., Giustetto, M., Zhu, H., Chen, M., Bartsch, D., Bailey, C.H., and Kandel, E.R. (1999). A transient, neuron-wide form of CREB-mediated long-term facilitation can be stabilized at specific synapses by local protein synthesis. *Cell* 99, 221-237.

Coburn, C.M., and Bargmann, C.I. (1996). A putative cyclic nucleotide-gated channel is required for sensory development and function in *C. elegans*. *Neuron* 17, 695-706.

Colbert, H.A., Smith, T.L., and Bargmann, C.I. (1997). OSM-9, a novel protein with structural similarity to channels, is required for olfaction, mechanosensation, and olfactory adaptation in *Caenorhabditis elegans*. *J. Neurosci.* 17, 8259-8269.

Craig, A.M., Blackstone, C.D., Huganir, R.L., and Banker, G. (1994). Selective clustering of glutamate and gamma-aminobutyric acid receptors opposite terminals releasing the corresponding neurotransmitters. *Proc. Natl. Acad. Sci.* 91, 12373-12377.

Craven, S.E., and Brecht, D.S. (1998). PDZ proteins organize synaptic signaling pathways. *Cell* 93, 495-498.

DeChiara, T.M., Bowen, D.C., Valenzuela, D.M., Simmons, M.V., Poueymirou, W.T., Thomas, S., Kinetz, E., Compton, D.L., Rojas, E., Park, J.S., Smith, C., DiStefano, P.S., Glass, D.J., Burden, S.J., and Yancopoulos, G.D. (1996). The receptor tyrosine kinase MuSK is required for neuromuscular junction formation *in vivo*. *Cell* 85, 501-512.

Drewes, G., Ebner, A., Preuss, U., Mandelkow, E.M., Mandelkow, E. (1997). MARK, a novel family of protein kinases that phosphorylate microtubule-associated proteins and trigger microtubule disruption. *Cell* 89, 297-308.

Fannon, A.M., and Colman, D.R. (1996). A model for central synaptic junctional complex formation based on the differential adhesive specificities of the cadherins. *Neuron* 17, 423-434.

Feng, G., Tintrup, H., Kirsch, J., Nichol, M.C., Kuhse, J., Betz, H., and Sanes, J.R. (1998). Dual requirement for gephyrin in glycine receptor clustering and molybdoenzyme activity. *Science* 282, 1321-1324.

Fenster, S.D., Chung, W.J., Zhai, R., Cases-Langhoff, C., Voss, B., Garner, A.M., Kaempf, U., Kindler, S., Gundelfinger, E.D., and Garner, C.C. (2000). Piccolo, a presynaptic zinc finger protein structurally related to bassoon. *Neuron* 25, 203-214.

Firestein, B.L., Brenman, J.E., Aoki, C., Sanchez-Perez, A.M., El-Husseini, A.E., and Brecht, D.S. (1999). Cypin: a cytosolic regulator of PSD-95 postsynaptic targeting. *Neuron* 24, 659-672.

Froehner, S.C., Luetje, C.W., Scotland, P.B., and Patrick, J. (1990). The postsynaptic 43K protein clusters muscle nicotinic acetylcholine receptors in *Xenopus* oocytes. *Neuron* 5, 403-10.

Gassmann, M., Casagrande, F., Orioli, D., Simon, H., Lai, C., Klein, R., and Lemke, G. (1995). Aberrant neural and cardiac development in mice lacking the ErbB4 neuregulin receptor. *Nature* 378, 390-394.

Gautam, M., Noakes, P.G., Mudd, J., Nichol, M., Chu, G.C., Sanes, J.R., and Merlie, J.P. (1995). Failure of postsynaptic specialization to develop at neuromuscular junctions of rapsyn-deficient mice. *Nature* 377, 232-236.

Gautam, M., Noakes, P.G., Moscoso, L., Rupp, F., Scheller, R.H., Merlie, J.P., and Sanes, J.R. (1996). Defective neuromuscular synaptogenesis in agrin-deficient mutant mice. *Cell* 85, 525-535.

Glass, D.J., Bowen, D.C., Stitt, T.N., Radziejewski, C., Bruno, J., Ryan, T.E., Gies, D.R., Shah, S., Mattsson, K., Burden, S.J., DiStefano, P.S., Valenzuela, D.M., DeChiara, T.M., and Yancopoulos, G.D. (1996). Agrin acts via a MuSK receptor complex. *Cell* 85, 513-523.

Glass, D.J., Apel, E.D., Shah, S., Bowen, D.C., DeChiara, T.M., Stitt, T.N., Sanes, J.R., and Yancopoulos, G.D. (1997). Kinase domain of the muscle-specific receptor tyrosine kinase (MuSK) is sufficient for phosphorylation but not clustering of acetylcholine receptors: required role for the MuSK ectodomain? *Proc. Natl. Acad. Sci.* 94, 8848-8853.

Glicksman, M.A., and Sanes, J.R. (1983). Differentiation of motor nerve terminals formed in the absence of muscle fibres. *J. Neurocytol.* 12, 661-671.

Goold, R., Chan, K.M., and Baines, A.J. (1995). Coordinated regulation of synapsin I interaction with F-actin by Ca²⁺/calmodulin and phosphorylation: inhibition of actin binding and bundling. *Biochemistry* 34, 1912-1920.

Grakoui, A., Bromley, S.K., Sumen, C., Davis, M.M., Shaw, A.S., Allen, P.M., and Dustin, M.L. (1999). The immunological synapse: a molecular machine controlling T cell activation. *Science* 285, 221-227.

Hall, A.C., Lucas, F.R., and Salinas, P.C. (2000). Axonal remodeling and synaptic differentiation in the cerebellum is regulated by WNT-7a signaling. *Cell* 100, 525-535.

Hazuka, C.D., Foletti, D.L., Hsu, S.C., Kee, Y., Hopf, F.W., and Scheller, R.H. (1999). The sec6/8 complex is located at neurite outgrowth and axonal synapse-assembly domains. *J. Neurosci.* 19, 1324-1334.

Hedgecock, E.M., Culotti, J.G., and Hall, D.H. (1990). The *unc-5*, *unc-6*, and *unc-40* genes guide circumferential migrations of pioneer axons and mesodermal cells on the epidermis in *C. elegans*. *Neuron* 4, 61-85.

Heisenberg, C.P., Tada, M., Rauch, G.J., Saúde, L., Concha, M.L., Geisler, R., Stemple, D.L., Smith, J.C., and Wilson, S.W. (2000). Silberblick/Wnt11 mediates convergent extension movements during zebrafish gastrulation. *Nature* 405, 76-81.

Hosaka, M., Hammer, R.E., and Sudhof, T.C. (1999). A phospho-switch controls the dynamic association of synapsins with synaptic vesicles. *Neuron* 24, 377-387.

Hunter, D.D., Porter, B.E., Bullock, J.W., Adams, S.P., Merlie, J.P., and Sanes, J.R. (1989). Primary sequence of a motor neuron-selective adhesive site in the synaptic basal lamina protein S-laminin. *Cell* 59, 905-913.

Ichtenko, K., Hata, Y., Nguyen, T., Ullrich, B., Missler, M., Moomaw, C., and Sudhof, T.C. (1995). Neuroligin 1: a splice site-specific ligand for beta-neurexins. *Cell* 81, 435-443.

Irie, M., Hata, Y., Takeuchi, M., Ichtenko, K., Toyoda, A., Hirao, K., Takai, Y., Rosahl, T.W., and Sudhof, T.C. (1997). Binding of neuroligins to PSD-95. *Science* 277, 1511-1515.

Ishii, N., Wadsworth, W.G., Stern, B.D., Culotti, J.G., and Hedgecock, E.M. (1992). UNC-6, a laminin-related protein, guides cell and pioneer axon migrations in *C. elegans*. *Neuron* 9, 873-881.

Jo, S.A., Zhu, X., Marchionni, M.A., and Burden, S.J. (1995). Neuregulins are concentrated at nerve-muscle synapses and activate ACh-receptor gene expression. *Nature* 373, 158-161.

Kaech, S.M., Whitfield, C.W., and Kim, S.K. (1998). The LIN-2/LIN-7/LIN-10 complex mediates basolateral membrane localization of the *C. elegans* EGF receptor LET-23 in vulval epithelial cells. *Cell* 94, 761-771.

Kemler, R. (1993). From cadherins to catenins: cytoplasmic protein interactions and regulation of cell adhesion. *Trends Genet.* 9, 317-321.

Kennedy, T.E., Serafini, T., de la Torre, J.R., and Tessier-Lavigne, M. (1994). Netrins are diffusible chemotropic factors for commissural axons in the embryonic spinal cord. *Cell* 78, 425-435.

Kim, J.H., Liao, D., Lau, L.F., and Huganir, R.L. (1998). SynGAP: a synaptic RasGAP that associates with the PSD-95/SAP90 protein family. *Neuron* 20, 683-691.

Kim, S.K. (1997). Polarized signaling: basolateral receptor localization in epithelial cells by PDZ-containing proteins. *Curr. Opin. Cell Biol.* 9, 853-859.

Kins, S., Betz, H., and Kirsch, J. (2000). Collybistin, a newly identified brain-specific GEF, induces submembrane clustering of gephyrin. *Nat. Neurosci.* 3, 22-29.

Kirsch, J., and Betz, H. (1995). The postsynaptic localization of the glycine receptor-associated protein gephyrin is regulated by the cytoskeleton. *J. Neurosci.* 15, 4148-4156.

Kirsch, J., and Betz, H. (1998). Glycine-receptor activation is required for receptor clustering in spinal neurons. *Nature* 392, 717-720.

Kohmura, N., Senzaki, K., Hamada, S., Kai, N., Yasuda, R., Watanabe, M., Ishii, H., Yasuda, M., Mishina, M., and Yagi, T. (1998). Diversity revealed by a novel family of cadherins expressed in neurons at a synaptic complex. *Neuron* 20, 1137-1151.

Komatsu, H., Mori, I., Rhee, J.S., Akaike, N., and Ohshima, Y. (1996). Mutations in a cyclic nucleotide-gated channel lead to abnormal thermosensation and chemosensation in *C. elegans*. *Neuron* 17, 707-718.

Kopczynski, C.C., Davis, G.W., and Goodman, C.S. (1996). A neural tetraspanin, encoded by *late bloomer*, that facilitates synapse formation. *Science* 271, 1867-1870.

Kose, H., Rose, D., Zhu, X., and Chiba, A. (1997). Homophilic synaptic target recognition mediated by immunoglobulin-like cell adhesion molecule Fasciclin III. *Development* 124, 4143-4152.

Kuromi, H., and Kidokoro, Y. (1998). Two distinct pools of synaptic vesicles in single presynaptic boutons in a temperature-sensitive *Drosophila* mutant, *shibire*. *Neuron* 20, 917-925.

Labeit, S., Gibson, T., Lakey, A., Leonard, K., Zeviani, M., Knight, P., Wardale, J., and Trinick, J. (1991). Evidence that nebulin is a protein-ruler in muscle thin filaments. *FEBS Lett.* 282, 313-316.

Labeit, S., and Kolmerer, B. (1995). The complete primary structure of human nebulin and its correlation to muscle structure. *J. Mol. Biol.* 248, 308-315.

Lahey, T., Gorczyca, M., Jia, X.X., and Budnik, V. (1994). The *Drosophila* tumor suppressor gene *dlg* is required for normal synaptic bouton structure. *Neuron* 13, 823-835.

Lee, K.F., Simon, H., Chen, H., Bates, B., Hung, M.C., and Hauser, C. (1995). Requirement for neuregulin receptor erbB2 in neural and cardiac development. *Nature* 378, 394-398.

Lee, S.H., Sheng, M. (2000). Development of neuron-neuron synapses. *Curr. Opin. Neurobiol.* 10, 125-131.

L'Etoile, N.D., and Bargmann, C.I. (2000). Olfaction and odor discrimination are mediated by the *C. elegans* guanylyl cyclase ODR-1. *Neuron* 25, 575-586.

Lu, B., Greengard, P., and Poo, M.M. (1992). Exogenous synapsin I promotes functional maturation of developing neuromuscular synapses. *Neuron* 8, 521-529.

Lucas, F.R., and Salinas, P.C. (1997). WNT-7a induces axonal remodeling and increases synapsin I levels in cerebellar neurons. *Dev. Biol.* 192, 31-44.

Matsumine, A., Ogai, A., Senda, T., Okumura, N., Satoh, K., Baeg, G.H., Kawahara, T., Kobayashi, S., Okada, M., Toyoshima, K., and Akiyama, T. (1996). Binding of APC to the human homolog of the *Drosophila* discs large tumor suppressor protein. *Science* 272, 1020-1023.

Matthes, D.J., Sink, H., Kolodkin, A.L., and Goodman, C.S. (1995). Semaphorin II can function as a selective inhibitor of specific synaptic arborizations. *Cell* 81, 631-639.

Meinertzhagen, I.A., Govind, C.K., Stewart, B.A., Carter, J.M., and Atwood, H.L. (1998). Regulated spacing of synapses and presynaptic active zones at larval

neuromuscular junctions in different genotypes of the flies *Drosophila* and *Sarcophaga*. *J. Comp. Neurol.* 393, 482-492.

Migaud, M., Charlesworth, P., Dempster, M., Webster, L.C., Watabe, A.M., Makhinson, M., He, Y., Ramsay, M.F., Morris, R.G., Morrison, J.H., O'Dell, T.J., and Grant, S.G. (1998). Enhanced long-term potentiation and impaired learning in mice with mutant postsynaptic density-95 protein. *Nature* 396, 433-439.

Monks, C.R., Freiberg, B.A., Kupfer, H., Sciaky, N., Kupfer, A. (1998). Three-dimensional segregation of supramolecular activation clusters in T cells. *Nature* 395, 82-86.

Naisbitt, S., Kim, E., Tu, J.C., Xiao, B., Sala, C., Valtschanoff, J., Weinberg, R.J., Worley, P.F., and Sheng, M. (1999). Shank, a novel family of postsynaptic density proteins that binds to the NMDA receptor/PSD-95/GKAP complex and cortactin. *Neuron* 23, 569-582.

Nitkin, R.M., Smith, M.A., Magill, C., Fallon, J.R., Yao, Y.M., Wallace, B.G., and McMahan, U.J. (1987). Identification of agrin, a synaptic organizing protein from Torpedo electric organ. *J. Cell Biol.* 105, 2471-2478.

Noakes, P.G., Gautam, M., Mudd, J., Sanes, J.R., and Merlie, J.P. (1995). Aberrant differentiation of neuromuscular junctions in mice lacking s-laminin/laminin beta 2. *Nature* 374, 258-262.

Nonet, M. L. (1999). Visualization of synaptic specializations in live *C. elegans* with synaptic vesicle protein-GFP fusions. *J. Neurosci. Methods* 89, 33-40.

Nose, A., Nagafuchi, A., and Takeichi, M. (1988). Expressed recombinant cadherins mediate cell sorting in model systems. *Cell* 54, 993-1001.

O'Brien, R.J., Xu, D., Petralia, R.S., Steward, O., Huganir, R.L., and Worley, P. (1999). Synaptic clustering of AMPA receptors by the extracellular immediate-early gene product Narp. *Neuron* 23, 309-323.

Porter, B.E., Weis, J., and Sanes, J.R. (1995). A motoneuron-selective stop signal in the synaptic protein S-laminin. *Neuron* 14, 549-559.

Prokop, A., Landgraf, M., Rushton, E., Broadie, K., and Bate, M. (1996). Presynaptic development at the *Drosophila* neuromuscular junction: assembly and localization of presynaptic active zones. *Neuron* 17, 617-626.

Rao, A., and Craig, A.M. (1997). Activity regulates the synaptic localization of the NMDA receptor in hippocampal neurons. *Neuron* 19, 801-12.

Rao, A., Kim, E., Sheng, M., and Craig, A.M. (1998). Heterogeneity in the molecular composition of excitatory postsynaptic sites during development of hippocampal neurons in culture. *J. Neurosci.* 18, 1217-1229.

Rongo, C., Whitfield, C.W., Rodal, A., Kim, S.K., and Kaplan, J.M. (1998). LIN-10 is a shared component of the polarized protein localization pathways in neurons and epithelia. *Cell* 94, 751-759.

Roos, J., and Kelly, R.B. (1999). The endocytic machinery in nerve terminals surrounds sites of exocytosis. *Curr. Biol.* 9, 1411-1414.

Rosahl, T.W., Spillane, D., Missler, M., Herz, J., Selig, D.K., Wolff, J.R., Hammer, R.E., Malenka, R.C., and Sudhof, T.C. (1995). Essential functions of synapsins I and II in synaptic vesicle regulation. *Nature* 375, 488-493.

Rose, D., Zhu, X., Kose, H., Hoang, B., Cho, J., and Chiba, A. (1997). Toll, a muscle cell surface molecule, locally inhibits synaptic initiation of the RP3 motoneuron growth cone in *Drosophila*. *Development* 124, 1561-1571.

Rose, D., and Chiba, A. (1999). A single growth cone is capable of integrating simultaneously presented and functionally distinct molecular cues during target recognition. *J. Neurosci.* 19, 4899-4906.

Sandrock, A.W. Jr, Dryer, S.E., Rosen, K.M., Gozani, S.N., Kramer, R., Theill, L.E., and Fischbach, G.D. (1997). Maintenance of acetylcholine receptor number by neuregulins at the neuromuscular junction in vivo. *Science* 276, 599-603.

Sanson, B., White, P., and Vincent, J.P. (1996). Uncoupling cadherin-based adhesion from wingless signalling in *Drosophila*. *Nature* 383, 627-630.

Sato-Harada, R., Okabe, S., Umeyama, T., Kanai, Y., and Hirokawa, N. (1996). Microtubule-associated proteins regulate microtubule function as the track for intracellular membrane organelle transports. *Cell Struct. Funct.* 21, 283-295.

Schaeffer, A. M., Hadwiger, G. D. and Nonet, M. L. (2000) *rpm-1*, a conserved neuronal gene that regulates targeting and synaptogenesis in *C. elegans*. *Neuron*, *in press*.

Schuster, C.M., Davis, G.W., Fetter, R.D., and Goodman, C.S. (1996A). Genetic dissection of structural and functional components of synaptic plasticity. I. Fasciclin II controls synaptic stabilization and growth. *Neuron* 17, 641-654.

Schuster, C.M., Davis, G.W., Fetter, R.D., and Goodman, C.S. (1996B). Genetic dissection of structural and functional components of synaptic plasticity. II. Fasciclin II controls presynaptic structural plasticity. *Neuron* 17, 655-67.

Sengupta, P., Chou, J.H., and Bargmann, C.I. (1996). *odr-10* encodes a seven transmembrane domain olfactory receptor required for responses to the odorant diacetyl. *Cell* 84, 899-909.

Serpinskaya, A.S., Feng, G., Sanes, J.R., and Craig, A.M. (1999). Synapse formation by hippocampal neurons from agrin-deficient mice. *Dev. Biol.* 205, 65-78.

Serra-Pagés, C., Medley, Q.G., Tang, M., Hart, A., and Streuli, M. (1998). Liprins, a family of LAR transmembrane protein-tyrosine phosphatase-interacting proteins. *J. Biol. Chem.* 273, 15611-15620.

Shapiro, L., Fannon, A.M., Kwong, P.D., Thompson, A., Lehmann, M.S., Grubel, G., Legrand, J.F., Als-Nielsen, J., Colman, D.R., and Hendrickson, W.A. (1995). Structural basis of cell-cell adhesion by cadherins. *Nature* 374, 327-337.

Shigemoto, R., Kulik, A., Roberts, J.D., Ohishi, H., Nusser, Z., Kaneko, T., and Somogyi, P. (1996). Target-cell-specific concentration of a metabotropic glutamate receptor in the presynaptic active zone. *Nature* 381, 523-525.

Shishido, E., Takeichi, M., and Nose, A. (1998). *Drosophila* synapse formation: regulation by transmembrane protein with Leu-rich repeats, CAPRICIOUS. *Science* 280, 2118-2121.

Son, Y.J., Scranton, T.W., Sunderland, W.J., Baek, S.J., Miner, J.H., Sanes, J.R., and Carlson, S.S. (2000). The synaptic vesicle protein SV2 is complexed with an alpha5-containing laminin on the nerve terminal surface. *J. Biol. Chem.* 275, 451-460.

Sone, M., Hoshino, M., Suzuki, E., Kuroda, S., Kaibuchi, K., Nakagoshi, H., Saigo, K., Nabeshima, Y., and Hama, C. (1997). Still life, a protein in synaptic terminals of *Drosophila* homologous to GDP-GTP exchangers. *Science* 275, 543-547.

Song, J.Y., Ichtchenko, K., Sudhof, T.C., and Brose, N. (1999). Neuroligin 1 is a postsynaptic cell-adhesion molecule of excitatory synapses. *Proc. Natl. Acad. Sci.* 96, 1100-1105.

Sugita, S., Khvochtev, M., and Sudhof, T.C. (1999). Neurexins are functional alpha-latrotoxin receptors. *Neuron* 22, 489-96.

Sugiyama, J.E., Glass, D.J., Yancopoulos, G.D., and Hall, Z.W. (1997). Laminin-induced acetylcholine receptor clustering: an alternative pathway. *J. Cell Biol.* 139, 181-191.

Sulston, J.E., Schierenberg, E., White, J.G., and Thomson, J.N. (1983). The embryonic cell lineage of the nematode *Caenorhabditis elegans*. *Dev. Biol.* 100, 64-119.

Suzuki, E., Rose, D., and Chiba, A. (2000). The ultrastructural interactions of identified pre- and postsynaptic cells during synaptic target recognition in *Drosophila* embryos. *J. Neurobiol.* 42, 448-459.

Tapon, N., and Hall, A. (1997). Rho, Rac and Cdc42 GTPases regulate the organization of the actin cytoskeleton. *Curr. Opin. Cell Biol.* 9, 86-92.

Tejedor, F.J., Bokhari, A., Rogero, O., Gorczyca, M., Zhang, J., Kim, E., Sheng, M., and Budnik, V. (1997). Essential role for dlg in synaptic clustering of Shaker K⁺ channels in vivo. *J. Neurosci.* 17, 152-159.

TerBush, D.R., Maurice, T., Roth, D., and Novick, P. (1996). The Exocyst is a multiprotein complex required for exocytosis in *Saccharomyces cerevisiae*. *EMBO J.* 15, 6483-6494.

Thomas, U., Kim, E., Kuhlendahl, S., Koh, Y.H., Gundelfinger, E.D., Sheng, M., Garner, C.C., and Budnik, V. (1997). Synaptic clustering of the cell adhesion molecule fasciclin II by discs-large and its role in the regulation of presynaptic structure. *Neuron* 19, 787-799.

- Tomschy, A., Fauser, C., Landwehr, R., and Engel, J. (1996). Homophilic adhesion of E-cadherin occurs by a co-operative two-step interaction of N-terminal domains. *EMBO J.* 15, 3507-3514.
- Trinick, J., and Tskhovrebova, L. (1999). Titin: a molecular control freak. *Trends Cell Biol.* 9, 377-380.
- Troemel, E.R., Chou, J.H., Dwyer, N.D., Colbert, H.A., and Bargmann, C.I. (1995). Divergent seven transmembrane receptors are candidate chemosensory receptors in *C. elegans*. *Cell* 83, 207-218.
- Tu, J.C., Xiao, B., Naisbitt, S., Yuan, J.P., Petralia, R.S., Brakeman, P., Doan, A., Aakalu, V.K., Lanahan, A.A., Sheng, M., and Worley, P.F. (1999). Coupling of mGluR/Homer and PSD-95 complexes by the Shank family of postsynaptic density proteins. *Neuron* 23, 583-592.
- Uchida, N., Honjo, Y., Johnson, K.R., Wheelock, M.J., and Takeichi, M. (1996). The catenin/cadherin adhesion system is localized in synaptic junctions bordering transmitter release zones. *J. Cell Biol.* 135, 767-779.
- Ullrich, B., Ushkaryov, Y.A., and Sudhof, T.C. (1995). Cartography of neuroligins: more than 1000 isoforms generated by alternative splicing and expressed in distinct subsets of neurons. *Neuron* 14, 497-507.
- Wallingford, J.B., Rowling, B.A., Vogeli, K.M., Rothbacher, U., Fraser, S.E., and Harland, R.M. (2000). Dishevelled controls cell polarity during *Xenopus* gastrulation. *Nature* 405, 81-85.
- Wan, H. I., DiAntonio, A., Fetter, R. D., Bergstrom, K., Strauss, R. and Goodman, C. S. (2000). Highwire regulates synaptic growth in *Drosophila*. *Neuron*, *in press*.

Wang, H., Bedford, F.K., Brandon, N.J., Moss, S.J., and Olsen, R.W. (1999). GABA(A)-receptor-associated protein links GABA(A) receptors and the cytoskeleton. *Nature* 397, 69-72.

White, J.G., Albertson, D.G., and Anness, M.A. (1978). Connectivity changes in a class of motoneurone during the development of a nematode. *Nature* 271, 764-766.

White, J.G., Southgate, E., Thomson, J.N., and Brenner, S. (1986). The structure of the nervous system of the nematode *C. elegans*. *Philosophical Transactions of the Royal Society of London* 314B, 1-340.

Winberg, M.L., Mitchell, K.J., and Goodman, C.S. (1998). Genetic analysis of the mechanisms controlling target selection: complementary and combinatorial functions of netrins, semaphorins, and IgCAMs. *Cell* 93, 581-591.

Wood, W.B., and the Community of *C. elegans* Researchers. (1988). "The Nematode *Caenorhabditis elegans*." Cold Spring Harbor Laboratory Press, ix-xiii.

Wu, Q., and Maniatis, T. (1999). A striking organization of a large family of human neural cadherin-like cell adhesion genes. *Cell* 97, 779-790.

Zhen, M., and Jin, Y. (1999). The liprin protein SYD-2 regulates the differentiation of presynaptic termini in *C. elegans*. *Nature* 401, 371-375.

Zhen, M., Xun, H., Bamber, B. and Jin, Y. (2000). Regulation of presynaptic terminal organization by *C. elegans* RPM-1, a putative GTP-GDP exchanger with a Ring-H2 finger domain. *Neuron*, *in press*.

Chapter 2

The G α protein ODR-3 mediates olfactory and nociceptive function and controls cilium morphogenesis in *C. elegans* olfactory neurons

(published in Neuron, Vol. 20, pp. 55-67, 1998)

The G α Protein ODR-3 Mediates Olfactory and Nociceptive Function and Controls Cilium Morphogenesis in *C. elegans* Olfactory Neurons

Kayvan Roayaie,* Justin Gage Crump,*
Alvaro Sagasti, and Cornelia I. Bargmann†
Howard Hughes Medical Institute
Programs in Developmental Biology,
Neuroscience, and Genetics
Department of Anatomy
University of California
San Francisco, California 94143

Summary

The G α -like G α protein ODR-3 is strongly and selectively implicated in the function of *C. elegans* olfactory and nociceptive neurons. Either loss of *odr-3* function or overexpression of *odr-3* causes severe olfactory defects, and *odr-3* function is essential in the ASH neurons that sense noxious chemical and mechanical stimuli. In the nociceptive neurons, ODR-3 may interact with OSM-9, a channel similar to the mammalian capsaicin receptor implicated in pain sensation; in AWC olfactory neurons, ODR-3 may interact with another signal transduction pathway. ODR-3 exhibits an unexpected ability to regulate morphogenesis of the olfactory cilia. In *odr-3* null mutants, the fan-like AWC cilia take on a filamentous morphology like normal AWA cilia, whereas ODR-3 overexpression in AWA transforms its filamentous cilia into a fan-like morphology.

Introduction

Many sensory neurons have elaborate cilia that contribute to sensory function through their structural properties and their localization of signaling proteins (Barber, 1974; Tamar, 1992). Specialized vertebrate sensory cilia include the outer segments of rod and cone photoreceptors, the kinocilium associated with the stereocilia of vertebrate mechanosensory and auditory hair cells, and olfactory cilia (Figure 1A). Little is known about the mechanisms by which these specialized cilia are generated and shaped.

Olfactory cilia are the site at which odorants first interact with olfactory receptor proteins. In the nematode *C. elegans*, olfaction is mediated by ciliated neurons that are associated with the two amphid chemosensory organs (Bargmann and Mori, 1997). *C. elegans* senses volatile attractants using two pairs of olfactory neurons: the AWA neurons mediate responses to diacetyl and pyrazine, and the AWC neurons mediate responses to benzaldehyde, isoamyl alcohol, and 2-butanone (Bargmann et al., 1993). Like olfactory neurons in other animals, these neurons have elaborate cilia (Figures 1B and 1C; Ward et al., 1975; Ware et al., 1975). The AWA cilia are filamentous and extensively branched, whereas

the AWC cilia form a large sheet of membrane that encircles the tip of the nose (Ward et al., 1975; Ware et al., 1975; Perkins et al., 1986). Water-soluble attractants, repellents, and pheromones are sensed by amphid-associated neurons with simple single or double cilia (e.g., ASE and ASH neurons).

C. elegans detects odors using receptors such as the diacetyl receptor ODR-10, a predicted G protein-coupled receptor that is localized to the AWA olfactory cilia (Sengupta et al., 1996). *odr-10* mutants have a specific defect in their ability to detect the odorant diacetyl, and heterologous expression of ODR-10 in ectopic *C. elegans* neurons or human 293 cells confers diacetyl responsiveness on those cells (Troemel et al., 1997; Zhang et al., 1997). ODR-10 is unrelated in sequence to the mammalian olfactory or vomeronasal receptors, but it has seven transmembrane domains and key residues characteristic of G protein-coupled receptors. About 200 additional *odr-10*-like genes and an equal number of genes from other potential families of G protein-coupled receptors might encode other chemosensory receptors in *C. elegans* (Troemel et al., 1995; E. Troemel and C. I. B., unpublished data).

Two types of *C. elegans* sensory channels have been identified by analyzing mutants with olfactory defects. AWC-mediated olfaction requires the activity of a cyclic nucleotide-gated channel encoded by the *tax-2* and *tax-4* genes (Coburn and Bargmann, 1996; Komatsu et al., 1996). The TAX-2/TAX-4 channel is similar to the vertebrate visual and olfactory channels and implicates cGMP or cAMP as a second messenger in *C. elegans* sensory pathways. It is also required in sensory neurons that detect water-soluble attractants (ASE) and thermal gradients (AFD). AWA-mediated olfaction is generated by an alternative pathway that requires a novel putative channel encoded by the *osm-9* gene (Colbert et al., 1997). *osm-9* is also required for avoidance of noxious osmotic, volatile, and mechanical stimuli that are detected by the ASH sensory neurons. The dual mechanical and chemical sensitivity of ASH is reminiscent of pain-sensing (nociceptive) neurons in vertebrates (Kaplan and Horvitz, 1993). Amazingly, OSM-9 has extensive similarity to the capsaicin receptor, which is implicated in vertebrate pain sensation (Caterina et al., 1997; Colbert et al., 1997). Both of these channels are distantly related to the *Drosophila* phototransduction channel TRP, which is regulated by G protein signaling (Tsunoda et al., 1997).

Many G proteins are implicated in vertebrate and invertebrate olfaction. In the vertebrate olfactory system, odorants increase levels of cAMP, which opens an olfactory cyclic nucleotide-gated channel in the olfactory cilia (Pace et al., 1985; Firestein et al., 1991). The G α -like G α protein is concentrated in the ciliated sensory endings of the olfactory neurons, suggesting that it mediates the odor-induced increases in cAMP (Jones and Reed, 1989). Indeed, G α mutant mice have profound defects in odorant-induced activity (Belluscio et al., 1998 [this issue of *Neuron*]). Mammalian vomeronasal neurons,

* These authors contributed equally to this work.
† To whom correspondence should be addressed.

UCSF LIBRARY

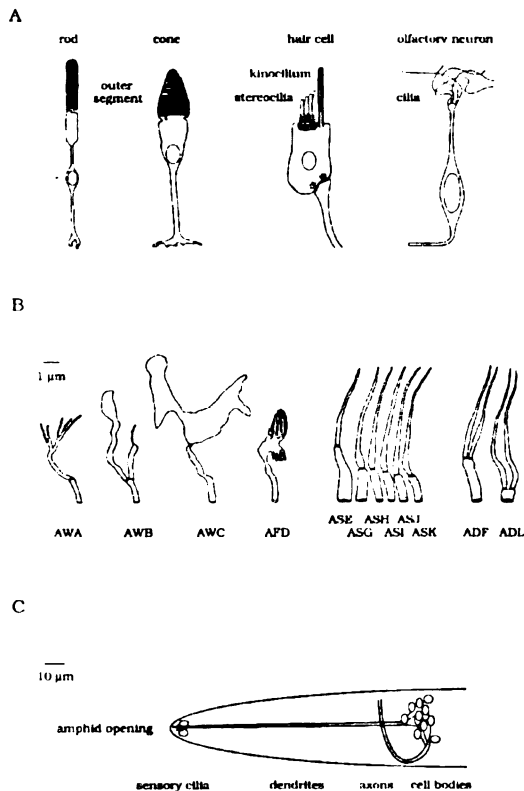


Figure 1. Morphologies of Sensory Cilia

(A) Cilium morphologies of vertebrate photoreceptors (rods and cones), mechanoreceptors (hair cells), and olfactory neurons. The entire cell is shown in each case (except for the olfactory axon); drawings are not to scale.

(B) *C. elegans* cilium morphologies, adapted from Perkins et al. (1986). The ciliated endings of these sensory neurons are associated with the amphid opening at the tip of the nose. All have one or two transition zones at the base of the cilia (in the AFD neurons, this zone is embedded within one of the projections). The actual AWA morphology is probably much more complex than was appreciated from these electron micrograph reconstructions (see Figure 6).

(C) Overall structure of the amphid sensory organ. The bilaterally symmetric amphids each contain the endings of 11 chemosensory neurons and one thermosensory neuron. Only the left side is shown. At the tip of the nose, a small opening exposes the cilia of the ASE, ASG, ASH, ASI, ASJ, ASK, ADF, and ADL neurons. The AWA, AWB, and AWC cilia are enclosed within a sheath pocket that is continuous with the environment, and the thermosensory AFD neurons are not exposed. Anterior is at left and dorsal is up.

which detect pheromones, express either G_{12} or G_0 but not G_{olf} (Halpern et al., 1995; Berghard and Buck, 1996). The targets of G_{12} and G_0 in the vomeronasal system are unknown. Another signaling pathway is used in insect olfaction, which expresses a specialized G_q protein and requires phospholipase C activity for olfactory transduction (Woodard et al., 1992; Talluri et al., 1995). Sensation of sweet and bitter taste in vertebrates requires a transducin-like G_α protein, gustducin, which might regulate phosphodiesterases in taste cells (Ruiz-Avila et al., 1995; Wong et al., 1996).

C. elegans odr-3 mutants were isolated in a behavioral screen for animals that failed to chemotax to benzaldehyde (Bargmann et al., 1993). They have diminished responses to all odors detected by the AWA and AWC neurons, but they retain responses to high concentrations of odors. They are also defective in the chemosensory and mechanosensory functions of the ASH neurons. Here, we show that *odr-3* encodes a G_i -like G_α protein that is expressed in AWA, AWC, ASH, and two other pairs of chemosensory neurons. Although it is coexpressed in sensory neurons with similar *gpa* G_α proteins, *odr-3* and the *gpa* genes have mostly distinct functions. The ODR-3 protein is localized to the sensory cilia, where the initial events of odorant detection occur. *odr-3* activity affects morphogenesis of the AWA and AWC cilia, suggesting that this G_α protein specifies one aspect of cilium morphology.

Results

odr-3 Encodes a G Protein α Subunit

odr-3 was cloned by rescue of its osmotic avoidance phenotype with cosmid clones and subclones from the genetically defined *odr-3* interval (Figure 2A and Experimental Procedures). The coding sequence of a novel G_α subunit was entirely contained on pODR3-1, a clone that rescued *odr-3* mutants. Three subclones that failed to rescue *odr-3* disrupted the *G_\alpha* gene, identifying it as the likely *odr-3* coding region.

A full-length *odr-3* cDNA was isolated and sequenced (see Experimental Procedures). *odr-3* encodes a predicted protein of 356 amino acids that is a member of the G_α family and shares the highest degree of homology (57% amino acid identity) with *gpa-3* (G protein α ; Lochrie et al., 1991), a sensory G_α protein from *C. elegans* (Figures 2B, 2C, and 2D). With respect to the vertebrate classes of G_α subunits, *odr-3* is most closely related to the G_i/G_o family (47% amino acid identity to G_{i2}). This similarity is less striking than the similarity between *C. elegans* homologs of G_o , G_q , and G_s and their vertebrate counterparts, which share >68% amino acid identity (Mendel et al., 1995; Segalat et al., 1995; Brundage et al., 1996; Korswagner et al., 1997).

The amino terminus of ODR-3 contains consensus sites for myristylation and palmitoylation (daggers in Figure 2B), posttranslational modifications that can localize G_α proteins to the plasma membrane (Wedegaertner et al., 1995). The G_α residues important in guanine nucleotide binding and GTP hydrolysis are conserved in ODR-3 (boldface in Figure 2B; Rens-Domiano and Hamm, 1995). The carboxyl termini of G_α subunits are important in defining their interactions with seven transmembrane-domain receptors (Conklin and Bourne, 1993); this region of ODR-3 is unique.

odr-3 Null Mutants Are Defective in Olfaction and in Olfactory, Osmotic, and Mechanosensory Avoidance

An independent mutant screen for osmotic avoidance-defective mutants led to the isolation of an additional allele of *odr-3*, *n1605* (J. H. Thomas, personal communication). To determine whether all *odr-3* phenotypes were

NCBI LIBRARY
 N1605
 1507

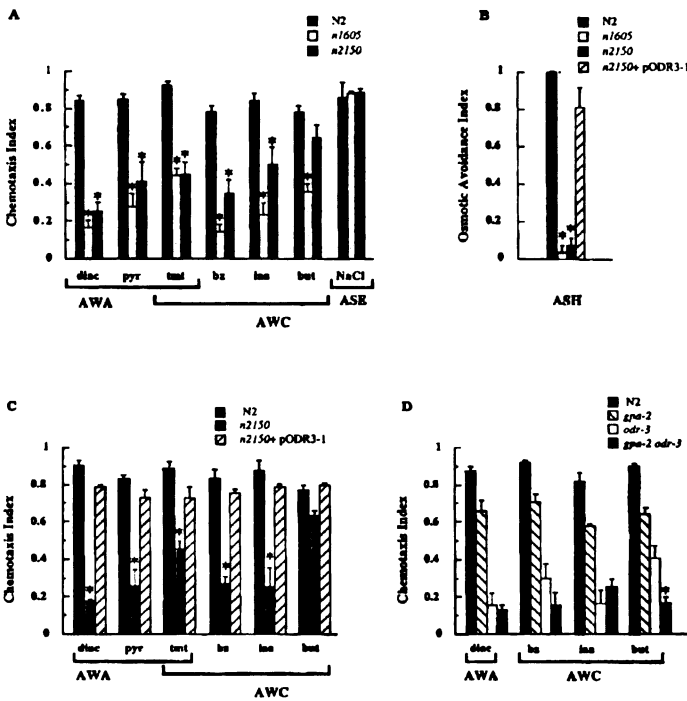


Figure 3. Behavioral Phenotypes of *odr-3* Mutants and Rescued Strains

(A) Chemotaxis responses of wild-type, *odr-3(n1605)*, and *odr-3(n2150)* strains. For all figures, abbreviations are as follows: diac, 1:1000 dilution of diacetyl; pyr, 10 mg/ml pyrazine; tmt, 1:1000 2,4,5-trimethylthiazole; bz, 1:200 benzaldehyde; iaa, 1:100 isoamyl alcohol; but, 1:1000 2-butanone; and NaCl, 0.2 M NaCl. All volatile odorants were diluted in ethanol. Asterisks denote numbers different from the control at $p < 0.01$. *odr-3(n1605)* was different from *odr-3(n2150)* for chemotaxis to 2-butanone ($p = 0.001$) and marginally different for chemotaxis to benzaldehyde ($p = 0.023$) and isoamyl alcohol ($p = 0.03$). There could be a residual function of the truncated *odr-3* protein in *odr-3(n2150)*, or these differences could be caused by other strain differences.

(B) Osmotic-avoidance responses of wild-type animals, *odr-3* mutants, and *odr-3(n2150)* mutants rescued with pODR3-1 DNA (10 ng/ μ l injection).

(C) Chemotaxis responses of wild-type animals, *odr-3(n2150)* mutants, and *odr-3(n2150)* mutants rescued with pODR3-1 DNA (10 ng/ μ l injection).

(D) Mutant phenotypes of *odr-3(n1605)*, *gpa-2(pk16)*, and *gpa-2(pk16) odr-3(n1605)* mutants. The *gpa-2 odr-3* double mutants differ from each single mutant at $p < 0.01$ (asterisk) for butanone chemotaxis; for all other odorants, double mutants were no more severe than *odr-3* alone.

Chemotaxis responses of wild-type animals, *odr-3* mutants, and *odr-3(n2150)* mutants rescued with pODR3-1 DNA (10 ng/ μ l injection). For all assays, controls were tested in parallel on the same day as the mutant strains to control for day-to-day variation of the assay. At least three independent assays were conducted for each data point. Error bars indicate the standard error of the mean (SEM).

caused by the same gene, we compared the behavioral effects of the independent *odr-3(n2150)* and *odr-3(n1605)* mutations. Like *odr-3(n2150)* animals, *odr-3(n1605)* mutants were defective in chemotaxis to all volatile attractants, including odorants sensed by both the AWA and the AWC olfactory neurons (Figure 3A). The severity of the mutant defects varied from mild (e.g., butanone chemotaxis) to severe (e.g., diacetyl chemotaxis). In all cases, *odr-3(n1605)* was comparable or more defective in its responses than *odr-3(n2150)*. Both alleles displayed normal chemotaxis to water-soluble attractants such as NaCl (Figure 3; data not shown). All of the olfactory defects of *odr-3(n2150)* mutants were rescued by the *odr-3* transgene, confirming that they were all caused by the same mutation (Figure 3C).

odr-3 mutants were defective in all avoidance responses mediated by the ASH sensory neurons. The ASH neurons are essential for osmotic avoidance and avoidance of light touch to the nose, both of which were defective in the *odr-3(n1605)* and *odr-3(n2150)* mutants (Figure 3B; data not shown). *odr-3* mutants were also highly defective in avoidance of the volatile repellent octanol in an assay that depends on ASH and ADL (data not shown).

The coding region of *odr-3* was sequenced in *n1605* and *n2150* mutants to determine the nature of the *odr-3* mutations (Figure 2B). Each mutant allele had a G-to-A transition mutation, consistent with the mutagenic spectrum of the mutagen ethylmethanesulfate. In *odr-3(n1605)*

animals, a glutamine at amino acid residue 22 was changed to a stop codon. This early nonsense mutation in the coding sequence suggests that *n1605* results in a complete loss of *odr-3* function. In *odr-3(n2150)* animals, an arginine at amino acid residue 180 was changed to a stop codon. This nonsense mutation would only produce the amino-terminal half of the protein, which would not function properly as a $G\alpha$ but might retain some ability to bind $G\beta\gamma$ subunits (Conklin and Bourne, 1993). The weaker behavioral phenotype of *odr-3(n2150)* may be due to activity of this partial protein, or it may be due to other differences in the strain backgrounds.

These behavioral data indicate that *odr-3* is essential for all AWA and ASH functions but less critical for some AWC responses. The mild butanone defects of *odr-3* null mutants suggest that a different $G\alpha$ protein may mediate responses to some odorants. The $G\alpha$ protein GPA-2 is expressed in the AWC neurons that detect butanone (Zwaal et al., 1997). *gpa-2* null mutants had nearly normal olfactory responses, including strong butanone chemotaxis (Figure 3D). However, *gpa-2 odr-3* double mutants were highly defective in butanone chemotaxis, indicating that the two G proteins act redundantly in the response to this odorant (Figure 3D).

***odr-3* Is Expressed in a Subset of Sensory Neurons**

In order to identify the cells that express *odr-3*, ~2.7 kb of the *odr-3* promoter was used to drive expression of

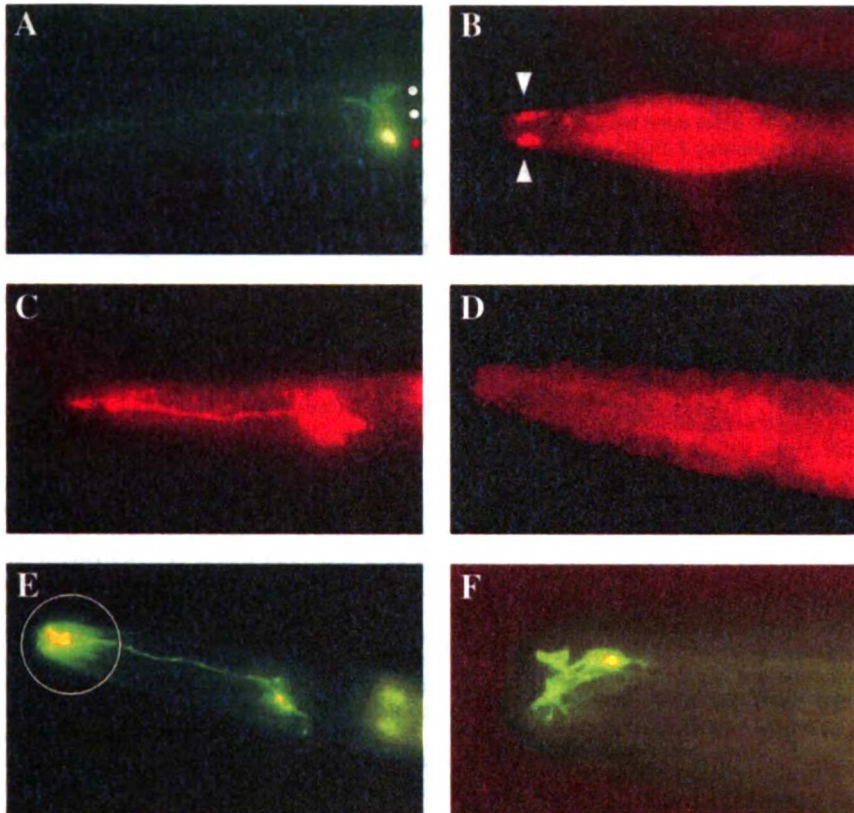


Figure 4. Expression of Endogenous ODR-3 Protein and *odr-3* Fusion Genes

- (A) Expression of pODR3::GFP-2, a transcriptional fusion of GFP to the initiation codon of *odr-3* (Figure 2A; lateral view). Strong expression in the AWC neuron is visible (red dot), along with weaker expression in ASH and AWB (white dots).
- (B) Expression of endogenous ODR-3 protein in the cilia of the AWC neurons (arrowheads), detected with anti-ODR3 antisera (dorsal view).
- (C) Expression of ODR-3 protein overexpressed from its own promoter (the plasmid pODR3-1, injected at 100 ng/ μ l), detected with anti-ODR3 antisera (lateral view). A cluster of cell bodies is visible, along with their sensory processes.
- (D) ODR-3 expression is not detectable with anti-ODR3 antisera in the *odr-3(n1605)* mutant strain.
- (E) Expression of pODR3::GFP-1, a translational fusion that incorporates the first 36 amino acids of ODR-3 into the fusion protein (lateral view). Expression is highly concentrated in the cilia (circled).
- (F) High magnification view of the AWC cilia expressing pODR3::GFP-1.

the green fluorescent protein (GFP) in transgenic animals (Chalfie et al., 1994). Expression of the GFP reporter gene was observed in five pairs of sensory neurons, the AWA, AWB, AWC, ASH, and ADF neurons (Figure 4A). The AWC neurons consistently expressed GFP most brightly, the AWB neurons less well, and the AWA, ASH, and ADF neurons only weakly (see Experimental Procedures). The expression of *odr-3* in the AWA and AWC neurons is consistent with the observed volatile attraction defect of mutant *odr-3* mutant animals, whereas expression in ASH could account for the osmotic-avoidance, octanol-avoidance, and nose-touch defects. *odr-3* mutants are also defective in AWB-mediated long-range avoidance (Troemel et al., 1997). This restricted pattern of GFP expression suggests that *odr-3* subserves a specialized function in sensory neurons.

Antibodies against the ODR-3 protein were generated and used to detect the endogenous ODR-3 protein in wild-type and mutant animals. The anti-ODR-3 antibodies stained only the ciliated endings of a few amphid

neurons in wild-type animals (Figure 4B). The AWC neurons were identified by the distinctive morphology of their ciliated endings, but the identity of the other cells expressing *odr-3* could not be established based on cilia morphology. However, the overall pattern of staining is consistent with the predicted pattern based on the GFP fusion gene, and no staining was observed outside the amphid region. To help identify the cells that expressed ODR-3, the anti-ODR-3 antibodies were also used to stain animals with high copy overexpression of the *odr-3* genomic clone. In these animals, the ODR-3 protein was detected in cell bodies as well as cilia, in a cluster of cells that appeared to be the AWA, AWB, AWC, ADF, and ASH cells that expressed *odr-3::GFP* transgenes (Figure 4C). The specificity of the antibody was confirmed by the absence of staining in the null mutant *odr-3(n1605)*, which should not express ODR-3 protein (Figure 4D).

In an effort to determine molecular cues necessary for localization of ODR-3 to the sensory cilia, portions

of ODR-3 were fused to GFP. The amino terminus of ODR-3 contains consensus sites for both myristylation and palmitoylation, posttranslational modifications that are required for proper localization and function of G α subunits (Wedegaertner et al., 1995). When the promoter and the first 36 amino acids of the *odr-3* coding region were fused to GFP, the strongest GFP expression was observed at the tip of the nose (Figure 4E), particularly in the distinctive AWC cilia (Figure 4F). The enriched expression of this transgene in the cilia indicates that the first 36 amino acids of ODR-3 have a preference for the ciliated endings of sensory neurons.

Overexpression of ODR-3 Causes Olfactory Defects but Not Osmotic Avoidance Defects

Overexpression of a G protein that is closely involved in olfactory function might lead to defective olfactory signaling. To achieve *odr-3* overexpression, the wild-type *odr-3* rescuing genomic clone was injected into *odr-3(+)* animals at 10-fold higher concentrations than were typically used to rescue the mutant phenotype. All five resulting overexpressing strains (*odr-3(xs)* strains) were found to have olfactory defects. One line carrying an extrachromosomal transgenic array was characterized in more detail. As was anticipated, this line had a much higher level of ODR-3 protein expression than wild-type animals (Figure 4C), and expression appeared to be restricted to the correct sensory neurons, albeit delocalized within those cells.

Overexpression of ODR-3 resulted in olfactory defects that were as strong or stronger than those of *odr-3(n1605)* animals (Figure 5A). The *odr-3(xs)* animals were severely defective in responses to all odorants sensed by both the AWA and AWC neurons, including odorants such as 2-butanone that were only mildly affected in the null mutants. However, animals overexpressing ODR-3 were not significantly defective in osmotic avoidance (Figure 5B). The absence of an osmotic-avoidance defect is unlikely to be due to low levels of ODR-3 in the ASH neurons, since anti-ODR-3 antibodies appeared to show similar staining of ASH, AWA, and AWC neurons in the *odr-3(xs)* strain (Figure 4C).

A clone in which the *odr-3* promoter was used to drive GFP did not cause olfactory defects when injected into *odr-3(+)* animals at high concentrations (data not shown). Therefore, high levels of the *odr-3* promoter did not disrupt expression of *odr-3* or other genes involved in olfactory behaviors. Nomarski microscopy and antibody staining of *odr-3(xs)* animals revealed that the olfactory neurons were not killed by the transgene. Thus, both the absence of *odr-3* function and excessive ODR-3 protein can disrupt olfactory responses.

Constitutively Active *odr-3* Causes Olfactory and Osmotic Avoidance Defects

The overexpression of ODR-3 could disrupt olfaction either through excessive G α activity or through titration of free G $\beta\gamma$ subunits by high levels of ODR-3 protein. In all known G α proteins, an even higher level of G α activity can be provided by generating constitutively active alleles. Altering the conserved glutamine corresponding to ODR-3 residue 206 to leucine leads to constitutive G α

activity by blocking the GTPase activity of G α proteins including G α_s , G α_q , G α_o , and G α_i (Conklin and Bourne, 1993; Rens-Domiano and Hamm, 1995). By analogy with these well-characterized proteins, an activated ODR-3 protein (ODR-3*) should have more G α activity than a comparable wild-type ODR-3 protein, but it should have less ability to titrate G $\beta\gamma$ subunits.

Expression of ODR-3* at high levels (*odr-3*(Q206L)xs*) caused olfactory defects in a wild-type background (Figure 5C) and also caused defects in osmotic avoidance that were not seen with expression of the wild-type ODR-3 protein (Figure 5D). The osmotic-avoidance defects caused by this mutant but not by the wild-type protein implicate G α in ASH signaling. Only slight defects were observed when this mutant was expressed at low levels.

Expression of either *odr-3*(Q206L)* or a second point mutant *odr-3(S47C)* at low levels did not rescue the olfactory or osmotic-avoidance defects of an *odr-3* mutant (Figures 5C–5F). *odr-3(S47C)* has a serine-to-cysteine mutation at residue 47; in G α_o or G α_q , a similar mutation produces a G protein that retains the ability to bind G $\beta\gamma$ subunits but has reduced affinity for GTP (Slepek et al., 1993, 1995). Thus, either ODR-3*(Q206L) or ODR-3(S47C) proteins might possess some G α activity, but neither should be modulated normally by receptors. Since these point mutations eliminate the normal rescuing activity of *odr-3*, it is likely that regulated *odr-3* activity, rather than some absolute level of ODR-3 protein, is essential for normal chemosensation. The *odr-3(S47C)* clone caused a moderate olfactory defect when expressed at high levels in a wild-type background, but it did not affect osmotic avoidance (Figures 5E and 5F).

***odr-3* Activity Specifies the Fan-like Morphology of the AWC Cilia**

The AWC neurons have cilia that form two extended, fan-like membrane sheets, while the AWA neurons have multiply branched filamentous cilia that are condensed around microtubules (Figure 1B; Ward et al., 1975; Ware et al., 1975; Perkins et al., 1986). In previous electron micrographs of *odr-3(n2150)* mutants, we noted that the AWC cilia were reduced in size (Bargmann et al., 1993). These ultrastructural defects suggest that mutations in *odr-3* affect AWC morphology. To examine the structure of the AWA and AWC neurons in greater detail, we made use of GFP fusion proteins that reveal individual olfactory cilia. An ODR-10::GFP fusion protein is localized to the AWA cilia (Sengupta et al., 1996), whereas an STR-2::GFP fusion protein is expressed at high levels in the AWC cilia (E. Troemel, personal communication; Figures 6A and 6F). *odr-10::GFP* or *str-2::GFP* transgenes were crossed into *odr-3(n1605)*, *odr-3(xs)*, *odr-3*(Q206L)xs*, and *odr-3(S47C)xs* strains. In all of these mutants, ODR-10::GFP was expressed in AWA and STR-2::GFP was expressed in AWC, indicating that the AWA and AWC cell fates were determined correctly.

As expected from the electron micrographs, *odr-3* loss-of-function mutations led to alterations in the AWC cilia (Figure 6B). These defects were examined using conventional and wide-field deconvolution microscopy (Hiraoka et al., 1991). In *odr-3(n1605)* mutants, AWC cilia

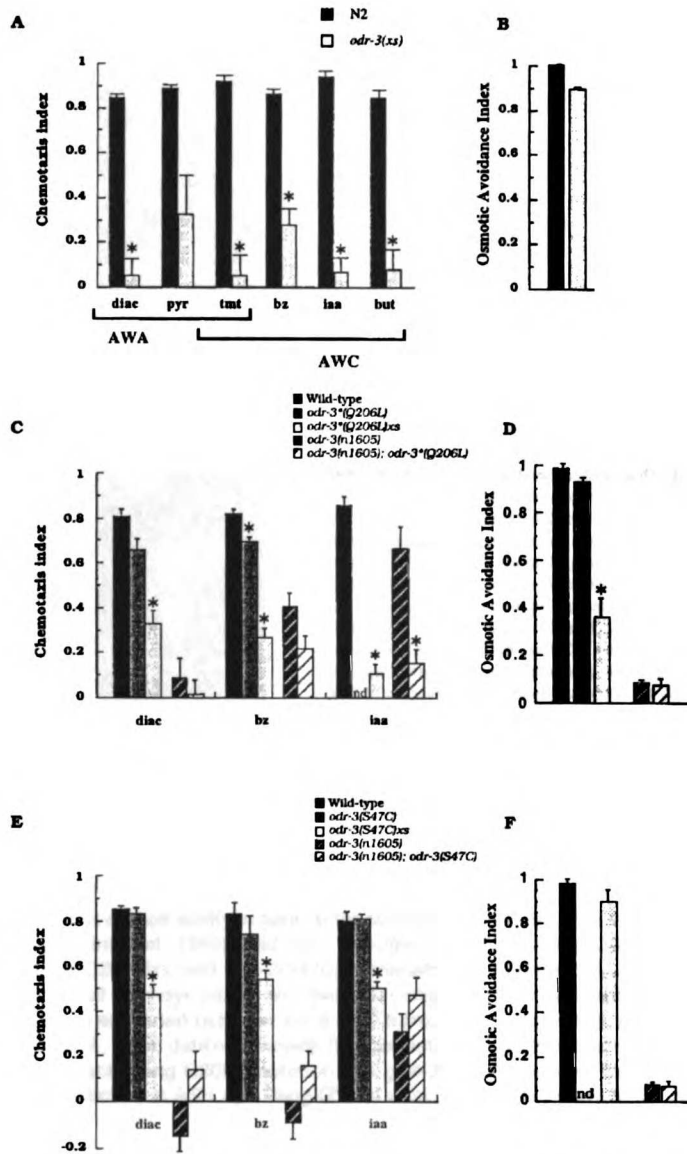


Figure 5. Behavioral Phenotypes of *odr-3* Overexpression and of *odr-3* Point Mutants
Chemotaxis responses ([A], [C], and [E]) and osmotic avoidance responses ([B], [D], and [F]) of wild-type animals (closed bars), wild-type animals bearing *odr-3* clones injected at 10 ng/ μ l (medium grey bars), and wild-type animals bearing *odr-3* clones injected at 100 ng/ μ l (open bars). *odr-3* mutant animals (closed cross-hatched bars) and *odr-3* mutants with clones injected at 10 ng/ μ l (open cross-hatched bars) are also included (compare injection of wild-type *odr-3* clones in Figures 3B and 3C). Asterisks denote values that are different from the controls at $p < 0.01$. Clones injected into *odr-3(+)* strains were compared to wild-type controls; clones injected into *odr-3(n1605)* were compared to *odr-3(n1605)* controls. When the wild-type clone was injected into *odr-3* mutants at 100 ng/ μ l, it rescued osmotic avoidance to wild-type levels, but it did not rescue diacetyl or benzaldehyde chemotaxis, presumably because it was overexpressed (data not shown). Each data point represents at least three independent assays. For the mutated *odr-3* clones, at least three independent transgenic lines were generated for each genotype and DNA concentration, and all behaved comparably in all assays. Error bars indicate the SEM.

always had filamentous branches, like AWA, instead of the extended fan-like sheets typical for AWC ($n = 112$ animals). The filamentous branches were often very long, perhaps to accommodate the excess AWC membrane. The AWA cilia were apparently normal in *odr-3(n1605)* mutants ($n = 38$).

Surprisingly, overexpression of *odr-3* led to reciprocal effects on the morphology of the AWA cilia (Figure 6G). In the *odr-3(xs)* strain, some branches of the AWA cilia were not filamentous but rather flattened and extended like AWC cilia, whereas most AWC cilia maintained the normal fan-like cilium morphology (Figures 6C and 6G; 62% of AWA cilia [$n = 50$] but only 13% of AWC cilia [$n = 105$] had altered morphologies). Thus, in either AWA or AWC, a low level of ODR-3 protein correlated with

AWA-like filamentous cilia, whereas a high level specified AWC-like fan-like cilia. This morphological effect was superimposed on a normal branching pattern; in all mutants, the AWA cilia split into many branches, whereas the AWC cilia had only one or two branches.

Although overexpression of wild-type *odr-3* did not disrupt AWC morphogenesis, both the *odr-3(Q206L)xs* strain and the *odr-3(S47C)xs* strain had highly aberrant, short filamentous AWC cilia (Figures 6D and 6E). Due to variable expression of the transgene, it was not possible to score the AWA cilia in *odr-3(Q206L)xs* or *odr-3(S47C)xs* strains.

The ASH neurons display a normal morphology in electron micrographs from *odr-3(n2150)* animals (Bargmann et al., 1993). Disruption of the ASH cilia can be

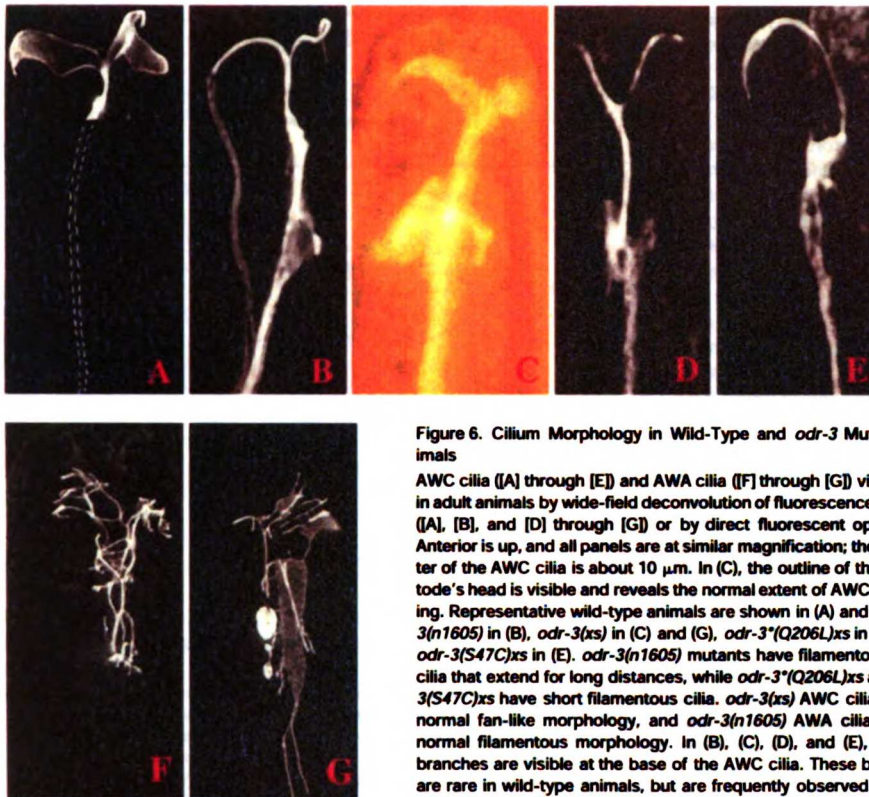


Figure 6. Cilia Morphology in Wild-Type and *odr-3* Mutant Animals

AWC cilia ([A] through [E]) and AWA cilia ([F] through [G]) visualized in adult animals by wide-field deconvolution of fluorescence images ([A], [B], and [D] through [G]) or by direct fluorescent optics (C). Anterior is up, and all panels are at similar magnification; the diameter of the AWC cilia is about 10 μm . In (C), the outline of the nematode's head is visible and reveals the normal extent of AWC spreading. Representative wild-type animals are shown in (A) and (F); *odr-3(n1605)* in (B), *odr-3(xs)* in (C) and (G), *odr-3*(Q206L)xs* in (D), and *odr-3(S47C)xs* in (E). *odr-3(n1605)* mutants have filamentous AWC cilia that extend for long distances, while *odr-3*(Q206L)xs* and *odr-3(S47C)xs* have short filamentous cilia. *odr-3(xs)* AWC cilia have a normal fan-like morphology, and *odr-3(n1605)* AWA cilia have a normal filamentous morphology. In (B), (C), (D), and (E), ectopic branches are visible at the base of the AWC cilia. These branches are rare in wild-type animals, but are frequently observed in GFP-expressing strains, even those that have normal responses to odors.

monitored as a loss of their ability to take up the fluorescent dye DiO (Perkins et al., 1986). Wild-type, *odr-3(null)*, *odr-3(xs)*, *odr-3*(Q206L)xs*, and *odr-3(S47C)xs* animals all exhibited normal ASH dye filling, and their ASH cilia were normal when examined using an *sra-6::GFP* transgene (Troemel et al., 1995; data not shown). By contrast, animals with the activating Q205L mutation in a *gpa-3* transgene are defective in ASH dye filling (Zwaal et al., 1997).

Discussion

The ODR-3 G α Protein Is Required for Olfaction, Osmosensation, and Mechanosensation

odr-3 is essential for normal responses to volatile odors. Unlike the previously described *C. elegans* G proteins, which have either very widespread (G_o , G_q , G_i ; Mendel et al., 1995; Segalat et al., 1995; Brundage et al., 1996; Korswagen et al., 1997) or very subtle (*gpa-2*, *gpa-3*; Zwaal et al., 1997) functions, ODR-3 is strongly and selectively implicated in olfactory function. Its expression in the AWA, AWB, and AWC olfactory neurons is consistent with previous evidence implicating G protein-coupled receptors in *C. elegans* olfaction. G protein-coupled receptors are also central to mammalian olfaction, but just as *C. elegans* olfactory receptors are

distinct from the mammalian receptors, the *C. elegans* G protein ODR-3 is distinct from the G_o -like vertebrate G protein $G_{\alpha o}$. These data, together with expression data from vomeronasal neurons and insect olfactory neurons, suggest that a variety of signaling pathways will operate in chemosensation.

Unexpectedly, we find that the ODR-3 G α protein is also essential for osmosensation and mechanosensation. These effects are likely to be due to ODR-3 G α action within the ASH sensory cilia. The ASH neurons may be analogous to the pain-sensing neurons of mammals that mediate avoidance of a wide array of noxious stimuli; our results with ODR-3 suggest that G protein-coupled receptors will initiate or regulate nociception.

One surprising aspect of *odr-3* function is that it acts in neurons that appear to use different sensory transduction pathways (Figure 7). *odr-3* is essential for all functions of the ASH and AWA neurons; the only other gene known to be required in these two neurons is *osm-9*, which encodes a novel predicted channel with extensive similarity to the capsaicin-sensitive receptor that is important in mammalian pain sensation (Caterina et al., 1997; Colbert et al., 1997). OSM-9 and the capsaicin receptor are more distantly related to the G protein-regulated *Drosophila* phototransduction channel TRP/TRPL (Tsunoda et al., 1997). Since ODR-3 and OSM-9

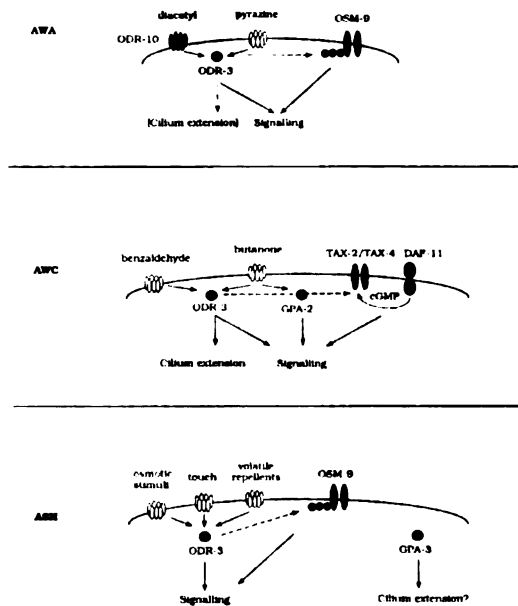


Figure 7. Summary of G α Function in Different Chemosensory Neurons

Shaded molecules are cloned, whereas unshaded receptors are hypothetical. The putative channels TAX-2, TAX-4, and OSM-9 represent potential targets for ODR-3 function (dotted lines). *odr-3* is essential for signaling in AWA, AWC, and ASH; it affects cilium morphology in AWC and can affect AWA cilium morphology when overexpressed.

functions are so similar in AWA and ASH, we speculate that the OSM-9/capsaicin receptor channel family will be regulated by G proteins such as ODR-3 and G α .

By contrast, the olfactory function of the AWC olfactory neurons requires *odr-3*, a cyclic nucleotide-gated channel encoded by *tax-2* and *tax-4*, and a transmembrane guanylyl cyclase encoded by *daf-11* (Coburn and Bargmann, 1996; Komatsu et al., 1996; D. Birnby and J. H. Thomas, personal communication), suggesting that *odr-3* regulates cyclic nucleotide production or degradation. *odr-3* could be a bifunctional G protein that couples to two signaling systems; alternatively, some of these neurons could require both *odr-3* and another G protein whose function has not been tested (e.g., *C. elegans* G α , G α , and G α , are all widely expressed, but these mutants move too poorly to be tested for sensory function).

odr-3 Activity Specifies the Shape of Olfactory Cilia

The reciprocal effects of *odr-3* levels on AWA and AWC cilia indicate that the amount of ODR-3 protein can determine the extent of cilium outgrowth. Like olfactory neurons in other animals, the AWA and AWC neurons have cilia with modified structures that may allow efficient odorant capture (Figures 1A and 1B). The AWA cilia are split into a large array of slender filamentous branches, whereas the AWC cilia extend in two fan-like flat sheets. Since alteration of ODR-3 levels can cause

reciprocal transformations between AWA and AWC morphologies, we propose that ODR-3 expression defines the unique fan-like extension of the AWC olfactory cilia.

Complex differentiated cilia and associated structures are characteristic of many types of sensory neurons. The *odr-3* phenotypes implicate heterotrimeric G protein signaling in cilium morphogenesis. There are two general ways in which *odr-3* could act: it could interact with a specific ligand-activated receptor that controls cilium development, or it could be part of a homeostatic mechanism that allows odorant-induced signaling to regulate the shape of the sensory cilia. Although there is no previous evidence for G protein function in cilium development, G proteins in other systems can contribute to cell polarity and morphogenesis. G protein-coupled receptors direct chemotaxis of leukocytes and *Dictyostelium* amoebae by reorganizing the actin cytoskeleton (Klotz and Jesaitis, 1994; Parent and Devreotes, 1996), and a *C. elegans* G β subunit is required to orient the polarity of embryonic cell divisions (Zwaal et al., 1996).

In *C. elegans*, at least 25 genes are required for normal structure of the sensory cilia, which are the only cilia in the animal (Starich et al., 1995). Nineteen candidate G α proteins are encoded in the sequenced regions of the *C. elegans* genome, including a G α , a G α , a G α , and at least 10 G α proteins of unknown function (Mendel et al., 1995; Segalat et al., 1995; Brundage et al., 1996; Korswagen et al., 1997; G. Jansen and R. Plasterk, personal communication). Perhaps some of the other G proteins also determine specific cilium properties. It is interesting that *gpa-3*^(Q205L) mutations, unlike *odr-3*^(Q206L) mutations, affect the ability of the ASH cilia to take up the fluorescent dye DiO (Zwaal et al., 1997).

Mutations that affect signal transduction components can indirectly cause cilium degeneration (Ranganathan et al., 1995). *Drosophila*, mouse, and human mutations that affect phototransduction cause degeneration, but not proliferation, of the photosensitive structures (Chang et al., 1993; Ranganathan et al., 1995; Sullivan and Daiger, 1996). *odr-3* is unlike these genes, since alteration of *odr-3* can either decrease or increase the area of olfactory cilia. However, the severe AWC alterations observed in *odr-3*^(Q206L)*xs* and *odr-3*^(S47C)*xs* strains might represent degenerative events caused by aberrant signaling.

Are all of the behavioral effects of *odr-3* due to its effects on cilia? Probably not: although malformation of the cilia probably decreases odorant sensitivity to some degree, the visible cilium defects cannot account for all *odr-3* sensory defects. For example, the *odr-3*^(xs) strain has appropriately extended AWC cilia and major defects in AWC-mediated olfaction, whereas the *odr-3*^(S47C) strain has very severe AWC cilium defects and milder AWC olfactory defects. Moreover, the AWC neurons of *odr-3* null mutants have severe defects in cilium morphology, but the AWA neurons are at most mildly affected, and the ASH neurons appear morphologically normal. Yet, *odr-3* null mutants are more defective in AWA and ASH behaviors than they are in AWC behaviors (Bargmann et al., 1993). The AWA cilia of *che-2* mutants are far more distorted than those of *odr-3* mutants (Lewis and Hodgkin, 1977), but *che-2* mutants are only

UNIVERSITY OF CALIFORNIA LIBRARY

mildly defective in chemotaxis to diacetyl, whereas *odr-3* mutants are severely defective (Bargmann et al., 1993). This result suggests that ODR-3 is directly involved in diacetyl detection, perhaps through interaction with the diacetyl receptor ODR-10.

Chemosensory G α Proteins Have Distinct but Partly Overlapping Functions

Unlike vertebrate olfactory neurons, individual *C. elegans* olfactory neurons express several odorant receptors and integrate information about multiple odorants (Bargmann et al., 1993; Troemel et al., 1995; Sengupta et al., 1996); our studies with *odr-3* indicate that individual sensory neurons can also utilize more than one G α protein. The AWC neurons detect both benzaldehyde and butanone, and *odr-3* mutants are severely defective in benzaldehyde chemotaxis but only mildly defective for butanone chemotaxis, whereas animals doubly mutant for *odr-3* and the similar protein *gpa-2* are severely defective in butanone chemotaxis. *gpa-2* and *gpa-3* have been previously implicated in developmental responses to the *C. elegans* dauer pheromone (Zwaal et al., 1997).

Despite the sequence similarity between *odr-3* and the *gpa* proteins, *gpa-2* is unable to substitute for most functions of *odr-3* in the AWC neurons where both are expressed, and *gpa-3* cannot substitute for *odr-3* in the avoidance function of the ASH neurons. Conversely, activated *gpa-3(Q205L)* mutations affect the ability of the ASH neurons to take up the dye DiO but do not cause ASH sensory defects (Zwaal et al., 1997), whereas *odr-3(Q206L)* mutations affect ASH sensory function but not ASH dye filling. This difference between *odr-3* and *gpa-3* implies that they interact with different effectors in ASH; one intriguing possibility is that *gpa-3* has a role in ASH cilium morphology that is analogous to the role of *odr-3* in AWC cilium morphology.

Responses to high concentrations of some odorants persist in *odr-3* null mutants (Bargmann et al., 1993) and even in *gpa-2 odr-3* double mutants (data not shown). Likewise, a residual olfactory response persists in G α knockout mice (Belluscio et al., 1998 [this issue of *Neuron*]). Similar observations were made in studies of the effects of gustducin mutations on mouse taste: gustducin-deficient mice have a 10- to 100-fold decrease in their sensitivity to sweet or bitter taste, depending on the assay, but they respond well to high concentrations of tastants (Wong et al., 1996). The residual response in gustducin mutants might be due to transducin, which is expressed in taste buds at lower levels (Ruiz-Avila et al., 1995). Unlike photoreceptors, which link rhodopsin to a single G α protein, chemosensory neurons may be able to deploy families of G α proteins during transduction. This distinction may arise from the fundamental differences between visual and olfactory reception. In the visual system, a few closely related opsin genes are responsible for all responses to light. By contrast, different chemosensory neurons contain widely divergent receptor proteins. There are at least three independent families comprising hundreds of vertebrate chemosensory receptor genes (Buck and Axel, 1991; Dulac and Axel, 1995; Herrada and Dulac, 1997; Matsunami and Buck, 1997; Ryba and Tirindelli, 1997) and at least

four independent families comprising hundreds of *C. elegans* chemosensory receptor genes (Troemel et al., 1995; Sengupta et al., 1996). G protein diversity may follow naturally from the receptor diversity involved in chemoreception.

Experimental Procedures

Strains

Wild-type animals were *C. elegans* variety Bristol, strain N2. Nematodes were grown at 20°C with plentiful food using standard methods (Brenner, 1974).

Strains used in this work included MT3644 *odr-3(n1605) V*, CX2818 *lin-15(n765ts) X*, CX2695 *odr-3(n2150) V lin-15(n765) X*, GS357 *unc-42(e270) arDf1 V/nT1 (n754) IV*, BW163 *ctDf1 V/nT1 (n754) IV*, MT5817 *nDf42 V/nT1 (n754) IV*, CX2369 *dpy-11(e224) odr-3(n2150) V*, GS352 *rol-4(sc63) arP3 arP1 unc-76(e911) V*, NL334 *gpa-2(pk16) V*, and DA869 *rol-4(sc8) lin-25(n545) him-5(e1467) unc-76(e911) V*.

Genetic Mapping and Cloning of *odr-3*

odr-3 had previously been mapped to the interval between *sqt-3* and *unc-61* on linkage group V (Bargmann et al., 1993). Subsequent mapping experiments localized the *odr-3* gene between the polymorphism *arP3* and the gene *eat-6*, as summarized below. The genetic deficiency *arDf1* complemented the *odr-3(n2150)* defects in osmotic avoidance and chemotaxis to benzaldehyde, indicating that it does not delete the *odr-3* gene. Since the *eat-6* locus is uncovered by *arDf1*, *odr-3* is to the right of *eat-6*. *arP3* is a Tc1-associated polymorphism, which is not deleted by *arDf1* (Tuck and Greenwald, 1995). *odr-3(n2150)* animals were mated with *rol-4(sc63) arP3 arP1 unc-76(e911) V* hermaphrodites. Nine out of 35 Rol non-Unc recombinants had lost the *arP3* polymorphism, and seven out of nine of these recombinants segregated *odr-3(n2150)*. This analysis placed *odr-3* to the left of *arP3*.

Overlapping cosmids from this region of the genome were introduced into *odr-3(n2150)* animals, and the resulting transgenic strains were tested for the ability to avoid areas of high osmotic strength (4 M fructose). Two overlapping cosmids, C34D1 and C34A12, were able to rescue the osmotic-avoidance defect of *odr-3(n2150)* mutants. Subclones from the region shared by both cosmids were injected to define the region containing the rescuing activity. A 7 kb EcoRV subclone (pODR3-1) rescued the osmotic-avoidance phenotype and was also sufficient to rescue the ability of *odr-3(n2150)* animals to respond to all odorants and to avoid octanol.

A 9 kb EcoRI-SphI fragment from the rescuing region was used to screen $\sim 1 \times 10^6$ plaques of a mixed stage *C. elegans* cDNA library. Three positive clones were isolated (Figure 2). Two cDNAs encoded proteins that were fully contained in a subclone that failed to rescue the *odr-3* mutant phenotype. The remaining clone encoded a partial cDNA with a high degree of homology to α subunits of heterotrimeric G proteins (G α). Reverse transcription-PCR experiments with *C. elegans* splice leader sequences SL1 and SL2 indicated that the G α message was trans-spliced to SL1 at its extreme 5' end, so the SL1 splice leader was used as a 5' primer in RT-PCR reactions to isolate a full-length cDNA clone from mixed-stage wild-type animals. The coding sequence of the G α was fully contained in the rescuing EcoRV subclone and was partially or entirely deleted from all subclones that failed to rescue, indicating that the G α coding region corresponded to the *odr-3* gene.

Behavioral Assays

Chemotaxis assays were performed on a round assay plate with a point source of attractant at one end and a control spot of diluent at the opposite end (Bargmann et al., 1993). The chemotaxis index was calculated as [(animals at attractant) - (animals in control area)] / (total number of animals).

Osmotic avoidance assays were performed as described (Culotti and Russell, 1978). Animals were placed within a high osmotic strength ring of 4 M fructose and counted after 10 min. The osmotic avoidance index was calculated as the fraction of worms still in the ring at the end of the assay.

LIBRARY
UNIVERSITY OF CALIFORNIA
SAN DIEGO

Volatile avoidance assays and nose-touch assays were performed as described (Kaplan and Horvitz, 1993; Troemel et al., 1995).

Germline Transformation

Germline transformations were performed using standard microinjection methods (Mello et al., 1991). All transformations were performed in strains containing *lin-15(n765)* with or without *odr-3* mutations. Coinjection mixes consisted of *lin-15* DNA pJM23 (50 ng/ μ l) and experimental DNA at various concentrations (5–100 ng/ml). Transgenic animals were identified by rescue of the multivulva phenotype of *lin-15(n765)* animals at 20°C. Independent lines were established from single rescued F1 animals. Transgenes were integrated using γ rays (Mello et al., 1991) or trimethylpsoralen treatment followed by UV irradiation (A. Santoso and C. I. B., unpublished data).

Molecular Biology Methods

General manipulations were performed using standard protocols (Sambrook et al., 1989). Genomic DNA from the mutant alleles was amplified by PCR, and purified PCR products were sequenced directly. Sequencing was performed with the *fmoI* sequencing kit (Promega) and an MJR thermal cycler. The Geneworks software package (Intelligenetics) was used in sequence analysis. BLAST (Altschul et al., 1990), CLUSTAL W (Thompson et al., 1994), and PHYLP (Felsenstein, 1996) packages were used to perform sequence comparisons and construct phylogenetic trees. Sequence of the *odr-3* region was confirmed with data courtesy of the *C. elegans* genome sequencing consortium, who identified this region as predicted gene C34D1.3 (Sulston et al., 1992). PCR reactions were performed using the following buffer: 50 mM KCl, 1.5 mM MgCl₂, 10 mM Tris-HCl (pH 8.3), and 0.01% gelatin. Primers used in sequencing and PCR are available upon request.

Antibody Staining

Antigen Preparation

A GST fusion was made to the last 106 amino acids of the *odr-3* coding region and injected into rabbits. Polyclonal sera were affinity-purified by binding to 6HIS-tagged full-length ODR-3 protein coupled to Affigel-15 resin (Biorad) and eluted with 3.5 M MgCl₂.

Staining

Animals were spread onto 0.1% polylysine-coated slides, heated on a 100°C block for 20 s, frozen on dry ice, and fixed by incubation in methanol (–20°C) for 5 min followed by incubation in acetone (–20°C) for 5 min. Samples were blocked in blocking solution (1× phosphate-buffered saline (PBS), 1% BSA (Sigma), 0.1% Tween-20) for 1 hr at room temperature, incubated with a 1:50 dilution of affinity-purified antibody overnight at 4°C, washed with PBS, incubated with a 1:500 dilution of Cy3 goat anti-rabbit IgG (Jackson Immunochemicals) at room temperature for 1 hr, and washed with PBS. DAPI (1 μ g/ml) was included to stain nucleic acids in the samples. All larval stages and adults showed comparable staining.

Generation and Analysis of *odr-3* Expression Constructs

pODR3::GFP-1

A 2.7 kb HindIII fragment of *pRV-1* was excised and ligated into the HindIII site of pTU#62 (Chalfie et al., 1994).

pODR-3::GFP-2

A fragment from the EcoRV site to the ATG of *odr-3* was amplified from *pODR3-1* and ligated into the SmaI site of pPD95.77 (A. Fire, S. Xu, N. Ahnn, and G. Seydoux, personal communication).

All cells expressing the *pODR-3::GFP-2* promoter fusion were identified in two independent integrated lines bearing the transgene. AWC had the strongest and most reliable expression (25 of 25 animals were GFP-positive), followed by AWB (22 of 25), AWA (8 of 25), ADF (6 of 25), and ASH (5 of 25). The GFP expression was always brightest in AWC, less bright in AWB, and faint in the other three cells, suggesting that AWA, ADF, and ASH express GFP at near the detection threshold. All larval stages and adults showed comparable expression. To ask whether other sequences in the *odr-3* introns or upstream region affect expression, we stained animals that overexpressed the 7 kb rescuing *odr-3* genomic clone with an anti-ODR-3 antibody. In the overexpressing lines, ODR-3 protein was in the cell bodies as well as the cilia, providing more

information than was available with the highly localized endogenous ODR-3 protein. All animals showed a cluster of five cells consistent with the cells named above (rigorous cell identification was not always possible in fixed animals). The five sensory neurons had approximately equal staining intensities. Some animals also showed weak staining of another cell, probably the interneuron AIN.

Generation and Analysis of *odr-3* Mutants

The *odr-3(S47C)* and the *odr-3(Q206L)* mutants were generated in *odr-3* subclones using specific PCR primers to create the mutations, sequenced, and reintroduced into the genomic *pODR3-1* clone. Clones were injected into *odr-3(+)* animals at either 10 ng/ml or 100 ng/ml, and into *odr-3(n1605)* animals at 10 ng/ml, using the *lin-15* cotransformation marker.

Microscopy

Images in Figure 6 were acquired with a scientific grade cooled CCD camera on a multiwavelength wide-field three-dimensional microscopy system (Hiraoka et al., 1991) in which the shutters, filters, and XYZ stage are all computer-driven. Samples were imaged using a 60× 1.4 NA lens (Olympus) and $n = 1.1518$ immersion oil. Three-dimensional data stacks of GFP-expressing samples were acquired in the FITC channel by moving the stage in successive 0.25 μ m focal planes through the sample, and out-of-focus light was removed with a constrained iterative deconvolution algorithm (Agard et al., 1989). Maximum intensity projections of the three-dimensional data stacks were generated using IVE software (Chen et al., 1996).

Other images were acquired by conventional fluorescence microscopy using a Zeiss Axioplan II microscope and a 40× Plan Achromat objective.

Acknowledgments

We are grateful to Orion Weiner and John Sedat for their guidance in deconvolution microscopy. We thank Henry Boume, Ira Herskowitz, Richard Axel, Sue Kirch, Jen Zallen, and Emily Troemel for discussion and comments on the manuscript; Heman Espinoza, Andrew Shiau, and Ramon Tabtiang for advice, reagents, and valuable discussions; Jim Thomas for the *odr-3(n1605)* strain; Simon Tuck and Iva Greenwald for the *arp3* strain; Bob Barstead for the cDNA library; Emily Troemel for the STR-2::GFP fusion gene; Andy Fire for the GFP vector; and the *Caenorhabditis* Genetic Center for some strains used in this work. This work was supported by the Howard Hughes Medical Institute. K. R., J. G. C., and A. S. are Predoctoral Fellows of the Howard Hughes Medical Institute, and C. I. B. is an Assistant Investigator of the Howard Hughes Medical Institute.

Received October 28, 1997; revised December 2, 1997.

References

- Agard, D.A., Hiraoka, Y., Shaw, P., and Sedat, J.W. (1989). Fluorescence microscopy in three dimensions. *Methods Cell Biol.* 30, 353–377.
- Altschul, S.F., Gish, W., Miller, W., Myers, E.W., and Lipman, D.J. (1990). Basic local alignment search tool. *J. Mol. Biol.* 215, 403–410.
- Barber, V.C. (1974). Cilia in sense organs. In *Cilia and Flagella*, M.A. Sleight, ed. (London: Academic Press), pp. 403–433.
- Bargmann, C.I., and Mori, I. (1997). Chemotaxis and thermotaxis. In *C. elegans II*, T.B.D.L. Riddle, B.J. Meyer, J.R. Priess, eds. (Cold Spring Harbor, NY: Cold Spring Harbor Laboratory Press), pp. 717–737.
- Bargmann, C.I., Hartwig, E., and Horvitz, H.R. (1993). Odorant-selective genes and neurons mediate olfaction in *C. elegans*. *Cell* 74, 515–527.
- Belluscio, L., Gold, G.H., Nemes, A., and Axel, R. (1998). Mice deficient in G_{α} are anosmic. *Neuron* 20, this issue, 69–81.
- Berghard, A., and Buck, L.B. (1996). Sensory transduction in vomeronasal neurons: evidence for $G_{\alpha o}$, $G_{\alpha i2}$, and adenylyl cyclase II as major components of a pheromone signaling cascade. *J. Neurosci.* 16, 909–918.

- Brenner, S. (1974). The genetics of *Caenorhabditis elegans*. *Genetics* **77**, 71–94.
- Brundage, L., Avery, L., Katz, A., Kim, U.-J., Mendel, J., Sternberg, P., and Simon, M. (1996). Mutations in a *C. elegans* G_{α} gene disrupt movement, egg laying, and viability. *Neuron* **16**, 999–1009.
- Buck, L., and Axel, R. (1991). A novel multigene family may encode odorant receptors: a molecular basis for odor recognition. *Cell* **65**, 175–187.
- Caterina, M.J., Schumacher, M.A., Tominaga, M., Rosen, T.A., Levine, J.D., and Julius, D. (1997). The capsaicin receptor: a heat-activated ion channel in the pain pathway. *Nature* **389**, 816–824.
- Chalfie, M., Tu, Y., Euskirchen, G., Ward, W.W., and Prasher, D.C. (1994). Green fluorescent protein as a marker for gene expression. *Science* **263**, 802–805.
- Chang, G.Q., Hao, Y., and Wong, F. (1993). Apoptosis: final common pathway of photoreceptor death in rd, rds, and rhodopsin mutant mice. *Neuron* **11**, 595–605.
- Chen, H., Hughes, D.D., Chan, T.A., Sedat, J.W., and Agard, D.A. (1996). IVE (Image Visualization Environment): a software platform for all three-dimensional microscopy applications. *J. Struct. Biol.* **116**, 56–60.
- Coburn, C.M., and Bargmann, C.I. (1996). A putative cyclic nucleotide-gated channel is required for sensory development and function in *C. elegans*. *Neuron* **17**, 695–706.
- Colbert, H.A., Smith, T.L., and Bargmann, C.I. (1997). OSM-9, a novel protein with structural similarity to channels, is required for olfaction, mechanosensation, and olfactory adaptation in *C. elegans*. *J. Neurosci.* **17**, 8259–8269.
- Conklin, B.R., and Bourne, H.R. (1993). Structural elements of G_{α} subunits that interact with $G\beta\gamma$, receptors, and effectors. *Cell* **73**, 631–641.
- Culotti, J.G., and Russell, R.L. (1978). Osmotic avoidance defective mutants of the nematode *Caenorhabditis elegans*. *Genetics* **90**, 243–256.
- Dulac, C., and Axel, R. (1995). A novel family of genes encoding putative pheromone receptors in mammals. *Cell* **83**, 195–206.
- Felsenstein, J. (1996). Inferring phylogenies from protein sequences by parsimony, distance, and likelihood methods. *Methods Enzymol.* **266**, 418–427.
- Firestein, S., Zufall, F., and Shepherd, G.M. (1991). Single odor-sensitive channels in olfactory receptor neurons are also gated by cyclic nucleotides. *J. Neurosci.* **11**, 3565–3572.
- Halpern, M., Shapiro, L.S., and Jia, C. (1995). Differential localization of G proteins in the opossum vomeronasal system. *Brain Res.* **677**, 157–161.
- Herrada, G., and Dulac, C. (1997). A novel family of putative pheromone receptors in mammals with a topographically organized and sexually dimorphic distribution. *Cell* **90**, 763–773.
- Hiraoka, Y., Swedlow, J.R., Paddy, M.R., Agard, D.A., and Sedat, J.W. (1991). Three-dimensional multiple-wavelength fluorescence microscopy for the structural analysis of biological phenomena. *Semin. Cell Biol.* **2**, 153–165.
- Jones, D.T., and Reed, R.R. (1989). G_{α} : an olfactory neuron specific-G protein involved in odorant signal transduction. *Science* **244**, 790–795.
- Kaplan, J., and Horvitz, H. (1993). A dual mechanosensory and chemosensory neuron in *Caenorhabditis elegans*. *Proc. Natl. Acad. Sci. USA* **90**, 2227–2231.
- Klotz, K.N., and Jesaitis, A.J. (1994). Neutrophil chemoattractant receptors and the membrane skeleton. *Bioessays* **16**, 193–198.
- Komatsu, H., Mori, I., Rhee, J.-S., Akaike, N., and Ohshima, Y. (1996). Mutations in a cyclic nucleotide-gated channel lead to abnormal thermosensation and chemosensation in *C. elegans*. *Neuron* **17**, 707–718.
- Korswagen, H.C., Park, J.H., Ohshima, Y., and Plasterk, R.H. (1997). An activating mutation in a *Caenorhabditis elegans* G_{α} protein induces neural degeneration. *Genes Dev.* **11**, 1493–1503.
- Lewis, J.A., and Hodgkin, J.A. (1977). Specific neuroanatomical changes in chemosensory mutants of the nematode *Caenorhabditis elegans*. *J. Comp. Neurol.* **172**, 489–510.
- Lochrie, M.A., Mendel, J.E., Sternberg, P.W., and Simon, M.I. (1991). Homologous and unique G protein α subunits in the nematode *Caenorhabditis elegans*. *Cell Reg.* **2**, 135–154.
- Matsunami, H., and Buck, L.B. (1997). A multigene family encoding a diverse array of putative pheromone receptors in mammals. *Cell* **90**, 775–784.
- Mello, C.C., Kramer, J.M., Stinchcomb, D., and Ambros, V. (1991). Efficient gene transfer in *C. elegans*: extrachromosomal maintenance and integration of transforming sequences. *EMBO J.* **10**, 3959–3970.
- Mendel, J., Korswagen, H., Liu, K., Hadju-Cronin, Y., Simon, M., Plasterk, R., and Sternberg, P. (1995). Participation of the protein G_{α} in multiple aspects of behavior in *C. elegans*. *Science* **267**, 1652–1655.
- Pace, U., Hanski, E., Salomon, Y., and Lancet, D. (1985). Odorant-sensitive adenylate cyclase may mediate olfactory reception. *Nature* **316**, 255–258.
- Parent, C.A., and Devreotes, P.N. (1996). Molecular genetics of signal transduction in Dictyostelium. *Annu. Rev. Biochem.* **65**, 411–440.
- Perkins, L.A., Hedgecock, E.M., Thomson, J.N., and Culotti, J.G. (1986). Mutant sensory cilia in the nematode *Caenorhabditis elegans*. *Dev. Biol.* **117**, 456–487.
- Ranganathan, R., Mallick, D.M., and Zuker, C.S. (1995). Signal transduction in *Drosophila* photoreceptors. *Annu. Rev. Neurosci.* **18**, 283–317.
- Rens-Domiano, S., and Hamm, H.E. (1995). Structural and functional relationships of heterotrimeric G-proteins. *FASEB J.* **9**, 1059–1066.
- Ruiz-Avila, L., McLaughlin, S.K., Wildman, D., McKinnon, P.J., Robichon, A., Spickofsky, N., and Margolskee, R.F. (1995). Coupling of bitter receptor to phosphodiesterase through transduction in taste receptor cells. *Nature* **376**, 80–85.
- Ryba, N.J.P., and Tirindelli, R. (1997). A new multigene family of putative pheromone receptors. *Neuron* **19**, 371–379.
- Sambrook, J., Fritsch, E.F., and Maniatis, T. (1989). *Molecular Cloning: A Laboratory Manual*. (Cold Spring Harbor, NY: Cold Spring Harbor Press).
- Segalat, L., Elkes, D., and Kaplan, J. (1995). G_{α} modulation of serotonin-controlled behaviors in *C. elegans*. *Science* **267**, 1648–1651.
- Sengupta, P., Chou, J.C., and Bargmann, C.I. (1996). *odr-10* encodes a seven transmembrane domain olfactory receptor required for responses to the odorant diacetyl. *Cell* **84**, 899–909.
- Slepak, V.Z., Quick, M.W., Aragay, A.M., Davidson, N., Lester, H.A., and Simon, M.I. (1993). Random mutagenesis of G protein α subunit $G(\alpha)$. Mutations altering nucleotide binding. *J. Biol. Chem.* **268**, 21889–21894.
- Slepak, V.Z., Katz, A., and Simon, M.I. (1995). Functional analysis of a dominant negative mutant of G α i2. *J. Biol. Chem.* **270**, 4037–4041.
- Starich, T.A., Herman, R.K., Kari, C.K., Yeh, W.H., Schackwitz, W.S., Schuyler, M.W., Collet, J., Thomas, J.H., and Riddle, D.L. (1995). Mutations affecting the chemosensory neurons of *Caenorhabditis elegans*. *Genetics* **139**, 171–188.
- Sullivan, L.S., and Daiger, S.P. (1996). Inherited retinal degeneration: exceptional genetic and clinical heterogeneity. *Molec. Med. Today* **2**, 380–386.
- Sulston, J., Du, Z., Thomas, K., Wilson, R., Hillier, L., Staden, R., Halloran, N., Green, P., Thierry-Mieg, J., Qiu, L., et al. (1992). The *C. elegans* genome sequencing project: a beginning. *Nature* **356**, 37–41.
- Talluri, S., Bhatt, A., and Smith, D.P. (1995). Identification of a *Drosophila* G protein alpha subunit (dGq alpha-3) expressed in chemosensory cells and central neurons. *Proc. Natl. Acad. Sci. USA* **92**, 11475–11479.
- Tamar, H. (1992). *Principles of Sensory Physiology* (Springfield, IL: Charles C. Thomas).
- Thompson, J.D., Higgins, D.G., and Gibson, T.J. (1994). CLUSTAL W: improving the sensitivity of progressive multiple sequence alignment through sequence weighting, position-specific gap penalties and weight matrix choice. *Nucleic Acids Res.* **22**, 4673–4680.
- Troemel, E.R., Chou, J.H., Dwyer, N.D., Colbert, H.A., and Bargmann,

- C.I. (1995). Divergent seven transmembrane receptors are candidate chemosensory receptors in *C. elegans*. *Cell* **83**, 207–218.
- Troemel, E.R., Kimmel, B.E., and Bargmann, C.I. (1997). Reprogramming chemotaxis responses: sensory neurons define olfactory preferences in *C. elegans*. *Cell* **91**, 161–169.
- Tsunoda, S., Sierralta, J., Sun, Y., Bodner, R., Suzuki, E., Becker, A., Socolich, M., and Zuker, C.S. (1997). A multivalent PDZ-domain protein assembles signaling complexes in a G-protein-coupled cascade. *Nature* **388**, 243–249.
- Tuck, S., and Greenwald, I. (1995). *lin-25*, a gene required for vulval induction in *Caenorhabditis elegans*. *Genes Dev.* **9**, 341–357.
- Ward, S., Thomson, N., White, J.G., and Brenner, S. (1975). Electron microscopical reconstruction of the anterior sensory anatomy of the nematode *Caenorhabditis elegans*. *J. Comp. Neurol.* **160**, 313–337.
- Ware, R.W., Clark, D., Crossland, K., and Russell, R.L. (1975). The nerve ring of the nematode *Caenorhabditis elegans*: sensory input and motor output. *J. Comp. Neurol.* **162**, 71–110.
- Wedegaertner, P.B., Wilson, P.T., and Bourne, H.R. (1995). Lipid modifications of trimeric G proteins. *J. Biol. Chem.* **270**, 503–506.
- Wong, G.T., Gannon, K.S., and Margolskee, R.F. (1996). Transduction of bitter and sweet taste by gustducin. *Nature* **381**, 796–800.
- Woodard, C., Alcorta, E., and Carlson, J. (1992). The *rdgB* gene of *Drosophila*: a link between vision and olfaction. *J. Neurogenet.* **8**, 17–31.
- Zhang, Y., Chou, J.H., Bradley, J., Bargmann, C.I., and Zinn, K. (1997). The *C. elegans* 7-transmembrane protein ODR-10 functions as an odorant receptor in mammalian cells. *Proc. Natl. Acad. Sci. USA* **94**, 12162–12167.
- Zwaal, R., Ahringer, J., van Leunen, H., Rushforth, A., Anderson, P., and Plasterk, R. (1996). G proteins are required for spatial orientation of early cell cleavages in *C. elegans* embryos. *Cell* **84**, 619–629.
- Zwaal, R.R., Mendel, J.E., Sternberg, P.W., and Plasterk, R.H.A. (1997). Two neuronal G proteins are involved in chemosensation of the *Caenorhabditis elegans* dauer-inducing pheromone. *Genetics* **145**, 715–727.

Chapter 3

Isolation of mutations that disrupt presynaptic vesicle clustering or trafficking in *C. elegans*

Summary

At synapses, presynaptic clusters of vesicles containing neurotransmitter localize adjacent to postsynaptic clusters of neurotransmitter receptors. Synaptic vesicles are generated in a series of steps that include transport along microtubules, endocytosis from the plasma membrane, and budding from the endosome. Clusters of mature vesicles target to synaptic sites where they associate with the actin cytoskeleton and a protein-rich thickening of the membrane known as the active zone. A screen for mutants with altered patterns of SNB-1::GFP-labelled vesicle clusters in the ASI chemosensory neurons identified 57 mutations. Vesicle or SNB-1::GFP trafficking defects were seen in *unc-104*, *unc-11*, *unc-51*, and *ky349* mutants, whereas vesicle clusters were disorganized in *sad-1*, *sad-2*, and *sad-3* mutants. In *sad-4(dm)* mutants axon and vesicle cluster morphologies were severely affected. *sad-1* and *sad-2* share many phenotypes and SAD-1 overexpression can rescue the synapse defects of *sad-2* animals, suggesting that *sad-2* is upstream of SAD-1 signaling. Additionally, *eat-7* mutants were found to have vesicle clusters that were less discrete. These mutants describe a pathway by which synaptic vesicles are generated, clustered, organized, and maintained at presynaptic sites within axons.

Introduction

Efficient neurotransmission requires that presynaptic vesicles containing neurotransmitter are concentrated in close proximity to sites of postsynaptic neurotransmitter receptors. At presynaptic terminals of most neurons vesicles are either docked at the plasma membrane and primed for calcium-dependent fusion or stored in clusters associated with the underlying actin cytoskeleton. Molecules important for exocytosis and its regulation by calcium signaling are localized to presynaptic active zones or associated with synaptic vesicles. The generation of clustered synaptic vesicles involves transport along microtubule tracks, maturation in endosomal compartments, aggregation into tight clusters, and targeting to synaptic regions. Vesicle clusters are maintained at the synapse

through cycles of exocytosis, endocytosis, and sometimes re-maturation in endosomal compartments. The activity-dependent regulation of the number and fusion competence of clustered synaptic vesicles may underlie presynaptic forms of facilitation and depression.

The signals that coordinate presynaptic vesicle clusters and active zones with postsynaptic receptors are best-characterized at the mammalian neuromuscular junction (NMJ) (reviewed in Sanes and Lichtman, 1999). During neuronal development, motor axons are precisely guided to the muscles they will innervate. Upon the axon's arrival at a target muscle, signals from the muscle to the neuron induce cytoskeletal changes in the axonal growth cone, the presynaptic clustering of neurotransmitter-filled vesicles, and the concentration of exocytotic machinery at the active zone. Mice deficient in agrin or MuSK have defects in muscle differentiation, and they also have presynaptic defects in vesicle aggregation and axon termination, suggesting that the muscle sends a retrograde signal to the neuron to induce presynaptic differentiation (DeChiara et al., 1996; Gautam et al., 1996). One candidate for a retrograde signal is laminin β 2, a component of the synaptic basal lamina. Laminin β 2 inhibits neurite outgrowth of cultured neurons (Porter et al., 1995), and in mice lacking laminin β 2 presynaptic differentiation is defective (Noakes et al., 1995). In the central nervous system (CNS) the secreted protein Wnt7A causes axonal remodeling and the accumulation of synapsin at presynaptic sites; in *Wnt7A* mutants the presynaptic differentiation of mossy fiber to granule cell synapses is delayed (Hall et al., 2000). The signaling pathways that act downstream of laminin β 2 and Wnt7A in this process are undefined.

Several presynaptic proteins may serve as either regulators or targets of the signals for presynaptic differentiation. Synapsin is a lipid-binding protein that associates with synaptic vesicles (Hosaka et al., 1999). Overexpression of synapsin I in *Xenopus* increased the number of clustered vesicles (Valtorta et al., 1995) and the frequency and amplitude of spontaneous synaptic currents (Lu et al., 1992). These effects were seen at the onset of synaptogenesis, suggesting a developmental role for synapsin in vesicle clustering. A mouse synapsin I/synapsin II double knockout has a 50% reduction in the number of clustered

synaptic vesicles (Rosahl et al., 1995). However, this defect could be explained by a role for synapsin in vesicle cluster maintenance. In *C. elegans*, the liprin protein SYD-2 controls the size of presynaptic structures; in *syd-2* mutant animals active zones and vesicle clustering regions were expanded (Zhen and Jin, 1999). As a vertebrate liprin interacts with tyrosine phosphatase receptors (Serra-Pages et al., 1995), tyrosine kinase signaling may be important for controlling the extent or shape of vesicle clusters.

The connectivity of the nematode *C. elegans* has been completely described in serial section electron micrographs and consists of 302 neurons that make about 7000 synapses (White et al., 1986), compared to 10^{12} neurons and 10^{15} synapses for humans. Thus, *C. elegans* is a genetically tractable system for studying presynaptic differentiation in neuron to neuron synapses. In order to identify new regulators of presynaptic vesicle clustering and trafficking in the CNS we have conducted direct visual screens in *C. elegans*. In this chapter we describe the identification of mutants that affect multiple steps in the generation of presynaptic vesicle clusters in the ASI chemosensory neurons. Mutations in *unc-104*, *unc-11*, *unc-51*, and *ky349* affect the trafficking and biogenesis of synaptic vesicles, and mutations in *sad-1*, *sad-2*, *sad-3*, and *eat-7* disrupt the organization of vesicle clusters. Additionally, we present evidence that *sad-2* is an upstream regulator of the SAD-1 kinase described in more detail in Chapter 4.

Results

Visualization of presynaptic vesicle clusters in chemosensory neurons

In order to visualize presynaptic vesicle clusters of neuron to neuron synapses in living animals, we expressed a fusion protein between the vesicle associated membrane protein synaptobrevin and green fluorescent protein (SNB-1::GFP) under the control of promoters specific for chemosensory neurons. SNB-1::GFP has been shown to be an accurate marker for presynaptic vesicle clusters in *C. elegans* (Nonet, 1999). SNB-1::GFP was expressed in either the ASI, AWC, ADL, or ASK neurons using the *str-3*, *str-2*, *sre-1*, or *sra-9* promoters. However, only SNB-1::GFP in the ASI neurons labeled vesicle clusters that were consistent

and discrete. The ASI neurons are a bilaterally symmetric pair of chemosensory neurons that control entry into an alternate developmental form, the dauer larvae, in response to environmental signals (Bargmann and Horvitz, 1991). Each ASI neuron has a dendrite that projects to the amphid pore and ends in a slender cilium, and an axon that enters the nerve ring and makes about 7-9 synapses onto an array of interneurons and other chemosensory neurons (White et al., 1986). In each ASI neuron of animals carrying an integrated array of p_{str-3} SNB-1::GFP, GFP fluorescence was visible in 7-9 evenly spaced clusters along the region of the axon that fasciculates with the nerve ring (Figures 1A, 2A). In addition, GFP fluorescence was visible in the cell body, and weaker fluorescence was occasionally observed in the dendrite in a diffuse pattern. The number of clusters observed per ASI neuron corresponds well with the number of ASI presynaptic specializations observed in electron microscopic reconstructions (White et al., 1986)

A screen for mutants that alter the pattern of SNB-1::GFP fluorescence

Using p_{str-3} SNB-1::GFP as a marker for ASI synapses we conducted a direct screen for mutants with abnormal patterns of GFP fluorescence. Hermaphrodites carrying p_{str-3} SNB-1::GFP were mutagenized with EMS, and their F2 progeny were enriched for an inability to chemotaxis to the odorant benzaldehyde and examined for defects in the pattern of fluorescence (see Experimental Procedures). We isolated 57 mutations that altered the pattern of SNB-1::GFP expression. We placed 24 recessive mutations that altered SNB-1::GFP expression but not axon outgrowth into 6 complementation groups: *unc-104*, *unc-11*, *unc-51*, and three new genes that we named *sad-1*, *sad-2*, and *sad-3* for synapses of the amphid defective. In addition, we isolated 9 weaker recessive mutations and one dominant mutation, *sad-4(dm)*, that specifically disrupted the SNB-1::GFP pattern, 21 recessive mutations that had defects in axon outgrowth, and a new complementation group, *ppd-1* for *p*orpoise *h*ead-1, defined by two mutations that disrupt head morphology (Table 1).

LIBRARY
UNIVERSITY OF CALIFORNIA
SAN DIEGO

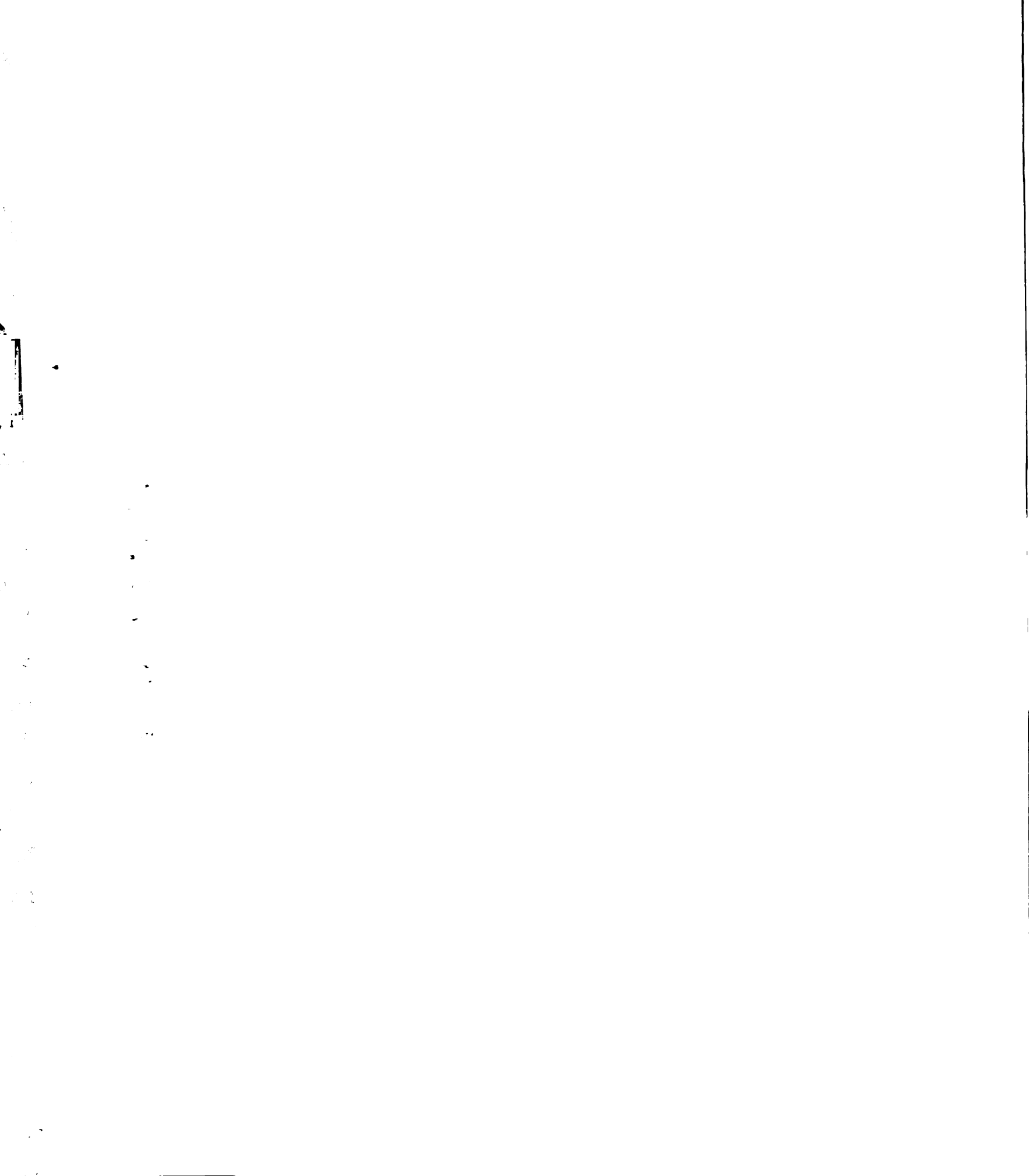
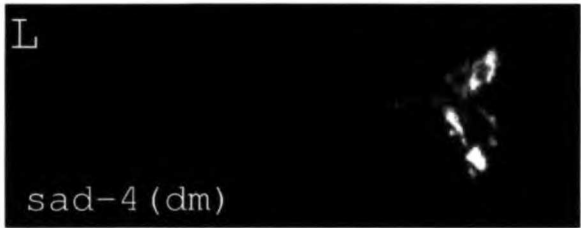
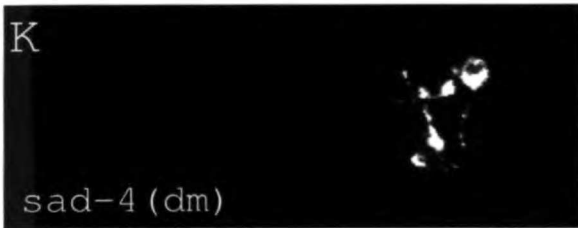
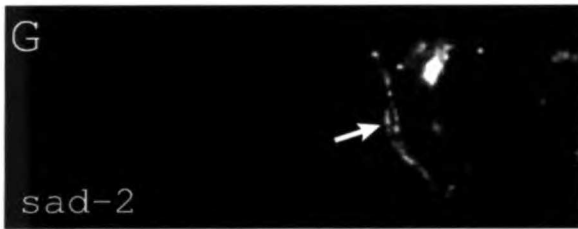
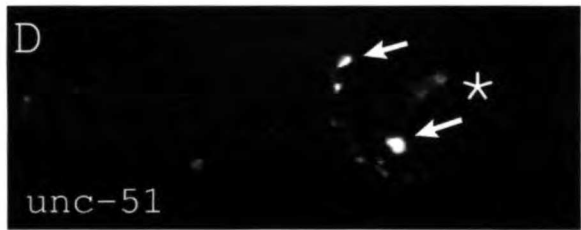
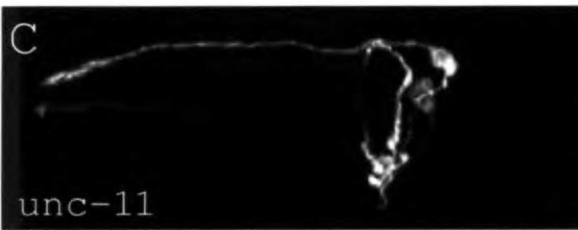
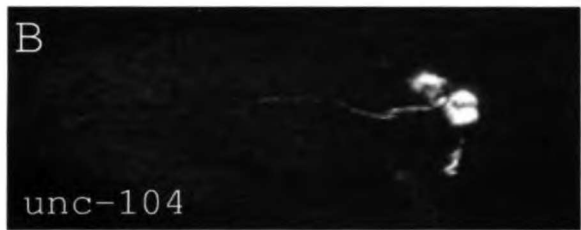
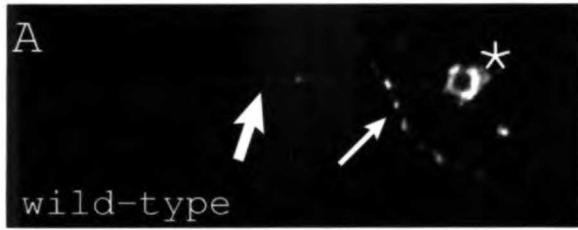


Table 1. Complete Summary of SNB-1::GFP screen

Mutant	# of Alleles		Phenotype	
			SNB-1::GFP	Movement
I. Vesicle Trafficking				
<i>unc-104</i>	4	<i>ky287, ky317, ky319, ky290(weak)</i>	only in cell body	paralyzed
<i>unc-11</i>	3	<i>ky280, ky291, ky325</i>	diffuse in axon and dendrite	coiler
<i>unc-51</i>	6	<i>ky286, ky321, ky322, ky323, ky324, ky347(weak)</i>	in large varicosities	paralyzed
<i>ky349</i>	1	<i>ky349</i>	overly vesicular in cell body; normal clusters in axon	
II. Vesicle Cluster Morphology				
<i>sad-1</i>	6	<i>ky281, ky289, ky326, ky330, ky332, ky344</i>	disorganized clusters	subtle unc
<i>sad-2</i>	3	<i>ky292, ky329, ky335</i>	disorganized clusters	mild unc
<i>sad-3/rpm-1</i>	2	<i>ky340, ky346</i>	disorganized clusters	mild unc
<i>sad-4(dm)</i>	1	<i>ky334</i>	very disorganized clusters; aberrant axon morphology	mild paralysis
unclassified	8	<i>ky285, ky293, ky295, ky328, ky333, ky336, ky337, ky343</i>	weakly disorganized clusters	subtle unc but varies
III. Axon Outgrowth				
unclassified	21	<i>ky283, ky284, ky294, ky296, ky297, ky298, ky299, ky300, ky301, ky303, ky304, ky305, ky306, ky307, ky327, ky338, ky348, ky350, ky351, ky354, ky356</i>	mainly premature termination but varies	varies
IV. Head Morphology				
<i>ppd-1</i>	2	<i>ky282, ky357</i>	cell body and axon shifted in position in adult; head drawn out to a point, looks like a "porpoise-head"	

UNIVERSITY OF CALIFORNIA LIBRARY

Figure 1. p_{str-3} SNB-1::GFP Phenotypes of *unc-104*, *unc-11*, *unc-51*, and *sad* Mutants
Confocal epifluorescence micrographs of p_{str-3} SNB-1::GFP expression in wild-type (A), *unc-104(ky319)* (B), *unc-11(ky291)* (C), *unc-51(ky321)* (D), *sad-1(ky281)* (E), *sad-1(ky330)* (F), *sad-2(ky292)* (G,H), *sad-2(ky335)* (I), *sad-3(ky346)* (J), and *sad-4(ky334dm)* (K,L) animals. Anterior is left, dorsal is up. Each ASI neuron sends a dendrite to the tip of the nose, where it ends in a cilium, and an axon into the nerve ring. In (A) the thick arrow denotes the dendrite, the thin arrow the axon, and the asterisk the cell body. In wild-type animals SNB-1::GFP clusters were regularly spaced along the ASI axon (A). In *unc-104* animals SNB-1::GFP fluorescence was concentrated in the cell body and absent from the axon (B). In *unc-11* animals SNB-1::GFP was diffusely distributed throughout the neuron (C). SNB-1::GFP accumulated in axon varicosities (arrows) and was often faint in the cell body (asterisk) in *unc-51* animals (D). In *sad-1*, *sad-2*, and *sad-3* mutants SNB-1::GFP clusters were absent in regions of the axon (E), spatially disorganized (F), more diffusely localized (G-I), or irregular in size (H-J). The arrow in (G) denotes a secondary branch emanating from the primary axon. In (C,E,F,H,J) axons from both ASI neurons can be seen, whereas in (A,D,G,I,K,L) only one axon can be seen.



1
2
3
4
5
6
7
8
9
10
11
12
13
14
15
16
17
18
19
20
21
22
23
24
25
26
27
28
29
30
31
32
33
34
35
36
37
38
39
40
41
42
43
44
45
46
47
48
49
50
51
52
53
54
55
56
57
58
59
60
61
62
63
64
65
66
67
68
69
70
71
72
73
74
75
76
77
78
79
80
81
82
83
84
85
86
87
88
89
90
91
92
93
94
95
96
97
98
99
100

Vesicle or SNB-1::GFP trafficking is disrupted in *unc-104*, *unc-11*, *unc-51*, and *ky349* mutants

unc-104, *unc-11*, and *unc-51* mutants have severe locomotion defects and likely affect early stages of vesicle trafficking and biogenesis. Previous analysis had shown that in *unc-104(e1265)* mutants SNB-1::GFP localized to the cell body and was absent from axons. *unc-104* encodes a kinesin required for the transport of synaptic vesicles (Otsuka et al., 1991). Similar to *unc-104(e1265)*, the new *unc-104* mutants had SNB-1::GFP depleted from the axon and enriched in the cell body (Figure 1B). Whereas the alleles *ky287*, *ky317*, and *ky319* were similar in severity to *e1265*, the allele *ky290* had SNB-1::GFP and locomotion defects that were less pronounced. In *unc-11* animals GFP fluorescence was diffusely localized throughout the plasma membrane of the neuron (Figure 1C). *unc-11* is an AP180 protein implicated in synaptic vesicle endocytosis that is essential for SNB-1 localization to vesicles (Nonet et al., 1999). In *unc-51* animals GFP fluorescence accumulated in one or two large varicosities in the axon, usually at the end of the axon and/or close to the cell body (Figure 1D). In addition, there was often less fluorescence in the cell body. *unc-51* encodes a protein kinase that affects axon outgrowth and guidance and may alter trafficking of membrane vesicles in neurons (Ogura et al., 1994). In the ASI neurons, *unc-51* affects synaptic vesicle clusters but not axon guidance. *unc-14* and *unc-51* interact genetically, and their protein products interact biochemically (Ogura et al., 1997); *unc-14* animals had qualitatively similar but much weaker SNB-1::GFP phenotypes than *unc-51* animals (data not shown). In *ky349* animals vesicle clusters were normal but SNB-1::GFP was concentrated in several large varicosities in the cell body (data not shown). *ky349* may affect the membrane trafficking of SNB-1 through the endoplasmic reticulum and Golgi such that some SNB-1 accumulates in intermediate compartments. *ky349* was mapped to the X chromosome.

Vesicle clusters are disorganized in *sad-1*, *sad-2*, and *sad-3* mutants

1
2
3
4
5
6
7
8
9
10
11
12
13
14
15
16
17
18
19
20
21
22
23
24
25
26
27
28
29
30
31
32
33
34
35
36
37
38
39
40
41
42
43
44
45
46
47
48
49
50
51
52
53
54
55
56
57
58
59
60
61
62
63
64
65
66
67
68
69
70
71
72
73
74
75
76
77
78
79
80
81
82
83
84
85
86
87
88
89
90
91
92
93
94
95
96
97
98
99
100

Whereas mutations in *unc-104*, *unc-11*, *unc-51*, and *ky349* seem to affect the trafficking of vesicles and/or SNB-1, mutations in *sad-1*, *sad-2*, and *sad-3* affect the organization of SNB-1::GFP clusters. We isolated six alleles of *sad-1*, three alleles (*ky281*, *ky289*, and *ky344*) of *sad-2*, and two alleles of *sad-3* (*ky340* and *ky346*). *sad-1* is discussed in detail in Chapter 4. *sad-1* and *sad-2* displayed indistinguishable and highly penetrant SNB-1::GFP phenotypes; all alleles were equally severe and not temperature sensitive. However, the nature of the SNB-1::GFP defect in the ASI neurons was variable from animal to animal. In some animals regions of the axon appeared to lack vesicle clusters (Figure 1E), whereas in other animals regions of the axon had densely packed vesicle clusters (Figure 1F). In other animals regions of the axon displayed more diffuse SNB-1::GFP fluorescence (Figures 1G,I), or vesicle clusters were irregular in size (Figures 1H,I). The phenotypes of many animals could be interpreted as a combination of these defects.

The p_{str-3} SNB-1::GFP defects in *sad-3* mutants were qualitatively similar to those of *sad-1* and *sad-2* but less penetrant and harder to score (Figure 1J). In collaboration with Mei Zhen and Yishi Jin we showed that *sad-3* is allelic with *rpm-1*. Both alleles of *sad-3* fail to complement *rpm-1* and a missense mutation in *rpm-1* was found in *sad-3(ky346)* (M.Z. and Y.J., personal communication; Zhen et al., 2000). *rpm-1* mutants have defects in the organization of the presynaptic vesicle clusters of the GABAergic VD and DD motor neurons (Zhen et al., 2000). In contrast, in *sad-1* and *sad-2(ky292)* mutants SNB-1::GFP clusters appeared more diffuse and weaker than normal (Chapter 4 and M.Z. and Y.J., personal communication). Interestingly, whereas *sad-1* and *sad-2* mutants displayed a stronger and more easily scored SNB-1::GFP phenotype than *sad-3/rpm-1* in ASI neurons, *sad-3/rpm-1* mutants displayed a stronger phenotype than *sad-1* and *sad-2* in the VD and DD motor neurons. This difference is observed even in putative null mutants of *sad-1* and *rpm-1*. Other differences between the mutants can also be observed; for example, whereas *rpm-1* mutants often have several active zones associated with a single vesicle cluster in VD and DD motor neurons, this phenotype is not observed in *sad-1* mutants (Zhen et al., 2000 and Chapter 4). We conclude that *sad-1* and *sad-2* are more central to sensory neuron synapses,

1
 2
 3
 4
 5
 6
 7
 8
 9
 10
 11
 12
 13
 14
 15
 16
 17
 18
 19
 20
 21
 22
 23
 24
 25
 26
 27
 28
 29
 30
 31
 32
 33
 34
 35
 36
 37
 38
 39
 40
 41
 42
 43
 44
 45
 46
 47
 48
 49
 50
 51
 52
 53
 54
 55
 56
 57
 58
 59
 60
 61
 62
 63
 64
 65
 66
 67
 68
 69
 70
 71
 72
 73
 74
 75
 76
 77
 78
 79
 80
 81
 82
 83
 84
 85
 86
 87
 88
 89
 90
 91
 92
 93
 94
 95
 96
 97
 98
 99
 100

whereas *sad-3/rpm-1* is more central to GABAergic synapses, though all genes act in several cell types.

Vesicle clusters and sensory axon morphology are abnormal in *sad-4(dm)* mutants

SNB-1::GFP localization, sensory axon morphology, and locomotion were more severely affected in the dominant *sad-4(dm)* mutant than in the other *sad* mutants. In *sad-4(dm)* animals SNB-1::GFP was highly disorganized and accumulated in large clumps (Figures 1K,L). This phenotype differed from that of *unc-51* animals in that SNB-1::GFP was distributed throughout the axon and was not decreased in the cell body. ASI axons of *sad-4(dm)* animals followed a shorter trajectory into the nerve ring than wild-type axons and had multiple varicosities. In some animals we observed minor axon outgrowth defects. *sad-4(dm)* mutants were very lethargic and moved poorly, suggesting that multiple neurons are affected in these animals. The SNB-1::GFP clustering defects are probably not a simple consequence of axon abnormalities, as SNB-1::GFP clusters are still relatively normal in other mutants that affect axon outgrowth (see Chapter 4). It is unclear whether *sad-4(dm)* disrupts vesicle biogenesis or clustering, though if it affects biogenesis it would have to do so at a step of vesicle maturation different from the step affected in *unc-51* animals. No attempts were made to map *sad-4(dm)*.

***sad-2* mutants are mildly uncoordinated, have extra axon outgrowth, and retain ASI function**

In contrast to *unc-104*, *unc-11*, and *unc-51* animals, which display severe uncoordination, *sad-2* animals are only mildly uncoordinated. *sad-2* mutants are more uncoordinated than *sad-1* mutants; animals move in reverse more than normal, weakly coil, and are lethargic. In *sad-2* animals the ASI cell bodies migrated to their correct locations and their primary axons assumed their normal position and morphology in the nerve ring. However, as in *sad-1* animals, sensory axons sometimes made ectopic branches in the nerve ring (Figure 1G)

1
2
3
4
5
6
7
8
9
10
11
12
13
14
15
16
17
18
19
20
21
22
23
24
25
26
27
28
29
30
31
32
33
34
35
36
37
38
39
40
41
42
43
44
45
46
47
48
49
50
51
52
53
54
55
56
57
58
59
60
61
62
63
64
65
66
67
68
69
70
71
72
73
74
75
76
77
78
79
80
81
82
83
84
85
86
87
88
89
90
91
92
93
94
95
96
97
98
99
100

and failed to terminate at their normal position. In particular, the axons of AWC chemosensory neurons failed to terminate in 14% of *sad-2* animals (n=106) (data not shown). To test whether the ASI neurons were functional in *sad-2* mutants we analyzed *unc-31; sad-2* double mutants. Ablation of the ASI neurons in an *unc-31* background causes animals to constitutively enter the alternative dauer larval form even in the presence of food (Avery et al., 1993). *unc-31; sad-2* animals formed virtually no dauer larvae in the presence of food, suggesting that in *sad-2* animals the ASI neurons are present and able to function (data not shown).

***sad-2* maps near *sad-1* on LGX**

In attempts to positionally clone *sad-2* we mapped *sad-2(ky292)* by following the ASI SNB-1::GFP phenotype. *sad-2* mapped to the X chromosome between the Tc1 polymorphisms stP72 and stP2 and to the right of *dpy-6*. *sad-2* was not covered by the deficiencies mnDf1, mnDf20, mnDf43, or mnDf10. Inconclusive data put *sad-2* to the left of and very near *unc-9*, though this should be repeated. *sad-1* is located near but to the right of *unc-9*. One candidate for *sad-2* was an AMPK β subunit corresponding to open reading frame F55F3.1 (*sad-1* encodes a kinase with homology to an AMPK α subunit). However, sequencing of all predicted exons and exon/intron boundaries of F55F3.1 revealed no mutations in *sad-2(ky292)* animals.

Overexpression of SAD-1 in *sad-2* mutants rescued synapse defects but caused synthetic axon defects

sad-2 maps to a region near *sad-1*, and the two mutants share many phenotypes. Even though *sad-2* and *sad-1* complement each other, we reasoned that *sad-2* and *sad-1* might represent different classes of alleles of the same gene. For example, different classes of alleles within the *unc-84* locus can complement each other (Malone et al., 1999). To test the possibility that *sad-2* and *sad-1* are allelic, we overexpressed SAD-1 in *sad-2* at levels that fully rescued the SNB-1::GFP defects of *sad-1* animals. When overexpressed at higher levels in wild-

1948

1949

type animals SAD-1 causes ectopic vesicle clusters, sensory axon defects, and paralysis (described in more detail in Chapter 4). However, at the levels used for rescue overexpressed SAD-1 caused no axon or locomotion defects in rescued *sad-1* animals. By contrast, when SAD-1 was expressed at the same levels in a *sad-2* background, we observed paralysis and ASI axon outgrowth and guidance defects in 45% of animals (n=49) (data not shown). Additionally, in 65% of animals in which axons were normal SNB-1::GFP clusters were more well-defined and organized than clusters in *sad-2* animals not overexpressing SAD-1. These results show that SAD-1 can rescue the synapse defects of *sad-2* animals while synthetically causing axon defects and paralysis in *sad-2* animals. To see if there were molecular lesions in the *sad-1* locus, we sequenced all exons and exon/intron boundaries in *sad-2(ky292)* animals but found no mutations. Though it is possible that *sad-2(ky292)* is mutated in *sad-1* regulatory sequences, we conclude that *sad-2* is not an allele of *sad-1* and is rather most likely an upstream regulator of SAD-1 activity. The identification of the gene mutated in *sad-2* animals will ultimately differentiate between these two possibilities.

Vesicle clusters were less discrete in *eat-7(ad450)* mutants

In the course of looking for candidate downstream targets of the SAD-1 kinase (see Chapter 4), we became interested in the *C. elegans* synapsin homolog. Synapsin has been proposed to cluster vesicles during synapse development (Lu et al., 1992), and its affinity for synaptic vesicles is regulated by PKA phosphorylation (Hosaka et al., 1999). We envisioned that one function of SAD-1 could be to regulate vesicle cluster size by the phosphorylation-dependent control of synapsin activity. The semidominant mutant *eat-7(ad450)* has been mapped to an interval that contains the synapsin gene. *eat-7(ad450)* was identified in a screen for mutants that feed poorly (Avery, 1993). *eat-7(ad450)* animals have been described as narcoleptic because they spontaneously enter into states in which locomotion, defecation, and pharyngeal pumping cease; animals resume normal functions when disturbed by the observer. In synapsin I/synapsin II knockout mice neurons are unable to sustain action potentials upon repeated stimulation (Rosahl et al., 1995). We hypothesized that the narcoleptic

WILSON LIBRARY

10
11
12
13
14
15
16
17
18
19
20
21
22
23
24
25
26
27
28
29
30
31
32
33
34
35
36
37
38
39
40
41
42
43
44
45
46
47
48
49
50
51
52
53
54
55
56
57
58
59
60
61
62
63
64
65
66
67
68
69
70
71
72
73
74
75
76
77
78
79
80
81
82
83
84
85
86
87
88
89
90
91
92
93
94
95
96
97
98
99
100

Figure 2. In *eat-7(ad450)* Animals Vesicle Clusters are Less Discrete

Confocal epifluorescence micrographs of p_{str-3} SNB-1::GFP expression in wild-type (A) and *eat-7(ad450)* (B-D) animals. Anterior is left, dorsal is up. In wild-type animals vesicles formed discrete clusters along the axon (A). In *eat-7(ad450)* animals SNB-1::GFP clusters were wider and not well-separated from each other.

1
2
3
4
5
6
7
8
9
10
11
12
13
14
15
16
17
18
19
20
21
22
23
24
25
26
27
28
29
30
31
32
33
34
35
36
37
38
39
40
41
42
43
44
45
46
47
48
49
50
51
52
53
54
55
56
57
58
59
60
61
62
63
64
65
66
67
68
69
70
71
72
73
74
75
76
77
78
79
80
81
82
83
84
85
86
87
88
89
90
91
92
93
94
95
96
97
98
99
100



4
11
12
13
14
15
16
17
18
19
20
21
22
23
24
25
26
27
28
29
30
31
32
33
34
35
36
37
38
39
40
41
42
43
44
45
46
47
48
49
50
51
52
53
54
55
56
57
58
59
60
61
62
63
64
65
66
67
68
69
70
71
72
73
74
75
76
77
78
79
80
81
82
83
84
85
86
87
88
89
90
91
92
93
94
95
96
97
98
99
100
101
102
103
104
105
106
107
108
109
110
111
112
113
114
115
116
117
118
119
120
121
122
123
124
125
126
127
128
129
130
131
132
133
134
135
136
137
138
139
140
141
142
143
144
145
146
147
148
149
150
151
152
153
154
155
156
157
158
159
160
161
162
163
164
165
166
167
168
169
170
171
172
173
174
175
176
177
178
179
180
181
182
183
184
185
186
187
188
189
190
191
192
193
194
195
196
197
198
199
200
201
202
203
204
205
206
207
208
209
210
211
212
213
214
215
216
217
218
219
220
221
222
223
224
225
226
227
228
229
230
231
232
233
234
235
236
237
238
239
240
241
242
243
244
245
246
247
248
249
250
251
252
253
254
255
256
257
258
259
260
261
262
263
264
265
266
267
268
269
270
271
272
273
274
275
276
277
278
279
280
281
282
283
284
285
286
287
288
289
290
291
292
293
294
295
296
297
298
299
300
301
302
303
304
305
306
307
308
309
310
311
312
313
314
315
316
317
318
319
320
321
322
323
324
325
326
327
328
329
330
331
332
333
334
335
336
337
338
339
340
341
342
343
344
345
346
347
348
349
350
351
352
353
354
355
356
357
358
359
360
361
362
363
364
365
366
367
368
369
370
371
372
373
374
375
376
377
378
379
380
381
382
383
384
385
386
387
388
389
390
391
392
393
394
395
396
397
398
399
400
401
402
403
404
405
406
407
408
409
410
411
412
413
414
415
416
417
418
419
420
421
422
423
424
425
426
427
428
429
430
431
432
433
434
435
436
437
438
439
440
441
442
443
444
445
446
447
448
449
450
451
452
453
454
455
456
457
458
459
460
461
462
463
464
465
466
467
468
469
470
471
472
473
474
475
476
477
478
479
480
481
482
483
484
485
486
487
488
489
490
491
492
493
494
495
496
497
498
499
500
501
502
503
504
505
506
507
508
509
510
511
512
513
514
515
516
517
518
519
520
521
522
523
524
525
526
527
528
529
530
531
532
533
534
535
536
537
538
539
540
541
542
543
544
545
546
547
548
549
550
551
552
553
554
555
556
557
558
559
560
561
562
563
564
565
566
567
568
569
570
571
572
573
574
575
576
577
578
579
580
581
582
583
584
585
586
587
588
589
590
591
592
593
594
595
596
597
598
599
600
601
602
603
604
605
606
607
608
609
610
611
612
613
614
615
616
617
618
619
620
621
622
623
624
625
626
627
628
629
630
631
632
633
634
635
636
637
638
639
640
641
642
643
644
645
646
647
648
649
650
651
652
653
654
655
656
657
658
659
660
661
662
663
664
665
666
667
668
669
670
671
672
673
674
675
676
677
678
679
680
681
682
683
684
685
686
687
688
689
690
691
692
693
694
695
696
697
698
699
700
701
702
703
704
705
706
707
708
709
710
711
712
713
714
715
716
717
718
719
720
721
722
723
724
725
726
727
728
729
730
731
732
733
734
735
736
737
738
739
740
741
742
743
744
745
746
747
748
749
750
751
752
753
754
755
756
757
758
759
760
761
762
763
764
765
766
767
768
769
770
771
772
773
774
775
776
777
778
779
780
781
782
783
784
785
786
787
788
789
790
791
792
793
794
795
796
797
798
799
800
801
802
803
804
805
806
807
808
809
810
811
812
813
814
815
816
817
818
819
820
821
822
823
824
825
826
827
828
829
830
831
832
833
834
835
836
837
838
839
840
841
842
843
844
845
846
847
848
849
850
851
852
853
854
855
856
857
858
859
860
861
862
863
864
865
866
867
868
869
870
871
872
873
874
875
876
877
878
879
880
881
882
883
884
885
886
887
888
889
890
891
892
893
894
895
896
897
898
899
900
901
902
903
904
905
906
907
908
909
910
911
912
913
914
915
916
917
918
919
920
921
922
923
924
925
926
927
928
929
930
931
932
933
934
935
936
937
938
939
940
941
942
943
944
945
946
947
948
949
950
951
952
953
954
955
956
957
958
959
960
961
962
963
964
965
966
967
968
969
970
971
972
973
974
975
976
977
978
979
980
981
982
983
984
985
986
987
988
989
990
991
992
993
994
995
996
997
998
999
1000

phenotype of *eat-7(ad450)* animals was the behavioral correlate of the neuronal phenotype seen in synapsin I/synapsin II knockout mice. We observed that ASI SNB-1::GFP clusters in *eat-7(ad450)* animals were less discrete than in wild-type animals (Figures 2B-D). In addition, there was more SNB-1::GFP in the dendrite than normal, and in occasional *eat-7(ad450)* animals SNB-1::GFP was enriched at the base of the cilia. Whereas in *unc-11* mutants SNB-1::GFP was equally and uniformly distributed throughout the plasma membrane of both dendrites and axons (Figure 1C), in *eat-7(ad450)* mutants SNB-1::GFP was not uniformly distributed and was still enriched in the axon. In addition, the SNB-1::GFP defects of *eat-7(ad450)* animals were very similar to those of *syd-2* animals in ASI (data not shown). Vesicle clusters have been shown by electron microscopy to be expanded in size in *syd-2* mutants (Zhen and Jin, 1999). These results suggest that *eat-7(ad450)* affects vesicle clustering or cluster size and not SNB-1 endocytosis.

As vesicle clustering is also disrupted in synapsin I/synapsin II knockout mice (Rosahl et al., 1995), *eat-7* appeared to be a good candidate for a synapsin mutant. To test this, we sequenced exons 1-3 of the synapsin gene from the *eat-7(ad450)* mutant but found no mutations. For technical reasons we did not sequence exons 4 and 5 (see Experimental Procedures). As *eat-7(ad450)* is semidominant and the gene is not covered by cosmids (only a YAC), we did not attempt transformation rescue of *eat-7(ad450)* mutants. Thus, we do not know if the *eat-7* defects are caused by mutations in synapsin.

Discussion

Mutations that describe a synaptic vesicle pathway from biogenesis in the cell body to mature clusters at the synapse (Figure 3)

Step 1: *ky349*, trafficking of synaptic vesicle proteins through the secretory pathway?

One of the first steps in synaptic vesicle biogenesis is the transcytosis and maturation of future synaptic vesicle resident proteins, such as SNB-1, through

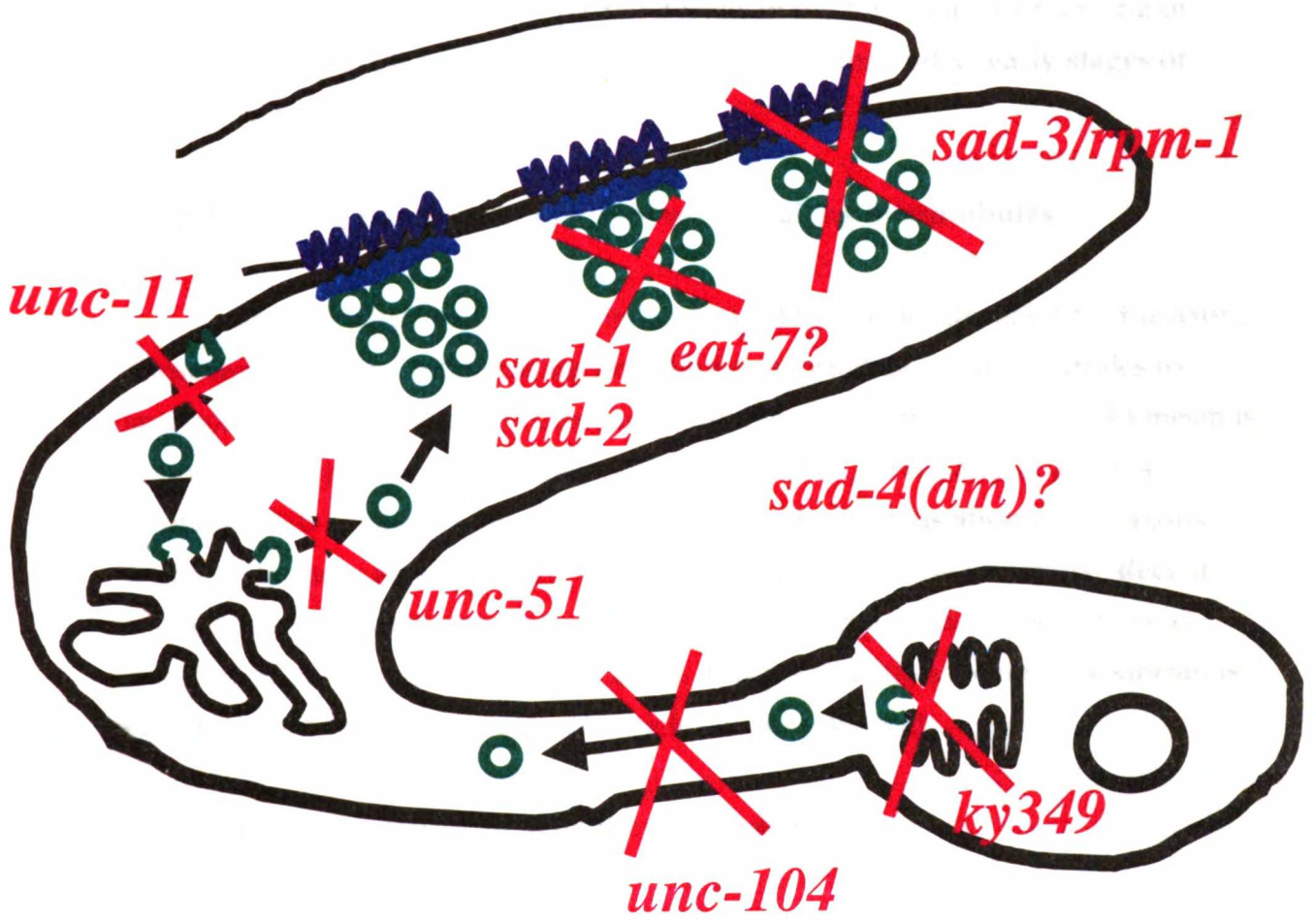
1940
1941
1942
1943
1944
1945
1946
1947
1948
1949
1950

1951
1952
1953
1954
1955
1956
1957
1958
1959
1960

Figure 3. Mutations That Define a Pathway from Vesicle Biogenesis to Mature Synaptic Vesicle Clusters

This model describes the lifecycle of synaptic vesicles. In this model *ky349* is (partially) required for the trafficking of vesicles or SNB-1 in the Golgi, *unc-104* for vesicle transport, *unc-51* for the budding of vesicles from the endosome, and *unc-11* for the incorporation of SNB-1 into endocytosing vesicles. At the synapse *sad-1* and *sad-2* may control the targeting and clustering of vesicles, *eat-7* the clustering of vesicles, and *sad-3/rpm-1* the organization of packets of vesicle clusters and active zones. It is unclear what step is affected in *sad-4(dm)* animals.

11
12
13
14
15
16
17
18
19
20
21
22
23
24
25
26
27
28
29
30
31
32
33
34
35
36
37
38
39
40
41
42
43
44
45
46
47
48
49
50
51
52
53
54
55
56
57
58
59
60
61
62
63
64
65
66
67
68
69
70
71
72
73
74
75
76
77
78
79
80
81
82
83
84
85
86
87
88
89
90
91
92
93
94
95
96
97
98
99
100



THE
LAW
OF
THE
STATE
OF
NEW
YORK
IN
RELATION
TO
THE
PRACTICE
OF
THE
PROFESSION
OF
THE
LAW

BY
JAMES
C. HAY
OF
NEW YORK
ATTORNEY AT LAW

the endoplasmic reticulum (ER) and Golgi. From the Golgi, synaptic vesicle proteins are sorted to immature vesicles that will take them to the axon for further maturation. In *ky349* mutants synaptic vesicle clusters still formed, suggesting that later steps of vesicle transport, biogenesis, and targeting were normal; but instead of being evenly distributed, SNB-1::GFP accumulated in several large varicosities in the cell body. The SNB-1::GFP varicosities could correspond to Golgi, lysosomes, or some other membrane compartment. We speculate that *ky349* may have partial defects in the trafficking or budding of vesicles from the ER or Golgi. Alternatively, *ky349* may affect early stages of SNB-1 trafficking or maturation.

Step 2: *unc-104*, transport of synaptic vesicles along microtubules

Once synaptic vesicle proteins are sorted to vesicles destined for the axon, these immature synaptic vesicles must be transported along microtubules to internal regions of the axon. Previous work has shown that the *unc-104* kinesin is required for synaptic vesicle transport (Otsuka et al., 1991), and in *unc-104* mutants SNB-1::GFP accumulated in the cell body and was absent from axons. These data show an early requirement for *unc-104* in vesicle transport. Recent work has shown that mature synaptic vesicles are transported to synapses as preformed clusters (Ahmari et al., 2000). It is possible that the *unc-104* kinesin is also required for this later step of vesicle cluster transport.

Step 3: *unc-11*, recycling of synaptic vesicle proteins

When immature synaptic vesicles arrive in the axon, they fuse with the plasma membrane and their transmembrane components such as SNB-1 are incorporated into the plasma membrane. A similar event occurs when calcium triggers a mature synaptic vesicle to fuse with the plasma membrane and release neurotransmitter. To maintain synaptic vesicle number, vesicles must be regenerated by endocytosis. This process involves the reincorporation of synaptic vesicle resident proteins into budding vesicles. The *unc-11* AP180 protein binds SNB-1 and is required for its recruitment to budding synaptic

1. The first part of the document discusses the importance of maintaining accurate records for all financial transactions. This includes recording all income, expenses, and assets in a timely and accurate manner. Proper record-keeping is essential for tax compliance and for providing accurate information to financial institutions.

2. The second part of the document focuses on the importance of budgeting and financial planning. By creating a realistic budget, individuals can better manage their finances, avoid debt, and achieve their long-term financial goals. Financial planning also helps to anticipate future needs and adjust accordingly.

vesicles (Nonet et al., 1999). As expected, in *unc-11* mutants SNB-1::GFP became diffusely distributed throughout the plasma membrane of the axon and dendrite. This shows that the targeting of SNB-1 to the axon is mediated solely by its association with synaptic vesicles.

Step 4: *unc-51*, budding of mature synaptic vesicles from endosomes

After endocytosis regenerates synaptic vesicles with most of their resident proteins, the majority of vesicles must pass through an endosomal intermediate to fully mature. We observed that SNB-1::GFP accumulated in one or two axonal varicosities in *unc-51* mutants. These varicosities may correspond to endosomes. *unc-51* is similar to the Apg1p kinase that acts at an early step in yeast autophagy, a process that involves membrane trafficking and the engulfment of cytoplasm (Matsuura et al., 1997). By analogy to the yeast phenotype, *unc-51* may be involved in the budding of synaptic vesicles from endosomes or other internal membrane compartments.

Step 5: *sad-1* and *sad-2*, recruitment of vesicle clusters to synapses (and inhibition of axon outgrowth)

During synaptogenesis synaptic vesicles can cluster independent of the postsynaptic target (Prokop et al., 1996) and seem to be transported as vesicle clusters to synaptic sites (Ahmari et al., 2000). Postsynaptic signals likely serve to recruit presynaptic structures to the developing synapse and to stop axons from further growing (Gautam et al., 1996; DeChiara et al., 1996). In both *sad-1* and *sad-2* mutants vesicle clusters were disorganized, suggesting a defect in the targeting of clusters to synaptic sites, and axons failed to properly terminate. The phenotypic similarities between *sad-1* and *sad-2* animals suggest that *sad-1* and *sad-2* are components of a common pathway; this pathway may be downstream of the postsynaptic signal that organizes presynaptic vesicle clusters and inhibits further axon outgrowth. SAD-1 overexpression can rescue the vesicle clustering defects of *sad-2* animals. In addition, overexpression of mild levels of SAD-1 caused synthetic axon defects in a *sad-2* background. One model

Figure 4. Genetic Model for *sad-1* and *sad-2* Interaction

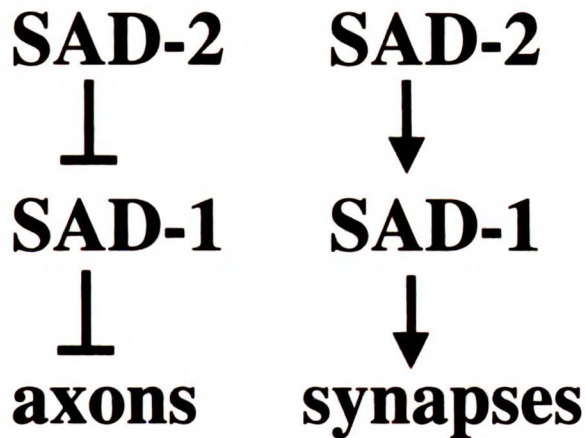
This model attempts to explain the complicated effects of SAD-1 overexpression on *sad-2* mutant animals. (A-D) illustrates model predictions for N2 (A), *sad-2* (B), SAD-1 overexpression (C), and *sad-2* + SAD-1 overexpression (D) animals. See text of the Discussion for details of the model.

1
2
3
4
5
6
7
8
9
10
11
12
13
14
15
16
17
18
19
20
21
22
23
24
25
26
27
28
29
30
31
32
33
34
35
36
37
38
39
40
41
42
43
44
45
46
47
48
49
50
51
52
53
54
55
56
57
58
59
60
61
62
63
64
65
66
67
68
69
70
71
72
73
74
75
76
77
78
79
80
81
82
83
84
85
86
87
88
89
90
91
92
93
94
95
96
97
98
99
100

101
102
103
104
105
106
107
108
109
110
111
112
113
114
115
116
117
118
119
120
121
122
123
124
125
126
127
128
129
130
131
132
133
134
135
136
137
138
139
140
141
142
143
144
145
146
147
148
149
150
151
152
153
154
155
156
157
158
159
160
161
162
163
164
165
166
167
168
169
170
171
172
173
174
175
176
177
178
179
180
181
182
183
184
185
186
187
188
189
190
191
192
193
194
195
196
197
198
199
200

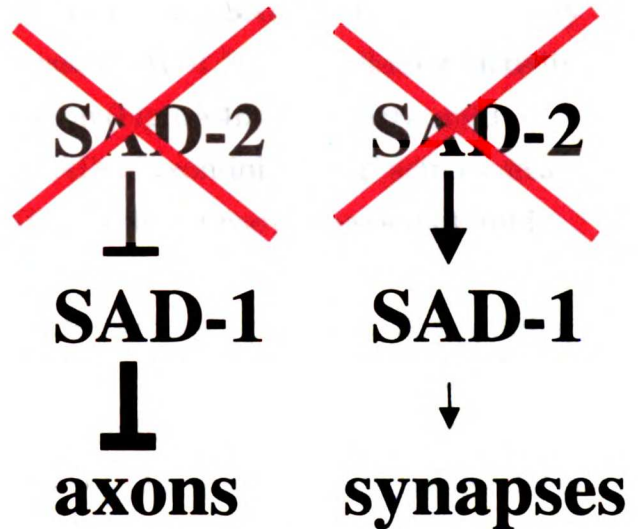
201
202
203
204
205
206
207
208
209
210
211
212
213
214
215
216
217
218
219
220
221
222
223
224
225
226
227
228
229
230
231
232
233
234
235
236
237
238
239
240
241
242
243
244
245
246
247
248
249
250
251
252
253
254
255
256
257
258
259
260
261
262
263
264
265
266
267
268
269
270
271
272
273
274
275
276
277
278
279
280
281
282
283
284
285
286
287
288
289
290
291
292
293
294
295
296
297
298
299
300

A



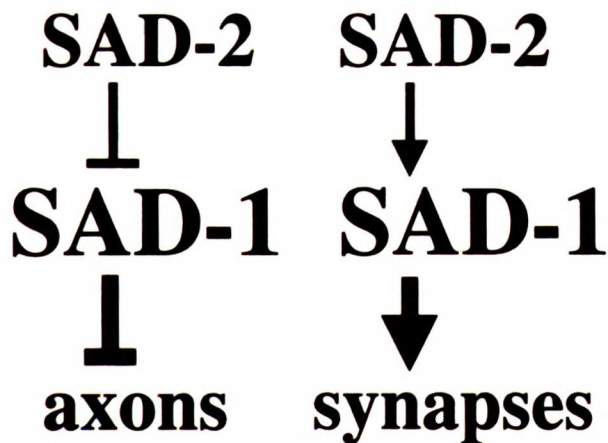
N2

B



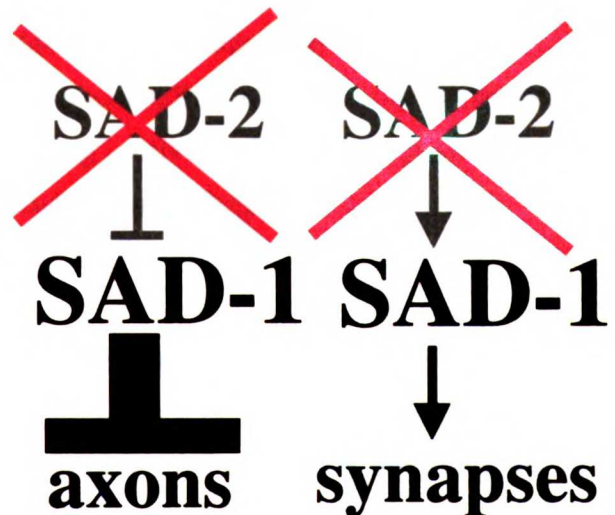
sad-2

C



mild OE(SAD-1)

D



**mild OE(SAD-1)
in *sad-2* mutant**

THE
UNITED
STATES
DEPARTMENT
OF
AGRICULTURE
WASHINGTON, D. C.
20250

OFFICE OF
FOREST SERVICE

REPORT OF
FOREST
INVESTIGATION
NO. 255
BY
R. B. WOODWARD
AND
R. M. WOODWARD
WATER RESOURCES
DIVISION
WASHINGTON, D. C.

to explain these results is that *sad-2* is an upstream activator of SAD-1 for synapse formation and an upstream inhibitor of SAD-1 for axon termination (Figure 4A). In a *sad-2* mutant there may not be enough SAD-1 "synapse" activity to promote synapse formation, yet the increased SAD-1 "axon-inhibiting" activity may not be sufficient to cause axon termination (Figure 4B). Similarly, mild overexpression of SAD-1 may not increase SAD-1 "axon-inhibiting" activity to a level sufficient to cause axon termination (Figure 4C). Overexpression of mild levels of SAD-1 would overcome the SAD-1 "synapse" activation barrier caused by loss of *sad-2*, thus rescuing the synapse defects in *sad-2* mutants. The additive effects of overexpressing SAD-1 and losing *sad-2* inhibition of SAD-1 "axon-inhibiting" activity would cause SAD-1 "axon-inhibiting" activity to reach levels sufficient to inhibit axon outgrowth (Figure 4D). One question with this model is why *sad-2* mutants do not have termination defects, as SAD-1 "axon-inhibiting" activity should be increased in *sad-2* mutants. One explanation may be that there are synaptic factors that depend on *sad-2* for activity and work in parallel with SAD-1 to inhibit axon outgrowth. Indeed, mutations in *sad-3/rpm-1* also cause defects in axon termination (Schaeffer et al., 2000). *sad-2* could have opposite effects on the two SAD-1 functions by regulating the localization of SAD-1 protein to synapses. When not localized to synapses, SAD-1 may have decreased "synapse" activity but increased "axon inhibiting" activity. The recent generation of anti-SAD-1 antibodies and SAD-1::GFP fusions (see Chapter 4) allows this model to be tested directly.

Step 6: *sad-3/rpm-1*, organization of presynaptic specializations

Presynaptic specializations are regularly spaced throughout the axon. In *sad-3* mutants SNB-1::GFP clusters were weakly disorganized in the ASI axons. In collaboration with M.Z and Y.J. we showed that *sad-3* is allelic with *rpm-1*. Mutations in *C. elegans rpm-1* (Zhen et al., 2000; Schaeffer et al., 2000) and its *Drosophila* homolog *Highwire* (Wan et al., 2000) led to a variety of presynaptic structural defects in sensory and motor neurons. These defects included reduced or disorganized presynaptic structures in *C. elegans* and hyperproliferation of synapses in *Drosophila*. In particular, at the *C. elegans* NMJ presynaptic structures

1. The first part of the document is a list of names and addresses of the members of the committee. The names are listed in alphabetical order, and the addresses are given in full. The list includes the names of the members of the committee, the names of the members of the sub-committee, and the names of the members of the advisory committee. The addresses are given in full, including the street, city, and state.

2. The second part of the document is a list of the names and addresses of the members of the committee. The names are listed in alphabetical order, and the addresses are given in full. The list includes the names of the members of the committee, the names of the members of the sub-committee, and the names of the members of the advisory committee. The addresses are given in full, including the street, city, and state.

3. The third part of the document is a list of the names and addresses of the members of the committee. The names are listed in alphabetical order, and the addresses are given in full. The list includes the names of the members of the committee, the names of the members of the sub-committee, and the names of the members of the advisory committee. The addresses are given in full, including the street, city, and state.

often fused together into aggregates containing multiple active zones and extended vesicle clusters, demonstrating that in *sad-3/rpm-1* mutants both vesicle clusters and active zones were disorganized. By contrast, in *sad-1* animals vesicle clusters were disorganized but active zones were normal. Whereas SAD-1 may function to couple vesicle clusters with active zones, SAD-3/RPM-1 may function to organize the spacing of packets of active zones and vesicle clusters.

Step 7: *sad-1*, *sad-2*, and *eat-7*, maintenance of synaptic vesicle clusters?

Once a functional synapse has formed, its shape must be maintained. Vesicles are in a constant state of flux as they undergo rounds of exocytosis and endocytosis. A neuron ensures that the size of vesicle clusters are controlled despite the high turnover rate of vesicles. In *sad-1* and *sad-2* animals vesicle clusters were irregular in size and less discrete, and in *eat-7(ad450)* animals vesicle clusters were even less discrete. One model is that *sad-1* and *sad-2* are required for the regulation of vesicle clustering, whereas *eat-7* is required for vesicle clustering itself. In the framework of this model the phenotype of *eat-7(ad450)* animals can be interpreted in one of two ways. If the semidominance of *eat-7(ad450)* reflects a gain-of-function property of *ad450*, then the SNB-1::GFP defect would be caused by increased clustering of vesicles such that vesicle clusters were expanded in size. Whereas, if the semidominance was due to a dominant negative property of *ad450*, then the diffuse SNB-1::GFP would be explained by a lack of vesicle clustering. One way to differentiate between these two possibilities is to examine the epistatic relationship between *eat-7(ad450)* and SAD-1 overexpression. If *ad450* is a dominant negative allele of *eat-7* than it may suppress the effects of SAD-1 overexpression.

The defects in cluster shape and size seen in *sad-1*, *sad-2*, and *eat-7(ad450)* mutants may result from either developmental defects in cluster formation, improper homeostasis of cluster morphology, or both. Indeed, SAD-1 protein is expressed both at the onset of synaptogenesis and well into adulthood, suggesting roles in both the development and maintenance of clusters (see Chapter 4).

SNB-1::GFP

1. The first part of the document is a list of names and addresses of the members of the committee. The names are listed in alphabetical order, and the addresses are given in full. The list includes the names of the members of the committee, the names of the members of the sub-committee, and the names of the members of the advisory committee. The addresses are given in full, including the street, city, and state.

2. The second part of the document is a list of the names and addresses of the members of the committee. The names are listed in alphabetical order, and the addresses are given in full. The list includes the names of the members of the committee, the names of the members of the sub-committee, and the names of the members of the advisory committee. The addresses are given in full, including the street, city, and state.

3. The third part of the document is a list of the names and addresses of the members of the committee. The names are listed in alphabetical order, and the addresses are given in full. The list includes the names of the members of the committee, the names of the members of the sub-committee, and the names of the members of the advisory committee. The addresses are given in full, including the street, city, and state.

Final thoughts on SNB-1::GFP screen

Although we set out to identify molecules specifically required for synapses between neurons, the mutants we recovered all affect the development of the neuromuscular junction as well. Interestingly, whereas mutations in *sad-1* and *sad-2* more strongly affected ASI synapses, mutations in *sad-3/rpm-1* more strongly affected the NMJ. One possibility is that *sad-1* and *sad-2* are more important for synapses between neurons, and *sad-3/rpm-1* is more important for synapses between neuron and muscle. Alternatively, the relative differences in phenotypic severity that we observed may depend on other factors such as type of neurotransmitter used. The comparative analysis of the requirements of *sad-1*, *sad-2*, and *sad-3/rpm-1* in additional types of synapses will help to address this question.

Multiple alleles were identified in each locus, suggesting that this visual screen is near genetic saturation. In addition, weak alleles of *unc-104* and *unc-51* were identified, showing that direct GFP visual screens can identify hypomorphic alleles that might not have otherwise been found in locomotion screens. However, *eat-7* and *syd-2* were missed in this screen despite having striking SNB-1::GFP defects in the ASI neurons. *eat-7* is represented by only the *ad450* semidominant allele; as it is semidominant *ad450* may not reflect the loss-of-function phenotype of *eat-7*. It may be that *eat-7* alleles were not found because loss-of-function *eat-7* does not cause striking synapse defects and *eat-7* alleles of the *ad450* class are rare. It is not known why *syd-2* was missed, though it should be noted that only one allele of *syd-2* was recovered in the motor neuron SNB-1::GFP screens (Zhen and Jin, 1999). Every screen has its biases. In the case of this screen, an enrichment scheme selected for animals with behavioral and locomotion defects. Lethal or genetically redundant genes would have been missed, as would genes that also affect earlier stages of neuronal development like axon outgrowth. We identified several mutations that had weak vesicle clustering defects, and we were unable to characterize them further. Nonetheless, we believe that this screen has identified the majority of the genes most important for the generation, organization, and maintenance of synaptic vesicle clusters. Secondary enhancer or suppressor screens are needed in order

1. The first part of the document is a list of names and addresses of the members of the committee. The names are listed in alphabetical order, and the addresses are given in full. The list includes the names of the members of the committee, the names of the members of the sub-committee, and the names of the members of the advisory committee. The addresses are given in full, including the street, city, and state.

2. The second part of the document is a list of the names and addresses of the members of the committee. The names are listed in alphabetical order, and the addresses are given in full. The list includes the names of the members of the committee, the names of the members of the sub-committee, and the names of the members of the advisory committee. The addresses are given in full, including the street, city, and state.

to identify additional molecules involved in the vesicle clustering pathway. Likewise, visual screens using markers for active zones and pre- and post-synaptic alignment will identify additional molecules important for other aspects of presynaptic development.

Experimental Procedures

Strains and Maintenance

Wild-type animals were *C. elegans* variety Bristol, strain N2. Animals were grown at 20°C on HB101 bacteria and maintained according to standard methods (Brenner, 1974). Some strains were provided by the *Caenorhabditis* Genetic Center, which is supported by the National Institutes of Health.

Screen for ASI SNB-1::GFP defects

p_{str-3} SNB-1::GFP was constructed by cloning a SphI-NheI PCR product containing 3kb of *str-3* upstream sequences into pSB121.51 (Nonet, 1999); an enhanced GFP from pPD95.75 was swapped with the GFP of pSB121.51 as an AgeI-ApaI fragment to increase fluorescence intensity. *lin-15(n765ts)* mutant animals were injected with p_{str-3} SNB-1::GFP at 100 ng/ul and a *lin-15(+)* pJM23 plasmid as a coinjection marker at 50 ng/ul (Huang et al., 1994). Transformants were maintained by picking animals rescued for the *lin-15* multivulval phenotype. The transgenic array was integrated into the genome using psoralen mutagenesis. One integrant, CX3572 *kyIs105; lin-15(n765ts)*, was outcrossed four times and used for subsequent analysis. For the screen, *kyIs105; lin-15(n765ts)* animals were mutagenized with EMS. F2 progeny were enriched for a lack of chemotaxis to a 1:200 point source of benzaldehyde and screened visually for SNB-1::GFP defects.

***sad-2* mapping and attempts at transformation rescue**

sad-2(ky292) was mapped with respect to Tc1 transposable element polymorphisms in the DP13 strain (Williams, 1995) by following the ASI SNB-1::GFP defects. Mapping localized the mutant to LGX between the stP72 and stP2 polymorphisms; in recovered *sad-2* mutants 2/18 recombination events

1. The first part of the document is a list of names and addresses of the members of the committee. The names are listed in alphabetical order, and the addresses are listed in the same order. The names are: [illegible]

2. The second part of the document is a list of the names and addresses of the members of the committee. The names are listed in alphabetical order, and the addresses are listed in the same order. The names are: [illegible]

3. The third part of the document is a list of the names and addresses of the members of the committee. The names are listed in alphabetical order, and the addresses are listed in the same order. The names are: [illegible]

occurred to the right of stP72 and 7/18 recombination events occurred to the left of stP2. Three-factor mapping was conducted to further localize *sad-2* on LGX. 0/3 *dpy-6* non *unc-18* and 5/5 non *dpy-6 unc-18* recombinants were mutant for *sad-2*. 0/5 *unc-9* non *unc-3* and 1/8 non *lin-2 unc-9* recombinants were mutant for *sad-2*, though when the one mutant non *lin-2 unc-9* recombinant was backcrossed and reisolated for *unc-9*, it did not appear as mutant for *sad-2* as the original recombinant. These data place *sad-2* near *unc-9* on LGX. More data is needed to further refine the *sad-2* map location.

Transgenic strains were created as previously described (Mello and Fire, 1995). Multiple lines from each injection were characterized for rescue of the SNB-1::GFP phenotype. Cosmids were injected at 20-50 ng/ul using the pJM67 *p_{elt-2}*GFP plasmid at 12 ng/ul as a coinjection marker (Fukushige et al., 1998). Transformants were maintained by picking animals expressing GFP in the gut. The following cosmids were injected either alone or in pools and failed to rescue the ASI SNB-1::GFP defects of *sad-2(ky292)* animals: pool SM1A (T24D3, T18D3, F45E6, C16D6, R01H5, R09A8, T07C5, F16H9, F22E10, T22H6, C52G5), pool SM1B (C52G5, T14G8, K02A4, C34E7, K03A11, F17H10, F09A5, F09D5), pool D (C13A12, C17H7, C55C7, C26H7, C09G10), pool E' (C16C5, C26B3, C02B4, C11F7, C06C5, C31B4, C07H2, C09A1), pool F (C07H2, C09A1, C52G5, C51A5, C43C2, C11D6, C34E7), C44H4, C04A11. These pools covered >90% of the region between *lin-2* and *unc-9*.

Synapsin sequencing in *eat-7* mutants

To identify possible mutations in *eat-7(ad450)*, the open reading frame and splice junctions of the predicted synapsin gene were PCR amplified from two separate genomic DNA preparations of *eat-7(ad450)* animals. PCR fragments were pooled and sequenced on both strands using an ABI sequencing machine (HHMI DNA facility). Synapsin is located on YAC Y38C1BA. An identified synapsin cDNA predicts exons corresponding to nucleotides 22235-21816 (1), 20531-20377 (2), 20241-19967 (3), 19364-19198 (4), and 19130-18909 (5) (Kao et al., 1999). An additional hypothesized 5' exon corresponding to nucleotides 28894-28790 has homology to the N-terminal A domain of mouse synapsins but was not found in the reported cDNAs. No mutations were found in exons 1-3 or the

1. The first part of the document is a list of names and titles, including the names of the authors and the titles of their respective works. This list is organized in a structured manner, likely representing a table of contents or a list of references.

2. The second part of the document is a list of names and titles, continuing the structured format seen in the first part. This section also appears to be a list of references or a table of contents.

3. The third part of the document is a list of names and titles, following the same structured format as the previous sections. This section likely contains the names of authors and the titles of their works.

hypothesized 5' exon. We did not sequence exons 4 and 5 since, despite using several primer combinations, we were unable to generate PCR products corresponding to this region of the synapsin gene from either wild-type or *eat-7(ad450)* animals. The following primers were used in the unsuccessful PCR: Y38-1 (5' ccgcaatacagatcaggc 3'), Y38-2 (5' gacgcagagcattctgcgtc 3'), Y38-1N (5' tggctagaagtgatcagaac 3'), Y38-2N (5' agcttcaaagttatggtggc 3'). Primer combinations Y38-1/Y38-2, Y38-1N/Y38-2N, Y38-1/Y38-2N, and Y38-1N/Y38-2 were used for PCR.

SAD-1 overexpression studies

For rescue of *sad-2(ky292)* the SacII deleted version of F15A2 was injected at 50 ng/ul with p_{elt-2} -GFP at 12 ng/ul. Two independent transgenic lines were analyzed for rescue of the ASI SNB-1::GFP defects of *sad-2(ky292)* animals. p_{str-3} -SNB-1::GFP was used to score synthetic axon defects.

Microscopy

Vesicle clusters of ASI neurons were visualized in *kyIs105; lin-15 (n765ts)* animals. AWC axons were visualized with an integrated *str-2*-GFP transgene (strain CX3621 *kyIs136 lin-15(n765ts)* X) (Troemel et al., 1999). Living animals were mounted on 2% agarose pads containing 3 mM sodium azide. Fluorescent animals were visualized using a Nikon Eclipse TE300 equipped with a Biorad MRC-1024 Laser Scanning Confocal Imaging System. Images were captured at 60X magnification and processed using the NIH Image and Adobe Photoshop programs.

1
2
3
4
5
6
7
8
9
10
11
12
13
14
15
16
17
18
19
20
21
22
23
24
25
26
27
28
29
30
31
32
33
34
35
36
37
38
39
40
41
42
43
44
45
46
47
48
49
50
51
52
53
54
55
56
57
58
59
60
61
62
63
64
65
66
67
68
69
70
71
72
73
74
75
76
77
78
79
80
81
82
83
84
85
86
87
88
89
90
91
92
93
94
95
96
97
98
99
100

101
102
103
104
105
106
107
108
109
110
111
112
113
114
115
116
117
118
119
120
121
122
123
124
125
126
127
128
129
130
131
132
133
134
135
136
137
138
139
140
141
142
143
144
145
146
147
148
149
150

References

Ahmari, S.E., Buchanan, J., and Smith, S.J. (2000). Assembly of presynaptic active zones from cytoplasmic transport packets. *Nat. Neurosci.* 3, 445-451.

Avery L. (1993). The genetics of feeding in *Caenorhabditis elegans*. *Genetics* 133, 897-917.

Avery, L., Bargmann, C..I, and Horvitz, H.R. (1993). The *Caenorhabditis elegans unc-31* gene affects multiple nervous system-controlled functions. *Genetics* 134, 455-464.

Bargmann, C.I., and Horvitz, H.R. (1991). Control of larval development by chemosensory neurons in *Caenorhabditis elegans*. *Science* 251, 1243-1246.

Brenner, S. (1974). The genetics of *Caenorhabditis elegans*. *Genetics* 77, 71-94.

DeChiara, T.M., Bowen, D.C., Valenzuela, D.M., Simmons, M.V., Poueymirou, W.T., Thomas, S., Kinetz, E., Compton, D.L., Rojas, E., Park, J.S., Smith, C., DiStefano, P.S., Glass, D.J., Burden, S.J., and Yancopoulos, G.D. (1996). The receptor tyrosine kinase MuSK is required for neuromuscular junction formation in vivo. *Cell* 85, 501-512.

Fukushige T, Hawkins MG, McGhee JD. (1998). The GATA-factor *elt-2* is essential for formation of the *Caenorhabditis elegans* intestine. *Dev. Biol.* 198, 286-302.

Gautam, M., Noakes, P.G., Moscoso, L., Rupp, F., Scheller, R.H., Merlie, J.P., and Sanes, J.R. (1996). Defective neuromuscular synaptogenesis in agrin-deficient mutant mice. *Cell* 85, 525-535.

THE UNIVERSITY OF
MICHIGAN LIBRARY
ANN ARBOR, MICHIGAN
48106-1000
SERIALS ACQUISITION
300 NORTH ZEEB ROAD
ANN ARBOR, MI 48106-1000
TEL: 734 763 1000
FAX: 734 763 1001
WWW: WWW.LIBRARY.MICHIGAN.EDU

UNIVERSITY OF
MICHIGAN LIBRARY
ANN ARBOR, MICHIGAN
48106-1000
SERIALS ACQUISITION
300 NORTH ZEEB ROAD
ANN ARBOR, MI 48106-1000
TEL: 734 763 1000
FAX: 734 763 1001
WWW: WWW.LIBRARY.MICHIGAN.EDU

Hall, A.C., Lucas, F.R., and Salinas, P.C. (2000). Axonal remodeling and synaptic differentiation in the cerebellum is regulated by WNT-7a signaling. *Cell* 100, 525-535.

Hosaka, M., Hammer, R.E., and Sudhof, T.C. (1999). A phospho-switch controls the dynamic association of synapsins with synaptic vesicles. *Neuron* 24, 377-387.

Huang LS, Tzou P, Sternberg PW. (1994). The *lin-15* locus encodes two negative regulators of *Caenorhabditis elegans* vulval development. *Mol. Biol. Cell.* 5, 395-411.

Kao, H.T., Porton, B., Hilfiker, S., Stefani, G., Pieribone, V.A., DeSalle, R., and Greengard, P. (1999). Molecular evolution of the synapsin gene family. *J. Exp. Zool.* 285, 360-377.

Lu, B., Greengard, P., and Poo, M.M. (1992). Exogenous synapsin I promotes functional maturation of developing neuromuscular synapses. *Neuron* 8, 521-529.

Malone, C.J., Fixsen, W.D., Horvitz, H.R., and Han, M. (1999). UNC-84 localizes to the nuclear envelope and is required for nuclear migration and anchoring during *C. elegans* development. *Development* 126, 3171-3181.

Matsuura, A., Tsukada, M., Wada, Y., and Ohsumi, Y. (1997). Apg1p, a novel protein kinase required for the autophagic process in *Saccharomyces cerevisiae*. *Gene* 192, 245-250.

Mello, C. and Fire, A. (1995). DNA transformation. *Methods Cell Biol.* 48, 451-482.

Noakes, P.G., Gautam, M., Mudd, J., Sanes, J.R., and Merlie, J.P. (1995). Aberrant differentiation of neuromuscular junctions in mice lacking s-laminin/laminin beta 2. *Nature* 374, 258-262.

THE
NATIONAL
ARCHIVES
COLLECTION
OF
THE
UNITED STATES
DEPARTMENT OF THE INTERIOR
BUREAU OF LAND MANAGEMENT
SALT LAKE CITY, UTAH

ETC
LAND MANAGEMENT
SALT LAKE CITY, UTAH
BUREAU OF LAND MANAGEMENT
SALT LAKE CITY, UTAH

Nonet, M. L. (1999). Visualization of synaptic specializations in live *C. elegans* with synaptic vesicle protein-GFP fusions. *J. Neurosci. Methods* 89, 33-40.

Nonet, M.L., Holgado, A.M., Brewer, F., Serpe, C.J., Norbeck, B.A., Holleran, J., Wei, L., Hartweg, E., Jorgensen, E.M., and Alfonso, A. (1999). UNC-11, a *Caenorhabditis elegans* AP180 homologue, regulates the size and protein composition of synaptic vesicles. *Mol. Biol. Cell.* 10, 2343-2360.

Ogura, K., Wicky, C., Magnenat, L., Tobler, H., Mori, I., Muller, F., and Ohshima, Y. (1994). *Caenorhabditis elegans unc-51* gene required for axonal elongation encodes a novel serine/threonine kinase. *Genes Dev.* 8, 2389-2400.

Ogura, K., Shirakawa, M., Barnes, T.M., Hekimi, S., and Ohshima, Y. (1997). The UNC-14 protein required for axonal elongation and guidance in *Caenorhabditis elegans* interacts with the serine/threonine kinase UNC-51. *Genes Dev.* 11, 1801-1811.

Otsuka, A.J., Jeyaprakash, A., Garcia-Anoveros, J., Tang, L.Z., Fisk, G., Hartshorne, T., Franco, R., and Born, T. (1991). The *C. elegans unc-104* gene encodes a putative kinesin heavy chain-like protein. *Neuron* 6, 113-122.

Porter, B.E., Weis, J., and Sanes, J.R. (1995). A motoneuron-selective stop signal in the synaptic protein S-laminin. *Neuron* 14, 549-559.

Prokop, A., Landgraf, M., Rushton, E., Broadie, K., and Bate, M. (1996). Presynaptic development at the *Drosophila* neuromuscular junction: assembly and localization of presynaptic active zones. *Neuron* 17, 617-626.

Rosahl, T.W., Spillane, D., Missler, M., Herz, J., Selig, D.K., Wolff, J.R., Hammer, R.E., Malenka, R.C., and Sudhof, T.C. (1995). Essential functions of synapsins I and II in synaptic vesicle regulation. *Nature* 375, 488-493.

Sanes, J.R., and Lichtman, J.W. (1999). Development of the vertebrate neuromuscular junction. *Annu. Rev. Neurosci.* 22, 389-442.

Schaeffer, A. M., Hadwiger, G. D. and Nonet, M. L. (2000) *rpm-1*, a conserved neuronal gene that regulates targeting and synaptogenesis in *C. elegans*. *Neuron*, *in press*.

Serra-Pages, C., Medley, Q.G., Tang, M., Hart, A., and Streuli, M. (1998). Liprins, a family of LAR transmembrane protein-tyrosine phosphatase-interacting proteins. *J. Biol. Chem.* 273, 15611-15620.

Troemel, E.R., Sagasti, A., and Bargmann, C.I. (1999). Lateral signaling mediated by axon contact and calcium entry regulates asymmetric odorant receptor expression in *C. elegans*. *Cell* 99, 387-398.

Valtorta, F., Iezzi, N., Benfenati, F., Lu, B., and Poo, M.M., and Greengard, P. (1995). Accelerated structural maturation induced by synapsin I at developing neuromuscular synapses of *Xenopus laevis*. *Eur. J. Neurosci.* 7, 261-270.

Wan, H. I., DiAntonio, A., Fetter, R. D., Bergstrom, K., Strauss, R. and Goodman, C. S. (2000). Highwire regulates synaptic growth in *Drosophila*. *Neuron*, *in press*.

White, J.G., Southgate, E., Thomson, J.N., and Brenner, S. (1986). The structure of the nervous system of the nematode *C. elegans*. *Philosophical Transactions of the Royal Society of London* 314B, 1-340.

Williams, B.D. (1995). Genetic mapping with polymorphic sequence-tagged sites. *Methods Cell. Biol.* 48, 31-58.

Zhen, M., and Jin, Y. (1999). The liprin protein SYD-2 regulates the differentiation of presynaptic termini in *C. elegans*. *Nature* 401, 371-375.

Zhen, M., Xun, H., Bamber, B. and Jin, Y. (2000). Regulation of presynaptic terminal organization by *C. elegans* RPM-1, a putative GTP-GDP exchanger with a Ring-H2 finger domain. *Neuron*, *in press*.

Chapter 4

The SAD-1 kinase organizes presynaptic vesicle clusters and arrests axon outgrowth in *C. elegans*

Summary

Synaptic development is a multistep process that involves the termination of axon outgrowth, presynaptic clustering of vesicles and active zone proteins, and postsynaptic clustering of neurotransmitter receptors and regulatory proteins. We report here the identification of a novel predicted serine/threonine kinase, SAD-1, that regulates presynaptic differentiation in *C. elegans*. In *sad-1* mutant animals presynaptic vesicle clusters in sensory and motor axons are smaller, diffusely distributed, mislocalized, and irregularly spaced. SAD-1 is selectively expressed in the nervous system and localizes to synapse-rich regions of the axons, where it can function cell-autonomously in presynaptic neurons. Strikingly, overexpression of SAD-1 can induce the formation of well-organized, evenly spaced vesicle clusters in dendrites, which are normally devoid of synapses. SAD-1 also affects the final stages of axon outgrowth: sensory axons fail to terminate appropriately in *sad-1* mutants, whereas overexpression of SAD-1 causes sensory axons to terminate prematurely. SAD-1 is related to PAR-1, a kinase that regulates cell polarity during asymmetric cell division. Like PAR-1, SAD-1 is polarized within cells; its local response to specific signals may recruit synaptic vesicles and inhibit axon elongation during synapse formation.

Introduction

The assembly of the nervous system occurs when neurons recognize appropriate targets and form electrical and chemical synapses with them. The signals that organize synaptogenesis are best-characterized at the mammalian neuromuscular junction (NMJ) (reviewed in Sanes and Lichtman, 1999). During neuronal development, motor axons are precisely guided to the muscles they will innervate. Upon the axon's arrival at a target muscle, signals between the neuron and muscle induce cytoskeletal changes in the axonal growth cone, the clustering of neurotransmitter-filled vesicles and exocytotic machinery at presynaptic active zones, the postsynaptic aggregation of neurotransmitter receptors and regulatory proteins, and the formation of a stable adhesion between the neuron and muscle. The neuron secretes the extracellular matrix

molecule agrin, which signals through the MuSK tyrosine kinase receptor to cluster acetylcholine receptors (Glass et al., 1996; Gautam et al., 1996; DeChiara et al., 1996). Mice deficient in agrin or MuSK have defects in muscle differentiation and also have presynaptic defects in vesicle aggregation and axon termination, suggesting that the muscle sends a retrograde signal to the neuron to induce presynaptic differentiation. One candidate for a retrograde signal is laminin β 2, a component of the synaptic basal lamina. Laminin β 2 inhibits neurite outgrowth of cultured neurons (Porter et al., 1995), and mice lacking laminin β 2 have defects in presynaptic differentiation (Noakes et al., 1995). The receptors and signaling pathways that act downstream of laminin β 2 are unknown.

Although many of the same principles governing NMJ synapse development probably apply to synapses between neurons, less is known about the molecules that regulate connectivity in the central nervous system (CNS) (reviewed in Lee and Sheng, 2000). Two classes of transmembrane proteins, the neurexin-neurologin complex (Butz et al., 1998) and cadherins (Kohmura et al., 1998; reviewed in Shapiro and Colman, 1999), have been implicated in neuron to neuron adhesion at CNS synapses. Synapses between neurons appear largely intact in agrin mutants (Serpinskaya et al., 1999). The secreted protein Wnt7A causes axonal remodelling and the accumulation of synapsin in cultured mossy fiber neurons; in *Wnt7A* mutants the presynaptic differentiation of mossy fiber granule cell synapses is delayed (Hall et al., 2000). In response to these or other factors, CNS neurons localize scaffold proteins at active zones, cluster vesicles nearby in a specialized cytoskeleton, and cease axon outgrowth. The signaling pathways that mediate these processes are undefined.

Several presynaptic proteins may serve as either regulators or targets of the signals for presynaptic differentiation. Synapsins are lipid-binding proteins that associate with synaptic vesicles (Hosaka et al., 1999) and have been implicated in their clustering at synaptic sites (Lu et al., 1992). A mouse synapsin I/synapsin II double knockout has a 50% reduction in the number of clustered synaptic vesicles (Rosahl et al., 1995). In *C. elegans*, the liprin protein SYD-2 controls the size of presynaptic specializations; in *syd-2* mutant animals active zones and vesicle clusters are expanded (Zhen and Jin, 1999). A vertebrate liprin

interacts with tyrosine phosphatase receptors (Serra-Pagés et al., 1995). Three large proteins, Piccolo, Bassoon (Fenster et al., 2000), and RPM-1/Highwire, localize at or near presynaptic specializations. Mutations in *C. elegans rpm-1* (Zhen et al., 2000; Schaeffer et al., 2000) and its *Drosophila* homolog *Highwire* (Wan et al., 2000) lead to a variety of presynaptic structural defects depending on the type of synapse studied. These defects include reduced or disorganized presynaptic structures in *C. elegans* and hyperproliferation of synapses in *Drosophila*.

To identify new regulators of presynaptic development, we conducted direct visual screens in *C. elegans* for mutations that affect presynaptic vesicle clusters in the ASI chemosensory neurons. We describe the identification of a mutant, *sad-1*, that affects presynaptic development. *sad-1* encodes a novel serine/threonine protein kinase that localizes to synapse-rich regions of the axon. In *sad-1* mutant animals presynaptic vesicle clusters are disorganized and sensory axons fail to terminate; conversely, when SAD-1 is overexpressed ectopic vesicle clusters form in the dendrite and sensory axons terminate prematurely. Thus, SAD-1 appears to be a key regulator of presynaptic morphology.

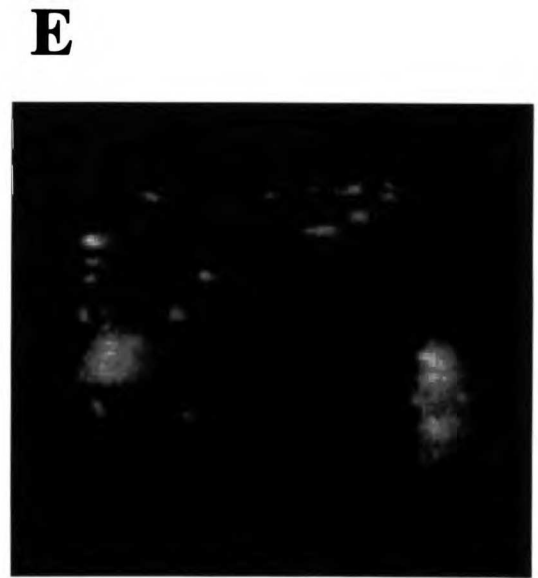
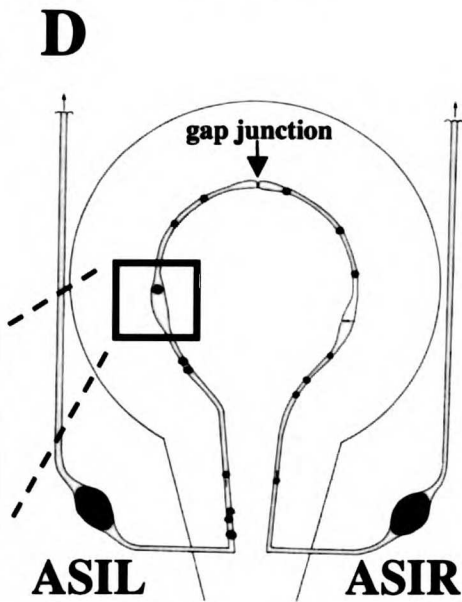
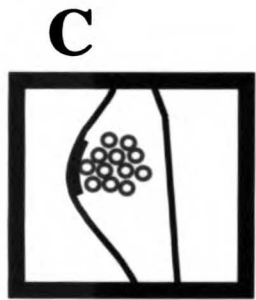
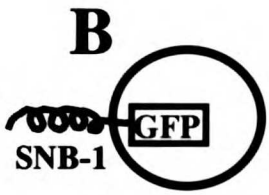
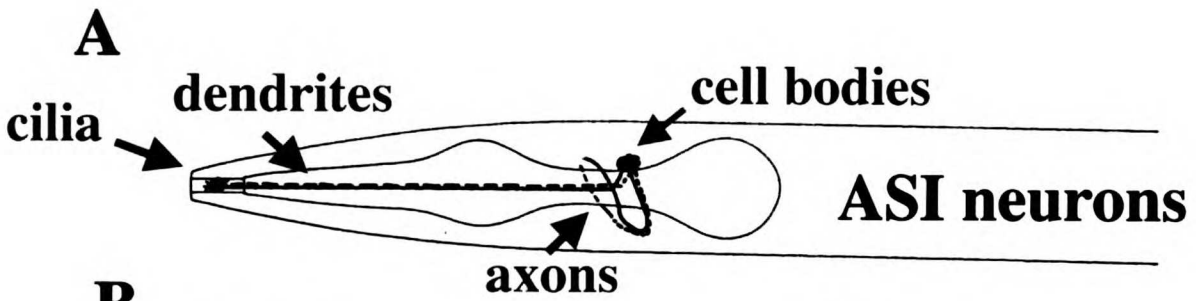
Results

Isolation of mutants with defective chemosensory synapses

The ASI neurons are a bilaterally symmetric pair of chemosensory neurons that control entry into an alternate developmental form, the dauer larvae, in response to environmental signals (Bargmann and Horvitz, 1991). Each ASI neuron has a dendrite that projects to the anterior sensory organ and ends in a slender cilium, and an axon that enters the nerve ring and makes about 7-9 synapses onto an array of interneurons and other chemosensory neurons (White et al., 1986) (see Figure 1A,D). In order to visualize the presynaptic specializations associated with ASI synapses in living animals, we expressed a fusion protein between the vesicle associated membrane protein synaptobrevin and green fluorescent protein (SNB-1::GFP) under the control of the ASI neuron-specific *str-3* promoter. SNB-1::GFP is an accurate marker for presynaptic vesicle

Figure 1. p_{str-3} SNB-1::GFP labels presynaptic vesicle clusters in the ASI chemosensory neurons

(A) Each ASI neuron sends a dendrite to the tip of the nose, where it ends in a cilium, and an axon into the nerve ring. Anterior is left, dorsal is up. (B) A SNB-1::GFP fusion localizes GFP to the luminal side of synaptic vesicles. (C) Diagram of a typical synapse, with vesicles and an active zone in a slight thickening. (D) Flattened cross-section showing the predicted presynaptic specializations of the ASI neurons (adapted from White et al., 1986). The two larger shaded ovals are the cell bodies of ASIL and ASIR. The axons of ASIL and ASIR form gap junctions at their dorsal ends. The smaller shaded circles within the axons represent clusters of synaptic vesicles (see inset (C)). (E) When expressed under the control of the ASI-specific *str-3* promoter, SNB-1::GFP allows the visualization of ASI presynaptic vesicle clusters in living animals. The confocal epifluorescence micrograph is in roughly the same orientation as (D) with dorsal up and anterior into the page. The large fluorescent regions are the ASI cell bodies. The smaller puncta correspond well with the vesicle clusters diagrammed in (D).



1. The first part of the document is a list of names and addresses of the members of the committee. The names are listed in alphabetical order, and the addresses are listed below each name. The list includes names such as Mr. J. H. Smith, Mr. J. B. Jones, and Mr. W. C. Brown.

2. The second part of the document is a list of the names and addresses of the members of the committee who were present at the meeting. The names are listed in alphabetical order, and the addresses are listed below each name. The list includes names such as Mr. J. H. Smith, Mr. J. B. Jones, and Mr. W. C. Brown.

3. The third part of the document is a list of the names and addresses of the members of the committee who were absent from the meeting. The names are listed in alphabetical order, and the addresses are listed below each name. The list includes names such as Mr. J. H. Smith, Mr. J. B. Jones, and Mr. W. C. Brown.

clusters in *C. elegans* (Nonet, 1999). In each ASI neuron of animals carrying an integrated array of p_{str-3} SNB-1::GFP, GFP fluorescence was visible in 7-9 evenly spaced clusters along the region of the axon that fasciculates with the nerve ring; in addition, GFP fluorescence was visible in the cell body (Figure 1, Figures 2A,B). Weaker fluorescence was occasionally observed in the dendrite in a diffuse pattern. The number of clusters observed in each ASI neuron corresponded well with the number of ASI presynaptic specializations observed in electron microscopic reconstructions (White et al., 1986) (compare Figures 1D and 1E). To confirm that SNB-1::GFP fluorescence corresponded to presynaptic vesicles and not some other compartment in ASI, we examined p_{str-3} SNB-1::GFP in the *unc-104* kinesin mutant. In *unc-104* mutant animals synaptic vesicles accumulate in the cell body and are largely absent from the axon (Otsuka et al., 1991). As expected for a marker of synaptic vesicles, p_{str-3} SNB-1::GFP fluorescence accumulated in the cell body in *unc-104(e1265)* mutant animals (data not shown).

Using p_{str-3} SNB-1::GFP as a marker for ASI synapses we conducted a screen for mutants with abnormal patterns of GFP fluorescence. Hermaphrodites carrying p_{str-3} SNB-1::GFP were mutagenized with EMS and their F2 progeny were examined for visible defects (see Experimental Procedures). We isolated 24 mutations in 6 complementation groups that affect the pattern of SNB-1::GFP expression: *unc-104*, *unc-11*, *unc-51*, and three new genes that we named *sad-1*, *sad-2*, and *sad-3* for synapses of the amphid defective (Table 1) (In Zhen et al., 2000 we report that *sad-3* is allelic with *rpm-1*). Multiple alleles were identified in each of these genes, suggesting that this visual screen is near genetic saturation.

The three *unc* genes isolated in our screen may all affect synaptic vesicle biogenesis or transport. As expected from our analysis of *unc-104(e1265)*, the new *unc-104* kinesin mutants had SNB-1::GFP localized to the cell body (data not shown). The allele *ky290* had weaker movement and SNB-1::GFP defects. In *unc-11* animals GFP fluorescence was diffusely localized throughout the plasma membrane of the neuron (described in more detail in Dwyer et al., 2000, submitted). *unc-11* is an AP180 protein implicated in synaptic vesicle endocytosis that is essential for SNB-1 localization to vesicles (Nonet et al., 1999).

1. The first part of the document is a list of names and addresses of the members of the committee. The names are listed in alphabetical order, and the addresses are given in full. The list includes the names of the members of the committee, the names of the members of the sub-committee, and the names of the members of the advisory committee. The addresses are given in full, including the street, city, and state.

2. The second part of the document is a list of the names and addresses of the members of the committee. The names are listed in alphabetical order, and the addresses are given in full. The list includes the names of the members of the committee, the names of the members of the sub-committee, and the names of the members of the advisory committee. The addresses are given in full, including the street, city, and state.

3. The third part of the document is a list of the names and addresses of the members of the committee. The names are listed in alphabetical order, and the addresses are given in full. The list includes the names of the members of the committee, the names of the members of the sub-committee, and the names of the members of the advisory committee. The addresses are given in full, including the street, city, and state.

Table 1. Summary of screen for SNB-1::GFP clustering defects in the ASI neurons

<u>Mutant</u>	<u>Number of Alleles Isolated</u>
<i>unc-104</i>	4 (<i>ky287, ky317, ky319</i>) and (<i>ky290</i>) _{weak}
<i>unc-11</i>	3 (<i>ky280, ky291, ky325</i>)
<i>unc-51</i>	6 (<i>ky286, ky321, ky322, ky323, ky324</i>) _{strong} and (<i>ky347</i>) _{weak}
<i>sad-1</i>	6 (<i>ky281, ky289, ky326, ky330, ky332, ky344</i>)
<i>sad-2</i>	3 (<i>ky292, ky329, ky335</i>)
<i>sad-3/rpm-1</i>	2 (<i>ky340, ky346</i>)

1. The first part of the document is a list of names and addresses of the members of the committee. The names are listed in alphabetical order, and the addresses are given in full. The list includes the names of the members of the committee, the names of the members of the sub-committee, and the names of the members of the advisory committee. The addresses are given in full, including the street name, the city, the state, and the zip code.

2. The second part of the document is a list of the names and addresses of the members of the committee. The names are listed in alphabetical order, and the addresses are given in full. The list includes the names of the members of the committee, the names of the members of the sub-committee, and the names of the members of the advisory committee. The addresses are given in full, including the street name, the city, the state, and the zip code.

3. The third part of the document is a list of the names and addresses of the members of the committee. The names are listed in alphabetical order, and the addresses are given in full. The list includes the names of the members of the committee, the names of the members of the sub-committee, and the names of the members of the advisory committee. The addresses are given in full, including the street name, the city, the state, and the zip code.

In *unc-51* animals GFP fluorescence accumulates in one or two large varicosities in the axon (data not shown). *unc-51* encodes a protein kinase that affects axon outgrowth and guidance and may alter trafficking of membrane vesicles in neurons (Ogura et al., 1994). We isolated both strong and weak *unc-51* alleles that affect synaptic vesicle clusters but not axon guidance in ASI. *unc-51* is similar to the Apg1p kinase that acts at an early step in yeast autophagy (Matsuura et al., 1997). By analogy to the yeast phenotype, *unc-51* may be involved in the budding of synaptic vesicles from endosomes or other internal membrane compartments.

***sad-1* mutants have disorganized vesicle clusters**

Whereas mutations in *unc-104*, *unc-11*, and *unc-51* have effects on trafficking of vesicles and/or synaptobrevin, mutations in *sad-1*, *sad-2*, and *sad-3/rpm-1* have defects in the organization of SNB-1::GFP clusters. We isolated six alleles (*ky281*, *ky289*, *ky326*, *ky330*, *ky332*, and *ky344*) of *sad-1* in the p_{str-3} SNB-1::GFP screen, and a seventh allele (*ju53*) in a similar type of screen using p_{unc-25} SNB-1::GFP (see below). The alleles *ky281*, *ky289*, *ky326*, *ky330*, *ky332*, and *ky344* displayed highly penetrant SNB-1::GFP defects in ASI. However, the nature of the SNB-1::GFP defect was variable from animal to animal. In some animals regions of the axon appeared to lack vesicle clusters (Figures 2C,D), whereas in other animals regions of the axon had densely packed vesicle clusters (Figures 2E,F). It was often difficult to determine whether the defect corresponded to a change in the number of vesicle clusters or irregularities in the spacing of clusters. In some animals vesicle clusters were irregular in size, often appearing smaller than normal (Figures 2E,F and data not shown). Also, regions of the axon sometimes displayed more diffuse SNB-1::GFP fluorescence (Figures 2G,H). The phenotypes of many animals could be interpreted as a combination of these defects.

sad-1 mutants also have presynaptic defects at neuromuscular junctions. p_{unc-25} SNB-1::GFP labels the presynaptic vesicle clusters of the GABAergic VD and DD motor neurons (Hallam and Jin, 1998 and Figure 3A). In wild-type animals this marker is expressed as discrete fluorescent puncta distributed along

1. The first part of the document is a list of names and addresses of the members of the committee. The names are listed in alphabetical order, and the addresses are given in full. The list includes names such as Mr. J. H. Smith, Mr. W. B. Jones, and Mr. C. D. Brown, among others.

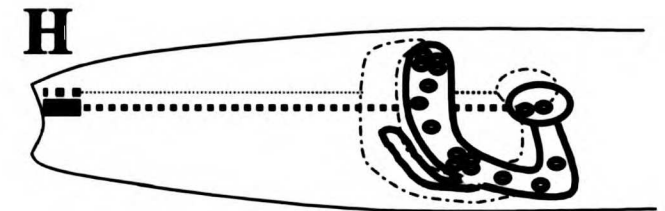
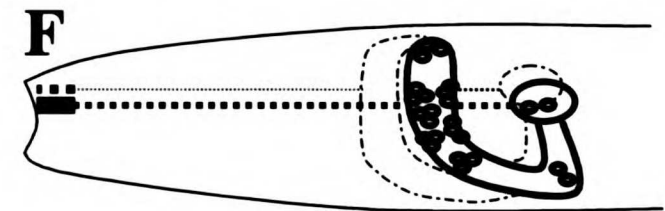
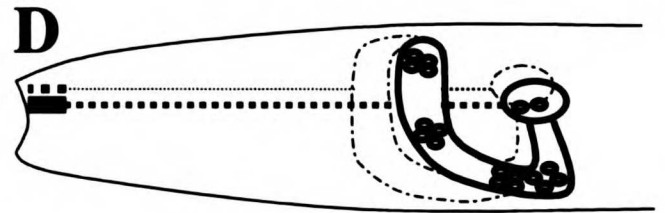
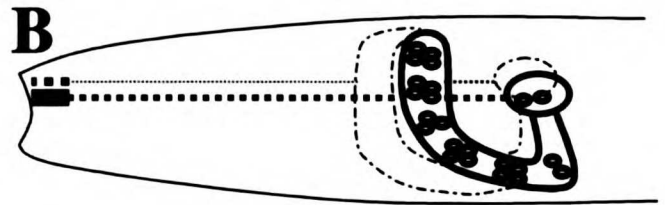
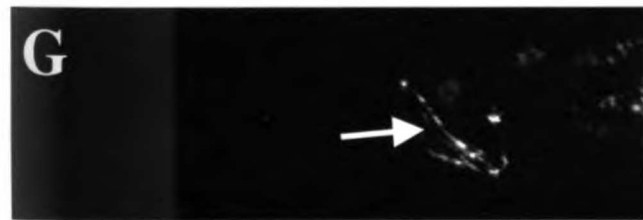
2. The second part of the document is a list of the names and addresses of the members of the committee who were present at the meeting. This list is also in alphabetical order and includes names such as Mr. J. H. Smith, Mr. W. B. Jones, and Mr. C. D. Brown, among others.

Figure 2. In *sad-1* mutants SNB-1::GFP clusters are disorganized and more diffuse in the ASI neurons

Confocal epifluorescence micrographs (A,C,E,G) and interpretive diagrams (B,D,F,H) of p_{str-3} SNB-1::GFP expression in wild-type (A,B) and *sad-1(ky330)* (C-H) animals. In wild-type animals SNB-1::GFP clusters were regularly spaced along the ASI axon (A,B). In *sad-1(ky330)* animals clusters were absent in regions of the axon (C,D), spatially disorganized (E,F), or diffusely localized (G,H). The arrow in (G) denotes a secondary branch emanating from the primary axon. Also, in (G) and to a lesser extent in (A,C,E) the axon of the contralateral ASI neuron is faintly visible. Scale bar: 10 μ m.

1. The first part of the document is a list of names and addresses of the members of the committee. The names are listed in alphabetical order, and the addresses are given in full. The list includes the names of the members of the committee, the names of the members of the sub-committee, and the names of the members of the advisory committee. The addresses are given in full, including the street name, the city, and the state.

2. The second part of the document is a list of the names and addresses of the members of the committee. The names are listed in alphabetical order, and the addresses are given in full. The list includes the names of the members of the committee, the names of the members of the sub-committee, and the names of the members of the advisory committee. The addresses are given in full, including the street name, the city, and the state.



1
2
3
4
5
6
7
8
9
10
11
12
13
14
15
16
17
18
19
20
21
22
23
24
25
26
27
28
29
30
31
32
33
34
35
36
37
38
39
40
41
42
43
44
45
46
47
48
49
50
51
52
53
54
55
56
57
58
59
60
61
62
63
64
65
66
67
68
69
70
71
72
73
74
75
76
77
78
79
80
81
82
83
84
85
86
87
88
89
90
91
92
93
94
95
96
97
98
99
100

101
102
103
104
105
106
107
108
109
110
111
112
113
114
115
116
117
118
119
120
121
122
123
124
125
126
127
128
129
130
131
132
133
134
135
136
137
138
139
140
141
142
143
144
145
146
147
148
149
150

the ventral and dorsal sides (Figure 3A). The pattern of VD and DD synaptic output is dynamically controlled during development. In the first larval stage (L1) the DD motor neurons, born embryonically, make synapses exclusively onto ventral muscle. However, at the end of the L1 stage, DD motor neurons eliminate the ventral synapses and establish connectivity with the dorsal muscle; at the same time the post-embryonic VD motor neurons begin to innervate ventral muscle (White et al., 1978). The *ju53* allele of *sad-1* was isolated as a mutant in which SNB-1::GFP clusters appeared smaller and less discrete (Figures 3B-D). GFP fluorescence was also weaker than normal. Similar VD and DD defects were observed for the *sad-1 ky330* and *ky332* alleles. Additionally, in *sad-1* mutants SNB-1::GFP was localized to both the ventral and dorsal side in the L1 stage (data not shown). This result suggests that in *sad-1* mutants synaptic vesicles are not properly anchored at or targeted to synaptic regions. *sad-1* may also affect the ventral-dorsal polarity of synapses in the L1 larval stage.

In contrast to *unc-104*, *unc-11*, and *unc-51* animals, which displayed severely uncoordinated locomotion, *sad-1* animals had only subtle defects in movement. *sad-1* mutants were partially defective in chemotaxis to volatile odorants (data not shown) and had mild defects in egg-laying. In *sad-1* animals the ASI cell bodies migrated to their correct locations and their primary axons assumed their normal position and morphology in the nerve ring. However, as discussed in more detail below, axons sometimes made ectopic branches in the nerve ring and failed to terminate at their normal position. To ask whether the ASI neurons are functional in *sad-1* mutants we analyzed *unc-31; sad-1* double mutants. Ablation of the ASI neurons in an *unc-31* background causes animals to constitutively enter the alternative dauer larval form despite the presence of food (Avery et al., 1993). This activity of ASI depends on its ability to release a TGF-beta-like peptide DAF-7 (Ren et al., 1996; Schackwitz et al., 1996). DAF-7 is most likely released from dark-core vesicles at extrasynaptic sites (White et al., 1986). *unc-31; sad-1* animals formed almost no dauer larvae in the presence of food, suggesting that in *sad-1* animals the ASI neurons are present and able to release DAF-7 peptide.

1. The first part of the document is a list of names and addresses of the members of the committee. The names are listed in alphabetical order, and the addresses are given in full, including the street name, number, and city.

2. The second part of the document is a list of the names and addresses of the members of the committee who have been elected to the office of chairman and vice-chairman.

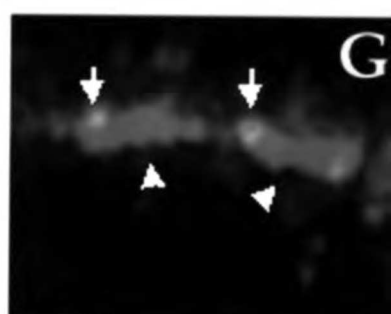
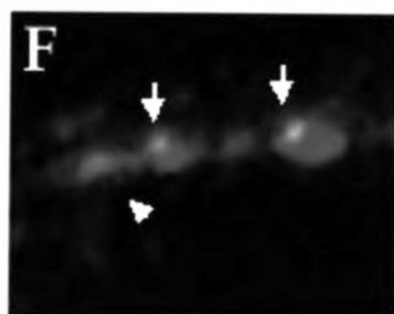
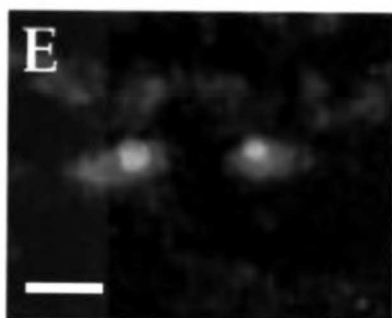
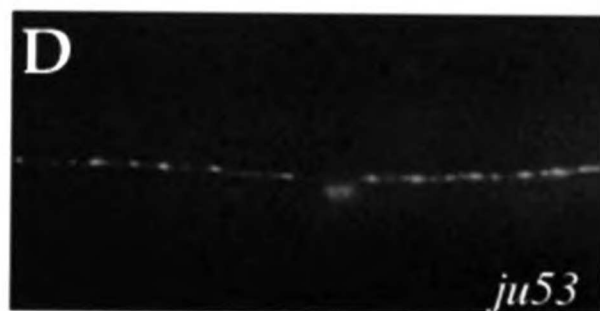
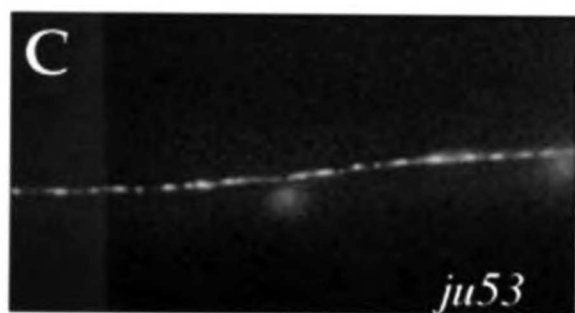
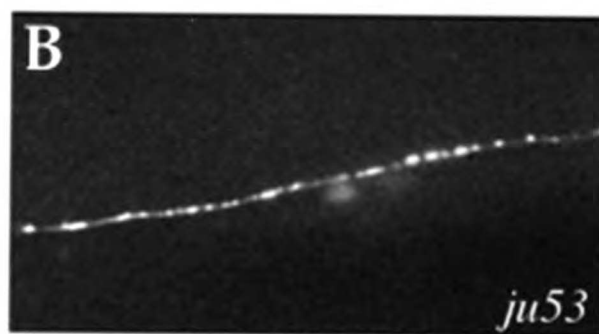
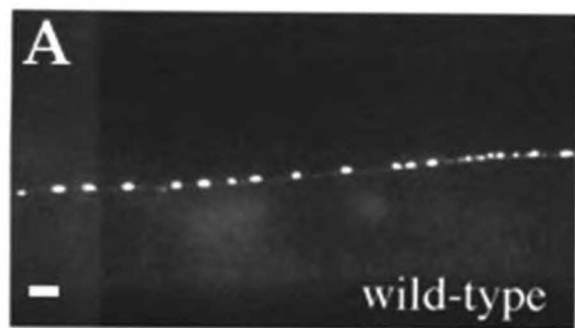
3. The third part of the document is a list of the names and addresses of the members of the committee who have been elected to the office of secretary and treasurer.

Figure 3. SNB-1::GFP clusters, but not SYD-2 localization, are disrupted at the NMJ of *sad-1* mutants

Fluorescence micrographs of wild-type (A) and *sad-1(ju53)* (B-D) animals expressing the p_{unc-25} SNB-1::GFP marker. p_{unc-25} SNB-1::GFP labels the presynaptic vesicle clusters of the GABAergic VD and DD motor neurons. In wild-type animals SNB-1::GFP clusters are of uniform size and regularly spaced (A). In *sad-1(ju53)* mutants these clusters appeared less discrete (B) or diffuse (C), and weaker in fluorescence (D). E-G show the expression of SYD-2 (red) and SNB-1::GFP (green) in wild-type (E) and *sad-1(ju53)* animals (F, G). SYD-2 localizes near or at presynaptic active zones. In wild-type animals, a single punctum of SYD-2 (red) is localized to the middle of SNB-1::GFP clusters (green) (E). In *sad-1(ju53)* animals, most SNB-1::GFP clusters were irregularly shaped (arrowheads), but SYD-2 puncta appeared normal (arrow) (F,G). Scale bars: 4 μ m.

1. The first part of the document discusses the importance of maintaining accurate records of all transactions. It emphasizes that proper record-keeping is essential for the integrity of the financial system and for the ability to detect and prevent fraud.

2. The second part of the document outlines the specific requirements for record-keeping, including the need to maintain original documents and to keep copies of all transactions. It also discusses the importance of regular audits and the role of internal controls in ensuring the accuracy of the records.



1. The first part of the document is a list of names and addresses of the members of the committee. The names are listed in alphabetical order, and the addresses are given in full. The list includes the names of the members of the committee, the names of the members of the sub-committee, and the names of the members of the advisory committee. The addresses are given in full, including the street, city, and state.

2. The second part of the document is a list of the names and addresses of the members of the committee. The names are listed in alphabetical order, and the addresses are given in full. The list includes the names of the members of the committee, the names of the members of the sub-committee, and the names of the members of the advisory committee. The addresses are given in full, including the street, city, and state.

3. The third part of the document is a list of the names and addresses of the members of the committee. The names are listed in alphabetical order, and the addresses are given in full. The list includes the names of the members of the committee, the names of the members of the sub-committee, and the names of the members of the advisory committee. The addresses are given in full, including the street, city, and state.

SYD-2, a presynaptic marker for active zones, is correctly localized in *sad-1* mutants

To investigate the extent of presynaptic defects in *sad-1* animals, we examined the localization of an active zone marker, SYD-2. SYD-2 localizes to small regions at presynaptic termini that are surrounded by SNB-1::GFP vesicle clusters (Zhen and Jin, 1999 and Figure 3E). The SYD-2 puncta remain localized to presynaptic termini in *unc-104* mutants, suggesting that SYD-2 is a component of presynaptic termini that is not associated with synaptic vesicles. Using the *unc-25* promoter we co-expressed SYD-2 and SNB-1::GFP in the VD and DD motor neurons in a *syd-2(ju37) sad-1(ju53)* double mutant and stained with anti-SYD-2 and anti-GFP antisera. p_{unc-25} SYD-2 fully rescued the SNB-1::GFP defects in VD and DD neurons in *syd-2(ju37)* mutants. Thus, this experiment allowed us to visualize SYD-2 and SNB-1 specifically in the VD and DD neurons in a *sad-1* mutant background. In the *sad-1* mutant, SNB-1::GFP clusters were less discrete in shape and the intensity of fluorescence was weaker, but the expression pattern of SYD-2 appeared normal (Figure 3F,G). In wild-type animals anti-SYD-2 staining reveals a dense pattern of puncta in the nerve ring; on a gross level we noticed no major differences in this staining between wild-type and *sad-1* animals (data not shown). We conclude that SAD-1 either is not required for active zone formation or is required only for the localization of a subset of active zone proteins. Consistent with this observation, *syd-2(ju37) sad-1(ju53)* double mutants showed a more severe phenotype than either single mutant alone (data not shown). This result suggests that *sad-1* functions in a different pathway from *syd-2*, which affects both vesicle clusters and active zones.

SAD-1 protein is a novel serine/threonine kinase

To understand the molecular nature of *sad-1* we cloned the gene. Cosmid F15A2 fully rescued the ASI and VD/DD SNB-1::GFP defects of *sad-1(ky332)*. A fragment of F15A2 that contained only a single predicted full-length open reading frame (ORF) also fully rescued *sad-1*, whereas fragments of F15A2 not containing this ORF failed to rescue (Figure 4A). We obtained a partial cDNA

1. The first part of the document is a list of names and addresses of the members of the committee. The names are listed in alphabetical order, and the addresses are listed below each name. The list includes names such as Mr. J. H. Smith, Mr. W. B. Jones, and Mr. C. D. Brown, among others.

2. The second part of the document is a list of the names and addresses of the members of the committee who were present at the meeting. This list is also in alphabetical order and includes names such as Mr. J. H. Smith, Mr. W. B. Jones, and Mr. C. D. Brown, among others.

Figure 4. SAD-1 protein is a novel serine/threonine kinase

(A) The *sad-1(ky332)* mutation was mapped near *odr-1* on the right arm of the X chromosome. A pool containing five cosmids rescued the ASI SNB-1::GFP defects of *sad-1(ky332)*. The cosmid F15A2 fully rescued the ASI SNB-1::GFP defects of *sad-1(ky332)* and the VD/DD SNB-1::GFP defects of *sad-1(ju53)*. A SacII deletion version of F15A2 and a 13.8kb fragment from F15A2 that contained a single predicted ORF (F15A2.6) also rescued *sad-1(ky332)*. Deleted versions of F15A2 not containing this ORF failed to rescue.

(B) A full-length cDNA corresponding to F15A2.6 predicts a 914 amino acid protein with strong homology to serine/threonine protein kinases. Mutations were found in the alleles *ju53*, *ky281*, *ky289*, *ky326*, *ky330*, and *ky344* (see text and D). SAD-1 has homologs in *Drosophila* (CG6114), ascidians (HrPOPK-1), and humans (partial EST). The kinase domain of SAD-1 (aa 42-298)(black shading) is 85% identical to that of CG6114 and 82% identical to that of HrPOPK-1. SAD-1 and its homologs share conservation in two regions outside of the kinase domain (grey shading)(aa 301-400: 61% identity (CG6114), 43% identity (HrPOPK-1); aa 589-755: 44% identity (CG6114), 39% identity (HrPOPK-1)). The kinase domains of SAD-1 and PAR-1 are 51% identical. Though SAD-1 and PAR-1 have a similar domain structure (note light grey shading, regions conserved in all PAR-1-like proteins) they share no homology outside of the kinase domain.

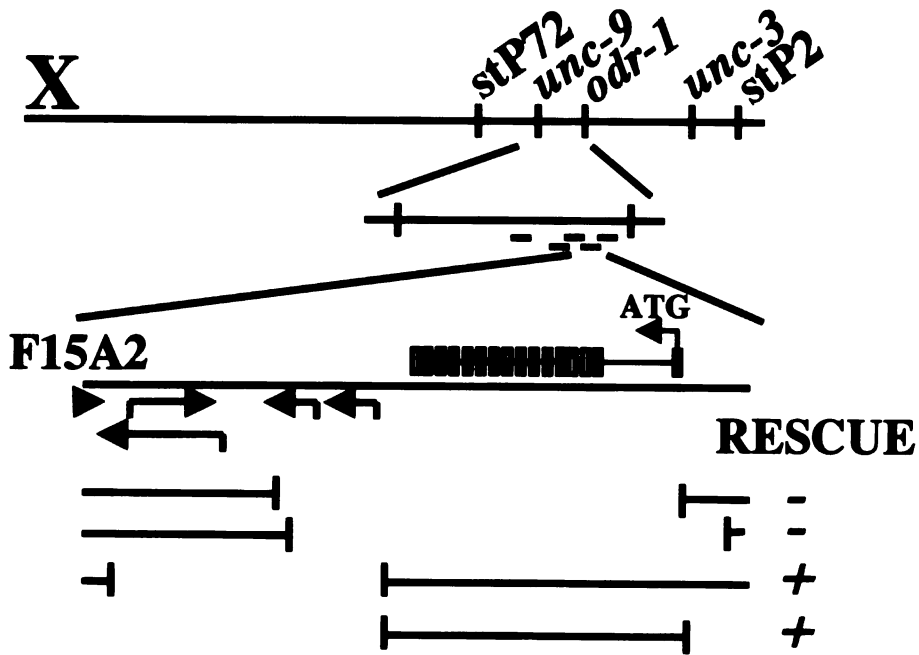
(C) Dendrogram of the kinase domains of AMPK/SNF-1 family members and CaMKII. The SAD-1 group and PAR-1 group are more closely related to each other than to human AMPK α 1 and yeast SNF1.

(D) Alignment of SAD-1, CG6114, HrPOPK-1, and the PAR-1 kinase domain. Identical residues are boxed and shaded. Similar residues are boxed. Black bar denotes the kinase domain. Grey bars denote regions of homology outside the kinase domain. Dots denote amino acids affected by point mutations in *sad-1*, the asterisk denotes the *ky289* stop codon, and ^ symbols denote truncation points in the *sad-1(ky344)* and *ky326* alleles.

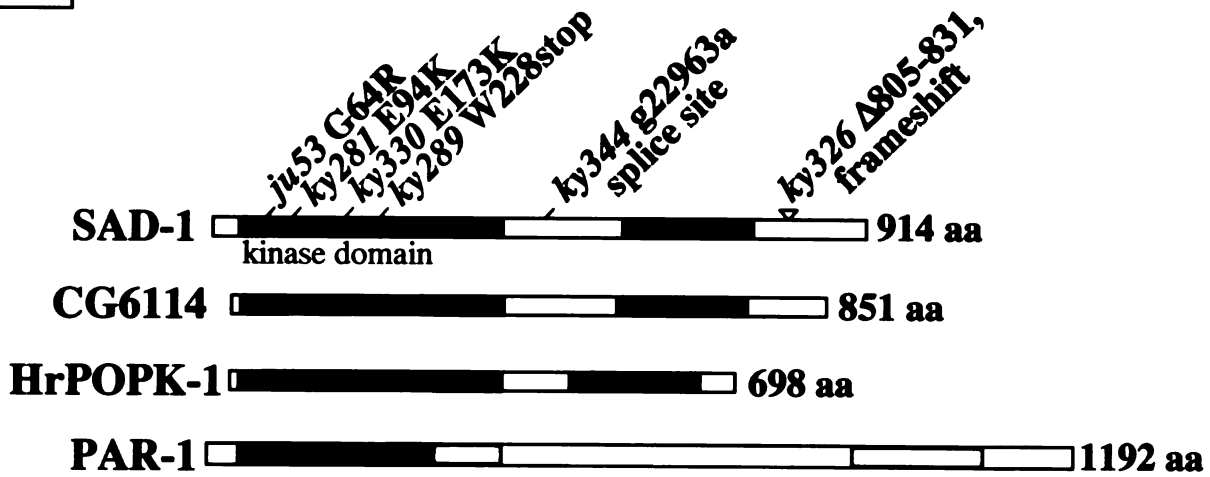
1. The first part of the document discusses the importance of maintaining accurate records of all transactions and activities. It emphasizes that this is crucial for ensuring transparency and accountability in the organization's operations.

2. The second part of the document outlines the specific procedures and protocols that must be followed to ensure that all records are properly maintained and updated. It details the roles and responsibilities of various staff members in this process.

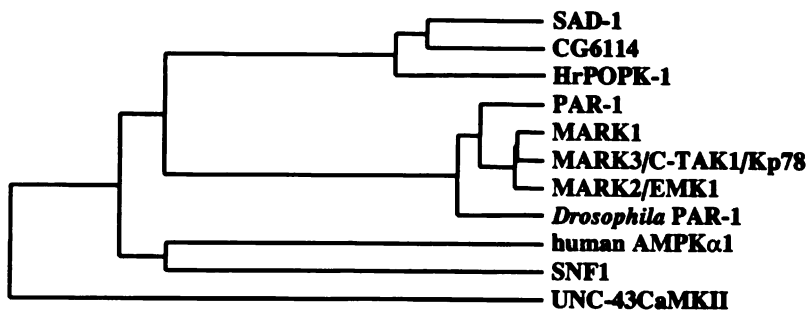
A



B



C



1. The first part of the document is a list of names and addresses of the members of the committee. The names are listed in alphabetical order, and the addresses are given in full, including the street name, city, and state.

2. The second part of the document is a list of the names and addresses of the members of the committee who have been elected to the office of chairman. The names are listed in alphabetical order, and the addresses are given in full, including the street name, city, and state.

SAD-1 1 MFEALKEVLGEINSLAAVNNELSSKIMSENIVSTRPVAQA QYICGPYKLE
CG614 1 MQKENNVTAENC QFVGPYRL
HrPOPK-1 1 MSNAPQPG QYVGPYKLE
FAR-1 kinase domain 1 V G K Y K L L

SAD-1 51 KTLGKGQTGLVKI TFCYERKVAIKIVKREKLSSEVLRVEREIAIMKL
CG614 22 KTLGKGQTGLVKI QVHCVIGKKVAIKIINREKLSSEVLRVEREIAIMKL
HrPOPK-1 18 KTLGKGQTGLVKI QVHCMTGKVAIKIINREKLSSEVLRVEREIAIMKL
FAR-1 kinase domain 8 K T I G K G N F A K V K L A K H V I T G H F V A I K I I D K T A L N P S S L Q K L F R E V K I M K Q

SAD-1 101 I E H P H V L H L Y D V Y E N K K Y L Y L L E H V S G G E L F D Y L V R K G R L M S K E A R K F F
CG614 72 I D H P H V L G L S D V Y E N K K Y L Y L I L E H V S G G E L F D Y L V K K G R L T P K E A R K F F
HrPOPK-1 68 I E H P H I L G L H D V Y E N K K Y L Y L I L E L V S G G E L F D Y L V O K G R L I P R E A R R F F
FAR-1 kinase domain 58 L D H P N I V K L Y Q V M E T F C T L Y L V L E Y A S G G E V F D Y L V A H G R M K E K E A R A K F

SAD-1 151 R Q I I S A L D F C H A H N I C H R D L K P E N L L D E R N N I K V A D F G M A S L O V E G S M L
CG614 122 R Q I I S A L D F C H S H S I C H R D L K P E N L L D E K N N I K I A D F G M A S L O P A G S M L
HrPOPK-1 118 R Q I I S A V D Y C H N H V C H R D L K P E N L L D E K N N I K V A D F G M A S L O P E G F L L
FAR-1 kinase domain 108 R Q I V S A V Q Y T H S K N I T H R D L K A E N L L D Q D M N I K I A D F G F S N T F S L G N K L

SAD-1 201 E T S C G S P H Y A C P E V I R G E K Y D G R K A D V W S C G V I L Y A L L V G A L P F D D D N L R
CG614 172 E T S C G S P H Y A C P E V I R G E K Y D G R K A D V W S C G V I L Y A L L V G A L P F D D D N L R
HrPOPK-1 168 E T S C G S P H Y A C P E V I R G E R Y D G R T A D V W S C G V I L F A L L V G A L P F D D D N L R
FAR-1 kinase domain 158 D T F C G S P P Y A A P E L F S G K Y D G P E V D V W S L G V I L Y T L V S G S L P F D G O N L K

SAD-1 251 N L L E K V K R G V F H I P H F V P A D V L S L R A M T E V D G K R Y S L A D V F R H P V S G
CG614 222 Q L L E K V K R G V F H I P H F V P P D C Q S L L R G M I E V N P D R R L T L A E I N R H P W V T A
HrPOPK-1 218 Q L L E K V K R G V F H I P H F V P P D A Q N L L R G M I D V R P D K R L L Q Q V L O H P W M R P
FAR-1 kinase domain 208 E L R E R V L R G K Y R I P F Y M S T D C E N L L K K T L V I N P O R R S S L D N I M K D R W M N V

SAD-1 301 T T K A D P . . . E L E L M G Q V V G T H V I T G E D S T D P D V L R H M N C L G C F K D K E K L
CG614 272 G K G K E L . . . E L E L M M E V G T H V I P T A T A V D P D V L N A I C S L G C F K E K E K L
HrPOPK-1 268 G S N S Y E G V L V T P D V V F V I D C V P L P E E E S V D P D V L A S M T S L G C F C N K E K L
FAR-1 kinase domain 258 G Y E D D E

SAD-1 348 I N E L S P K H N Y E K M V Y F L L D K R R R P A Q E D D T E I V L R G . . . A A Q N N D P P R
CG614 319 I Q E L L S S S H N T E K V Y F L L L E R K R R R P A L E D D D E I A Q K R S E L D A V D P P R
HrPOPK-1 318 L K N L I T E E Q N T E K V V Y M L L R R K R Y P S F D D D A D I S L P C K H P D A P R

SAD-1 366 K R T D S S R T S R Y P M . . . G S I A D G S P I N P R K . . . T Y G R N Q K S G R H S S L G G S P
CG614 369 K R L D T C R I N G T N A P S Y G O I S E G S P L T P R R Q A F N F R S Y S S T R N H Q R R S P T T
HrPOPK-1 363 K R V D S T S S L S S S N . . . G D D W C V N P I P Q R

SAD-1 440 T E S P R S T R D L F G S S S G S Y S A R A G E D R D R R S A R S T N S Y H Y T Q P V D P
CG614 419 V T S S V R S S S Y H S P T R C N S P M S S A Q Q Q A N A I S R P S P A A G T R H S T Y G D R D R
HrPOPK-1 388 . . . K M S A E S L C L T D S S S P L L S R K K S T E T H O R S Q B L T G E S N S R L V C N I S D

SAD-1 480 Q T L A E A R H Y R D A Q E R R E S R D S G R G S S R K E S K D
CG614 469 S G H H S S Y S R T P S H S S Q K S I E G D V V V V R E P R I E R R D S L R Q E R G G S P R D R G
HrPOPK-1 434 Q T K A E S K S R I N G T P V R R G T T C S

SAD-1 529 R S D K S A S S S S C K N D A S S T S S V H K Y S P P S V M S E S V V S S T M N S T N S S T N
CG614 519 D C G I P P G S P G . G N S S G S T S A S P S V H H R A N S G P T A I I V N P N G S P M M N S S
HrPOPK-1 466 G N Q P V P Q I N T P A S P N

SAD-1 573 S L I A G N S Q T S I G S T S G P R S K L N N I K N S F L G Y P R F H R R K S S N G T A E S D S E
CG614 568 P G M P G S P C N T P G G Q . L W K T R L T N I K N S F L G S P R F H R R K M Q V S A D E V H L T
HrPOPK-1 471 P R O R L A S L K N T F M G S P R F H R R K M Q A P S E D . . . V

SAD-1 623 D S Q M I D T T D L V K K S W F G S L A S S M S V E R D D T H C V P V G G K T L N S T K A E
CG614 616 P E S S P E L T K R S W F G N L I T T E K D E T F T I L V K G . K P I A I S V K A E
HrPOPK-1 503 E N Q G N S S S E L S K R S W F G N F M S S R Y S S T E H C D E L P Y A I A Y K N R T L N S V K S E

SAD-1 669 L I R A F L Q T H E L S H S V V G Q M C F R V E Y K R . G P T V G G S V F S G I K M N V D I I P S
CG614 656 L I H A F L S M A E L S H S V V S P T S F R V E Y K R . . N G N G P V M F O R H V K F Q V D I S A I
HrPOPK-1 553 L V H A F L S I P N L T H S M V S P T R F R C D Y R S S S G T S T S V F H O R S I K F Q V D I I Q H

SAD-1 718 P Q Q . V V I A G E T P T Y V V G F V L L A G P V R R F R L V E H L S A I L Q N S T O
CG614 704 C K Q G . D I A D M L F A L T F T L L S G N I R R F R R I C E H I Q S O V C S K R F
HrPOPK-1 603 S S L D R Q E N G K K P S S Q T V G S E T I A S L I S P I R R Y K R V L E L L O M O M S I V A A

SAD-1 761 Q R A D R Q Q A A L M V R P R R L S D S S V G S A C S D S E S N A S S I N M I A R H S D K T E T T
CG614 745 P G P S S P P T V T S V T Q A V S
HrPOPK-1 653 N Q O N K

SAD-1 811 S A T S S D P Y G P S P M R S V G S G T A N E Y K S P T P H R I R N T T A V T A S S S S A S N R Y G
CG614 762 E S S C G S V B S E R L S Y K R Q V I E N D M E N D S I F S Y K S G
HrPOPK-1 658 T S G E F S A F S H E I Q Q L C K T V N N L H Q D N S T M A I N N P N

SAD-1 861 P S S S S S G S Y S N N A D Y S Y H P . . . E Y S Q R S N G S S A P K N Q Y S P G S Q R S F A F S M F
CG614 797 N G R R A S T T N N N N A N P V D I P G S P I A V R S N S E T A E H E R N R E L Q S E R Q A T T M S
HrPOPK-1 683 H K S K V K

SAD-1 909 N K A D K V
CG614 847 G S A I A

THE UNIVERSITY OF CHICAGO
DIVISION OF THE PHYSICAL SCIENCES
DEPARTMENT OF CHEMISTRY
5708 SOUTH CAMPUS DRIVE
CHICAGO, ILLINOIS 60637

PHYSICAL CHEMISTRY
PHYSICAL CHEMISTRY
PHYSICAL CHEMISTRY
PHYSICAL CHEMISTRY
PHYSICAL CHEMISTRY

corresponding to this ORF (gift of Yuji Kohara) and performed RT-PCR to clone the 5' end of the gene. The major full-length cDNA is predicted to encode a protein of 914 amino acids. We sequenced all exons and intron/exon boundaries in the seven *sad-1* alleles and found molecular lesions in six (Figure 4B). We conclude that mutations in this ORF are responsible for the *sad-1* phenotype.

sad-1 encodes a novel protein predicted to encode a serine/threonine kinase. There are highly conserved homologs of *sad-1* in *Drosophila*, the ascidian *Halocynthia roretzi*, and humans, but the functions of these homologs are unknown. The *H. roretzi* homolog, HrPOPK-1, was discovered in a search for mRNAs that localize to the posterior pole of the ascidian one cell embryo (Sasakura et al., 1998); the *Drosophila* homolog was identified by the genome sequencing project (Adams et al., 2000); and the human homolog is represented by an expressed sequence tag (EST) from an infant brain cDNA library. All four homologs share an N-terminal kinase domain (>82% identity) followed by a short conserved region, an unconserved linker, and a conserved 167 amino acid C-terminal domain (>39% identity) (Figure 4B).

The SAD-1 kinase domain shows homology to the AMPK/SNF1 family of serine/threonine kinases, with strongest similarity in *C. elegans* to PAR-1 (Guo and Kemphues, 1995). SAD-1 and PAR-1 share extensive similarity throughout their kinase domains (51% identity) but are not conserved outside this domain (Figures 4B,D). PAR-1 is related to a family of vertebrate kinases that includes MARK1, MARK2/EMK1, and MARK3/C-TAK1/Kp78 (Drewes et al., 1998) (see Figure 4C for a phylogenetic analysis).

Six of the seven *sad-1* alleles have identical phenotypes, with one allele, *ju53*, exhibiting a less severe SNB-1::GFP phenotype. The allele *ky289* contains an early nonsense mutation that truncates the predicted protein in the middle of the kinase domain. *ky289* likely represents the null phenotype of *sad-1*. *ky281* and *ky330* contain charge substitutions in highly conserved regions of the kinase domain; in particular, the *ky330* E173K mutation occurs four residues from the active site aspartate residue that is conserved in almost all known kinases. These point mutations suggest that the kinase activity of SAD-1 is essential for its function. The weaker *ju53* allele is a glycine to arginine substitution in a less conserved region of the kinase domain. *ky344* and *ky326* encode proteins that

1. The first part of the document is a list of names and addresses of the members of the committee. The names are listed in alphabetical order, and the addresses are given in full. The list includes the names of the members of the committee, the names of the members of the sub-committee, and the names of the members of the advisory committee. The addresses are given in full, including the street name, the city, the state, and the zip code.

2. The second part of the document is a list of the names and addresses of the members of the committee. The names are listed in alphabetical order, and the addresses are given in full. The list includes the names of the members of the committee, the names of the members of the sub-committee, and the names of the members of the advisory committee. The addresses are given in full, including the street name, the city, the state, and the zip code.

retain an intact kinase domain but are missing C-terminal regions. *ky344* is a 5' splice site mutation at the border of intron 8 and exon 9 that is predicted to inhibit splicing and truncate SAD-1 soon after amino acid 475. *ky326* is a deletion of amino acids 805-831 that leads to a subsequent frameshift in the *sad-1* gene; the resultant protein would be effectively truncated at amino acid 805. These results suggest that the C-terminal 111 amino acids are also essential for SAD-1 function. An alternative explanation is that mutations in *ky344* and *ky326* affect the kinase domain indirectly by destabilizing *sad-1* mRNA. *C.elegans* transcripts containing premature stop codons are degraded through a pathway of *smg* genes; for example, in *smg-3* mutants nonsense transcripts are stabilized (Pulak and Anderson, 1993). The phenotype of *smg-3; sad-1(ky344)* animals was indistinguishable from that of *sad-1(ky344)* animals alone, suggesting that the protein itself is defective and not just the RNA (data not shown).

SAD-1 is expressed in neurons at the time of synaptogenesis and localizes to synapse-rich regions of axons

To determine where *sad-1* was expressed we used 5' regulatory elements from the *sad-1* locus to drive expression of GFP in transgenic animals. GFP was cloned in frame to the second exon of SAD-1 to create a protein fusion between the first 29 amino acids of SAD-1 and GFP (Figure 5A; this clone included 2 kb of upstream promoter sequences and the 6.6 kb first intron). In animals transgenic for the p_{sad-1} GFP construct fluorescence was seen throughout the entire nervous system beginning at late embryogenesis and continuing through adulthood (Figure 5B-D). We observed no expression in any tissues outside of the nervous system. Within the neurons, GFP fluorescence was uniformly distributed, indicating that the small portion of SAD-1 protein fused to GFP did not localize to a particular region. To confirm the *sad-1* expression suggested by p_{sad-1} GFP we generated antibodies against a unique region of SAD-1. Only weak expression of SAD-1 was visible in wild-type animals, but in animals overexpressing SAD-1 from the endogenous promoter and stained with anti-SAD-1 antibody, we observed fluorescence throughout the nervous system (Figures 5E,G and data not shown). As with p_{sad-1} GFP, expression was first seen in the late embryo. We

1. The first part of the document is a list of names and addresses of the members of the committee. The names are listed in alphabetical order, and the addresses are listed below each name. The list includes the names of the members of the committee, the names of the members of the sub-committee, and the names of the members of the advisory committee. The addresses are listed in the same order as the names.

2. The second part of the document is a list of the names and addresses of the members of the committee. The names are listed in alphabetical order, and the addresses are listed below each name. The list includes the names of the members of the committee, the names of the members of the sub-committee, and the names of the members of the advisory committee. The addresses are listed in the same order as the names.

Figure 5. SAD-1 expression and protein localization

(A-D) *sad-1* regulatory sequences were used to drive the expression of GFP (A). GFP was fused in frame to the second exon of *sad-1*. The portion of the *sad-1* locus used included 2 kb of upstream promoter sequences and the 6.6 kb first intron. p_{sad-1} GFP expression was seen exclusively in the nervous system beginning in the late embryo (B) and continuing through the life of the animal (C,D). (E,G) Anti-SAD-1 antibody staining of animals overexpressing SAD-1 from the endogenous promoter. (F,H) p_{str-3} SNB-1::GFP expression in the same animals. (E) In some animals fluorescence was confined to axons of the nerve ring (thick arrow) and ventral (white arrowhead) and dorsal (yellow arrowhead) cords, and to cell bodies (asterisk). No staining was observed in the sensory dendrites (thin arrow) or axon commissures. In these animals ASI neuron morphology was normal (F). (G) In other animals fluorescence was present in the dendrites (thin arrow) and commissures (yellow arrow) in addition to the axon and cell body staining seen in (E). In these animals axons were terminated (H, thick arrow) or otherwise defective, and some vesicle clusters appeared in the dendrite (H, thin arrow). (I) A full-length SAD-1::GFP fusion protein was expressed in the nervous system using the *unc-115* promoter. GFP was inserted in frame at amino acid 566 of the SAD-1 protein. Sequences 5' to GFP were from the *sad-1* cDNA and sequences 3' were from the *sad-1* genomic clone. Shading of domain structure as in Figure 4(B), GFP in green. (J) SAD-1::GFP localized to puncta within the axons of the nerve ring (thick arrow) and ventral (white arrowhead) and dorsal (yellow arrowhead) nerve cords but was faint or absent in the dendrites (thin arrow) and synapse-poor commissures. Additionally, SAD-1::GFP was observed in cell bodies, where it was excluded from the nucleus (asterisk). These animals were fixed with formaldehyde to eliminate gut autofluorescence. (K) A higher magnification of the ventral cord in animals expressing $p_{unc-115}$ SAD-1::GFP (green) and costained with anti-SYD-2 (red) antibodies. There is a high density of punctate staining in this region, but little colocalization of SAD-1::GFP and SYD-2 was evident (e.g. arrowhead). (L) A higher magnification of the dorsal cord in animals overexpressing SAD-1 from its own promoter and costained with anti-SAD-1 (red) and anti-SNT-1 (green) antibodies. Many SAD-1 puncta partially colocalized with SNT-1 puncta, as

1. The first part of the document is a list of names and addresses of the members of the committee. The names are listed in alphabetical order, and the addresses are given in full. The list includes the names of the members of the committee, the names of the members of the sub-committee, and the names of the members of the advisory committee. The addresses are given in full, including the street, city, and state.

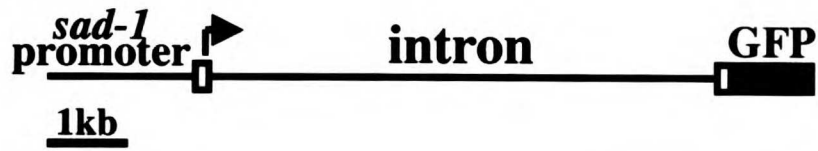
2. The second part of the document is a list of the names and addresses of the members of the committee. The names are listed in alphabetical order, and the addresses are given in full. The list includes the names of the members of the committee, the names of the members of the sub-committee, and the names of the members of the advisory committee. The addresses are given in full, including the street, city, and state.

evident by the yellow color (white arrowheads), or were immediately adjacent to SNT-1 puncta (orange arrowheads). Some SAD-1 puncta were not associated with SNT-1 puncta (yellow arrowheads). Scale bars: 10 μ m.

1. The first part of the document is a list of names and addresses of the members of the committee. The names are listed in alphabetical order, and the addresses are given in full. The list includes the names of the members of the committee, the names of the members of the sub-committee, and the names of the members of the advisory committee. The addresses are given in full, including the street, city, and state.

2. The second part of the document is a list of the names and addresses of the members of the committee. The names are listed in alphabetical order, and the addresses are given in full. The list includes the names of the members of the committee, the names of the members of the sub-committee, and the names of the members of the advisory committee. The addresses are given in full, including the street, city, and state.

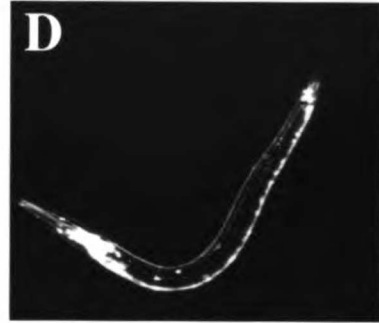
A



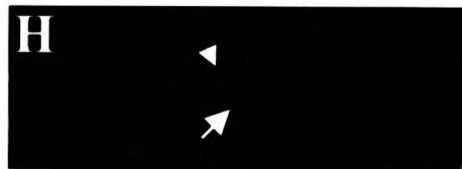
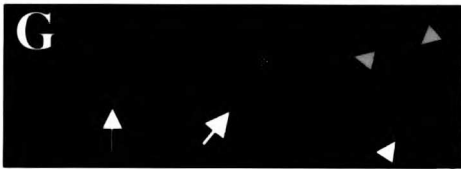
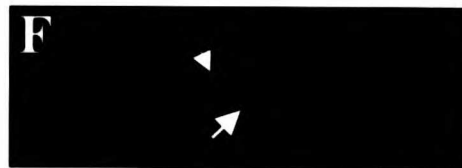
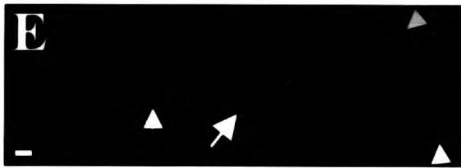
late embryo



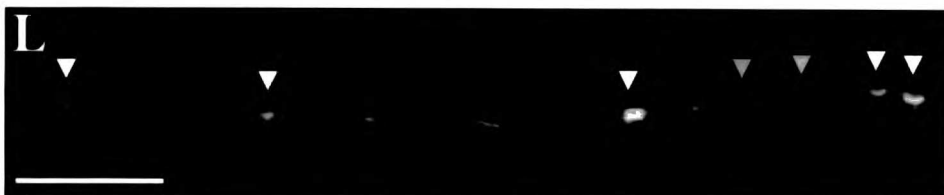
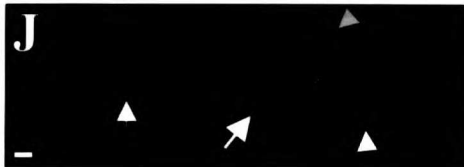
L1 larva



L2 larva



I



1. The first part of the document is a list of names and addresses of the members of the committee. The names are listed in alphabetical order, and the addresses are given in full. The list includes the names of the members of the committee, the names of the members of the sub-committee, and the names of the members of the advisory committee. The addresses are given in full, including the street, city, and state.

2. The second part of the document is a list of the names and addresses of the members of the committee. The names are listed in alphabetical order, and the addresses are given in full. The list includes the names of the members of the committee, the names of the members of the sub-committee, and the names of the members of the advisory committee. The addresses are given in full, including the street, city, and state.

observed no consistent anti-SAD-1 staining in *sad-1(ky289)* null animals, suggesting that the antibodies are specific for SAD-1 protein. The onset of *sad-1* expression in the late embryo is consistent with a role for SAD-1 in synaptogenesis, as this is the time when many synapses are first made.

Since *sad-1* animals have specific defects in synaptic development, we asked whether SAD-1 protein localizes to synaptic regions. The pan-neuronal *unc-115* promoter (Lundquist et al., 1998) was used to express a SAD-1::GFP fusion protein in which GFP was inserted in the variable linker region that connects the N-terminal kinase domain with the conserved C-terminal domain (Figure 5I). Both wild-type SAD-1 and this GFP fusion caused paralysis and other phenotypes when expressed at high concentrations (discussed in more detail below), but at the lower concentrations examined in this experiment $p_{unc-115}$ SAD-1::GFP did not cause locomotion defects. SAD-1::GFP fluorescence was most prominent in the nerve ring and the ventral and dorsal cords, regions of the axon where the majority of synapses are made (Figure 5J). Little or no staining was observed in the sensory dendrites or the axonal commissures, which are devoid of synapses. Weaker fluorescence was visible in the neuronal cell bodies excluded from the nucleus.

This general pattern of localization to synapses was confirmed using antibody staining of animals overexpressing SAD-1 from its own promoter. When SAD-1 localization was examined in animals that did not exhibit gain-of-function phenotypes (Figure 5F and see below) SAD-1 expression was very similar to that of $p_{unc-115}$ SAD-1::GFP. Staining was present in synapse-rich regions of the nerve ring and nerve cords and in the cell bodies, but no staining was observed in the sensory dendrites or axonal commissures (Figure 5E). This result suggests that at more physiological levels SAD-1 preferentially localizes to synaptic regions.

Both $p_{unc-115}$ SAD-1::GFP and SAD-1 stained with anti-SAD-1 antibodies appeared as a combination of punctate and diffuse staining within the axon (Figures 5J-L). The SAD-1::GFP puncta were unaltered in *unc-104* mutants, indicating that SAD-1 is not dependent on synaptic vesicles for localization (data not shown). Costaining of animals expressing $p_{unc-115}$ SAD-1::GFP with anti-SYD-2 antibodies revealed that SAD-1 and SYD-2 localize to different compartments

1. The first part of the document is a list of names and addresses of the members of the committee. The names are listed in alphabetical order, and the addresses are given in full. The list includes the names of the members of the committee, the names of the members of the sub-committee, and the names of the members of the advisory committee. The addresses are given in full, including the street, city, and state.

2. The second part of the document is a list of the names and addresses of the members of the committee. The names are listed in alphabetical order, and the addresses are given in full. The list includes the names of the members of the committee, the names of the members of the sub-committee, and the names of the members of the advisory committee. The addresses are given in full, including the street, city, and state.

within the axon that did not overlap (Figure 5K). However, SAD-1 is likely associated with synapses, as SAD-1 partially colocalized with SNT-1, the synaptotagmin protein associated with synaptic vesicles (Nonet et al., 1993)(Figure 5L). Most SNT-1 staining was either overlapping with or immediately adjacent to a spot of SAD-1 staining. This result suggests that SAD-1 is present at or near most synaptic vesicle clusters. Some SAD-1 staining was also observed in regions devoid of SNT-1; this staining may reflect a nonsynaptic role for SAD-1 or may be a consequence of SAD-1 overexpression. These results suggest that SAD-1 localizes to a perisynaptic region that is adjacent to the SYD-2 (active zone) region and near synaptic vesicles.

SAD-1 is present in motor neurons but not in the muscles they innervate; this observation suggests that SAD-1 functions cell-autonomously in the motor neurons to control presynaptic vesicle clustering. To test this hypothesis further we placed SAD-1 under the control of the *unc-25* promoter to drive expression specifically in the VD and DD motor neurons, and scored VD/DD SNB-1::GFP defects in *sad-1* animals expressing p_{unc-25} SAD-1. SNB-1::GFP vesicle clusters in *sad-1* animals expressing p_{unc-25} SAD-1 appeared more punctate and showed increased intensity compared to vesicle clusters in *sad-1* mutant animals, though they were not fully restored to wild-type (data not shown). We conclude that SAD-1 can function presynaptically to promote presynaptic differentiation, but may have either non-autonomous effects or specific temporal requirements for expression that are not fully met by the *unc-25* promoter.

SAD-1 overexpression induces ectopic vesicle clusters

Analysis of *sad-1* loss-of-function mutants suggested that SAD-1 is necessary for normal clustering of presynaptic vesicles. To determine whether SAD-1 is sufficient to induce vesicle clustering we analyzed the effects of increased SAD-1 activity. SAD-1 activity was increased by generating transgenic animals with high levels of a wild-type SAD-1 transgene expressed under its own promoter. Overexpression of SAD-1 caused severe locomotion defects (Figures 6A,B) as well as axon guidance defects (see below). However, the pattern of SNB-1::GFP clusters in the axons was superficially normal when axons

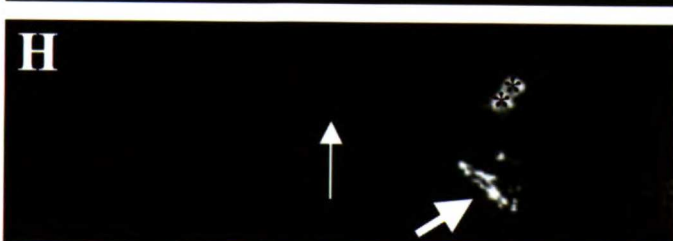
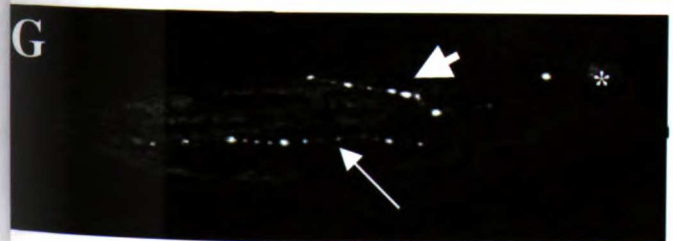
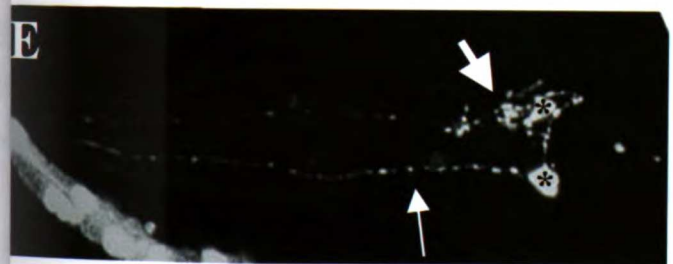
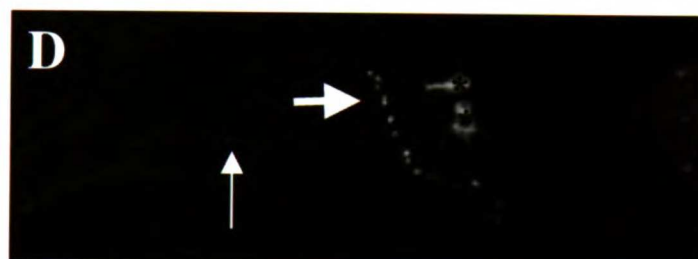
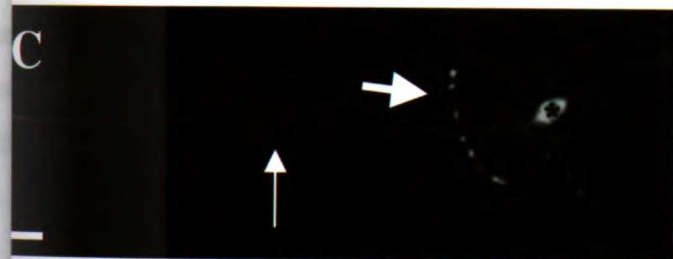
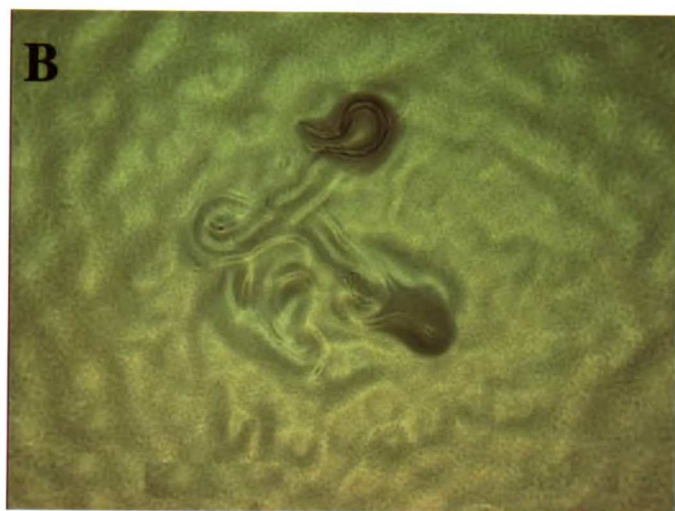
THE UNIVERSITY OF CHICAGO
DEPARTMENT OF CHEMISTRY
58 CHEMISTRY BUILDING
CHICAGO, ILLINOIS 60637
TEL: (773) 835-3131
FAX: (773) 835-3132
WWW: WWW.CHEM.UCHICAGO.EDU

PHYSICAL CHEMISTRY
LECTURE 1
THERMODYNAMICS
AND
STATISTICAL MECHANICS
PROF. J. CHEUNG

Figure 6. SAD-1 overexpression promotes the formation of vesicle clusters
(A) Wild-type animals moved in a sinusoidal pattern on a bacterial lawn. (B) Animals overexpressing SAD-1 from the endogenous promoter moved very little from where they were placed on the lawn, and their locomotion was severely uncoordinated. (C-H) Confocal epifluorescence micrographs showing expression of SNB-1::GFP in the ASI neurons of wild-type (C), SAD-1 overexpressing (D-G), and *unc-33(e204)* (H) animals. Anterior is left and dorsal is up. Thin arrows point to dendrites, thick arrows point to axons, and asterisks denote cell bodies. SNB-1::GFP clusters in the axons of SAD-1 overexpressing animals appeared more numerous (D,E) and perhaps more sharply defined (D) than the SNB-1::GFP clusters in the axons of wild-type animals (C). In some SAD-1 overexpressing animals SNB-1::GFP clusters were seen in the dendrites (E-G). Compare this to the faint, diffuse SNB-1::GFP fluorescence occasionally seen in the dendrites of wild-type animals (C). The axons of SAD-1 overexpressing animals were often prematurely terminated or misguided (E-G). In *unc-33(e204)* animals axons were affected to a similar degree, but SNB-1::GFP clusters were not visible in the dendrite (H). Scale bar: 10 μm .

1. The first part of the document is a list of names and addresses of the members of the committee. The names are listed in alphabetical order, and the addresses are given in full. The list includes the names of the members of the committee, the names of the members of the sub-committee, and the names of the members of the advisory committee. The addresses are given in full, including the street, city, and state.

2. The second part of the document is a list of the names and addresses of the members of the committee. The names are listed in alphabetical order, and the addresses are given in full. The list includes the names of the members of the committee, the names of the members of the sub-committee, and the names of the members of the advisory committee. The addresses are given in full, including the street, city, and state.



1. The first part of the document is a list of names and addresses of the members of the committee. The names are listed in alphabetical order, and the addresses are listed below each name. The list includes names such as Mr. J. H. Smith, Mr. J. B. Jones, and Mr. W. C. Brown.

2. The second part of the document is a list of the names and addresses of the members of the committee who have been elected to the office of chairman. The names are listed in alphabetical order, and the addresses are listed below each name. The list includes names such as Mr. J. H. Smith, Mr. J. B. Jones, and Mr. W. C. Brown.

were not malformed (Figure 6D). If anything, SAD-1 overexpressing animals appeared to have very bright clusters, suggesting an increased number of vesicles per cluster, and possibly an increased number of SNB-1::GFP clusters in axons (Figures 6D,E). Surprisingly, we also observed ectopic SNB-1::GFP clusters in the dendrite (Figures 6E-G). These dendritic clusters were similar in size and spacing to the normal axonal clusters in wild-type animals (Figure 6C). The appearance of dendritic vesicle clusters is not a secondary consequence of axon outgrowth defects, as similar clusters were not observed in other mutants that affected axon outgrowth (e.g. *unc-33(e204)* (Figure 6H) and data not shown). These results show that increased SAD-1 activity can promote SNB-1::GFP clusters in ectopic locations.

SAD-1 regulates axonal branching and termination

In *sad-1* animals the ASI neurons occasionally exhibited extra axon branches emanating from the primary axon in the area of the nerve ring (Figure 2G). To characterize this phenomenon more carefully at the single cell level we examined the axonal morphology of another chemosensory neuron, the AWC neuron, in *sad-1* animals. p_{str-2} GFP is expressed in a single AWC neuron (Troemel et al., 1999). AWC has an unbranched axon that extends ventrally, travels anteriorly to the nerve ring, circles the nerve ring, and terminates on the contralateral ventral side of the animal (Figure 7A). In wild-type animals expressing the p_{str-2} GFP reporter the AWC axon invariably terminated at the ventral side. In 18% (n=216) of *sad-1* animals the AWC axon failed to terminate at its correct position. Instead of terminating at the ventral side of the animal the AWC axon either reentered the nerve ring and returned to the dorsal side (Figure 7B) or traveled further posteriorly (Figure 7C) or anteriorly (Figure 7D). In addition, in 8% of these animals small ectopic branches emanated from the primary axon shaft (data not shown). In contrast to the ectopic sensory axon branches seen in mutants with altered electrical activity (Peckol et al., 1999), the branches in *sad-1* mutants were visible in early larvae and did not increase in penetrance over time. The failure of axons to terminate properly is not a secondary consequence of aberrant vesicle clustering; in *unc-104* mutants vesicle

1. The first part of the document is a list of names and addresses of the members of the committee. The names are listed in alphabetical order, and the addresses are given in full. The list includes the names of the members of the committee, the names of the members of the sub-committee, and the names of the members of the advisory committee. The addresses are given in full, including the street name, the city, the state, and the zip code.

2. The second part of the document is a list of the names and addresses of the members of the committee. The names are listed in alphabetical order, and the addresses are given in full. The list includes the names of the members of the committee, the names of the members of the sub-committee, and the names of the members of the advisory committee. The addresses are given in full, including the street name, the city, the state, and the zip code.

3. The third part of the document is a list of the names and addresses of the members of the committee. The names are listed in alphabetical order, and the addresses are given in full. The list includes the names of the members of the committee, the names of the members of the sub-committee, and the names of the members of the advisory committee. The addresses are given in full, including the street name, the city, the state, and the zip code.

Figure 7. Reciprocal axon phenotypes in *sad-1* mutants and SAD-1 overexpressing animals

Confocal epifluorescence micrographs of wild-type (A), *sad-1(ky332)* (B-D), *unc-104(e1265)* (E), and SAD-1 overexpressing (F-J) animals expressing p_{str-2} GFP (A-E, G-J) or p_{str-3} SNB-1::GFP (F). Anterior is left and dorsal is up. p_{str-2} GFP labels a single AWC neuron. In A-G arrows denote the axon termination points. In wild-type animals, the axon of the AWC neuron terminates at the ventral side of the animal (A). In 18% of *sad-1(ky332)* mutants the AWC axon fails to terminate at the proper position and either reenters the nerve ring (B) or continues posteriorly (C) or anteriorly (D). In *unc-104(e1265)* animals the AWC axon terminates at the proper location 100% of the time (E). In SAD-1 overexpressing animals the ASI (F) and AWC (G) axons were often prematurely terminated. In other SAD-1 overexpressing animals the axons were branched (H) and misguided (thick arrow) (I). Occasionally, dendrites of AWC neurons were also prematurely terminated (thin arrow) (I), and in rare cases the axon was missing (thick arrow) and the dendrite was prematurely terminated and misshapen (thin arrow) (J). Scale bar: 10 μ m.

1. The first part of the document discusses the importance of maintaining accurate records of all transactions. It emphasizes that proper record-keeping is essential for the integrity of the financial system and for the ability to detect and prevent fraud.

2. The second part of the document outlines the specific procedures that must be followed when recording transactions. It details the requirements for the format and content of records, as well as the responsibilities of the individuals involved in the recording process.

3. The third part of the document addresses the issue of the retention of records. It specifies the minimum period for which records must be kept and the conditions under which they may be destroyed or disposed of.

4. The fourth part of the document discusses the importance of the confidentiality of records. It outlines the measures that must be taken to protect records from unauthorized access and disclosure.

5. The fifth part of the document discusses the importance of the accuracy of records. It outlines the measures that must be taken to ensure that records are complete, correct, and reliable.

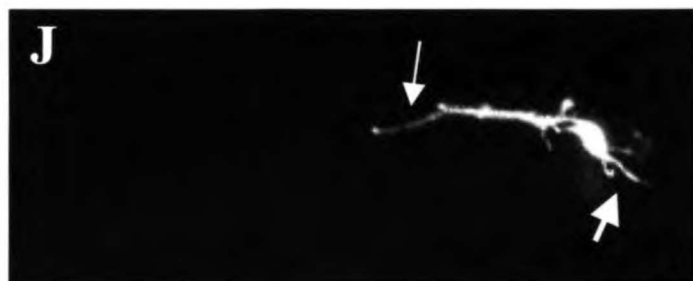
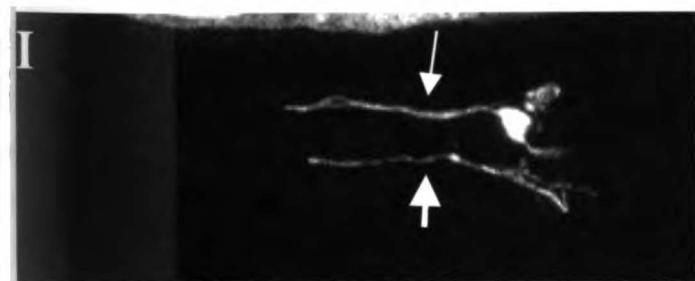
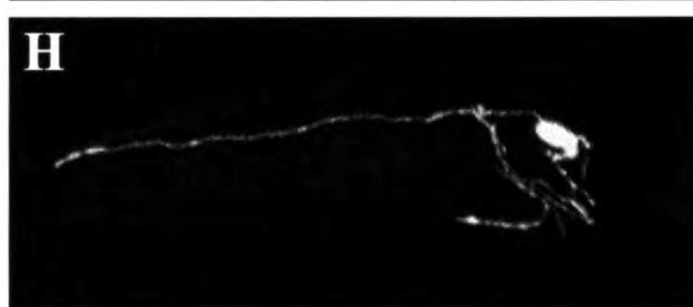
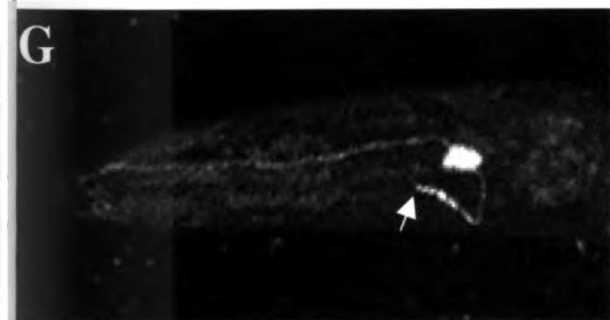
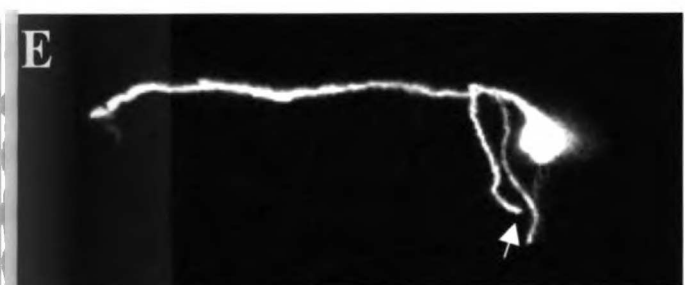
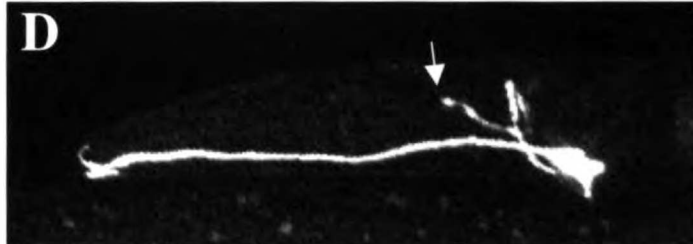
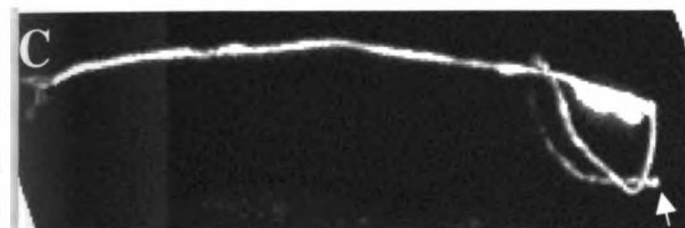
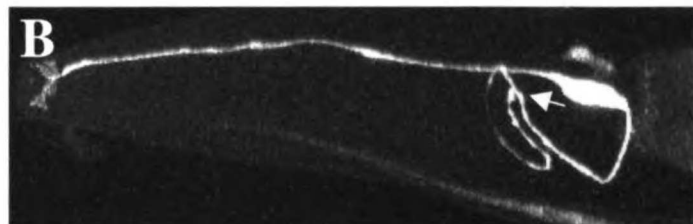
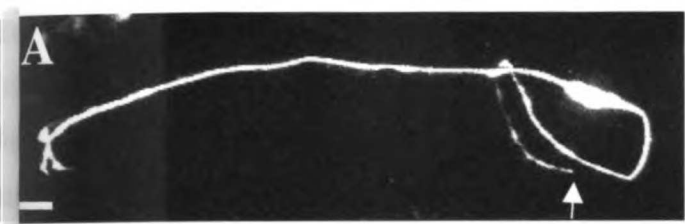
6. The sixth part of the document discusses the importance of the accessibility of records. It outlines the measures that must be taken to ensure that records are available to authorized personnel when needed.

7. The seventh part of the document discusses the importance of the security of records. It outlines the measures that must be taken to protect records from theft, loss, and damage.

8. The eighth part of the document discusses the importance of the integrity of records. It outlines the measures that must be taken to ensure that records are not tampered with or altered.

9. The ninth part of the document discusses the importance of the consistency of records. It outlines the measures that must be taken to ensure that records are prepared and maintained in a uniform manner.

10. The tenth part of the document discusses the importance of the transparency of records. It outlines the measures that must be taken to ensure that records are open to public scrutiny.



1. The first part of the document discusses the importance of maintaining accurate records of all transactions. It emphasizes that proper record-keeping is essential for the integrity of the financial system and for the ability to detect and prevent fraud.

2. The second part of the document outlines the specific requirements for record-keeping, including the need to maintain original documents and to keep them in a secure and accessible location.

3. The third part of the document discusses the role of the auditor in verifying the accuracy of the records. It notes that the auditor must exercise professional judgment and skepticism in evaluating the evidence provided by the client.

clusters are absent, yet axons terminate at the correct position and do not branch (Figure 7E). Conversely, the vesicle clustering defects cannot solely be a consequence of the axon defects as they were more highly penetrant than the axon defects (>95% vs. 26%).

In addition to the vesicle clustering defects described above, overexpression of SAD-1 caused animals to be paralyzed (Figure 6B). Animals overexpressing SAD-1 exhibited a spectrum of axon defects in both the ASI and AWC sensory neurons: these included premature termination (Figures 7F,G,J), axonal spreading and branching (Figure 7H), and severe guidance defects (Figures 6G and 7I). Occasionally, dendrite termination and branching were observed in the AWC neuron (Figure 7J). In the most severely affected strains with SAD-1 overexpression, ASI axon defects were present in 100% of the animals. In strains less severely affected for locomotion the most common defect of ASI and AWC axons was premature termination, suggesting that premature termination represents the less severe manifestation of SAD-1 overexpression. At presumably higher levels of SAD-1 overexpression axons became misguided and developed multiple branches (Figure 7H,I). At the presumably highest levels of SAD-1 overexpression, both the dendrite and axon were prematurely terminated and severely misshapen (Figure 7J). We observed a correlation between the presence of ASI neuron morphology defects and increased delocalization of SAD-1 protein. When SAD-1 was localized only to synapse-rich regions, the ASI neurons appeared morphologically normal (Figure 5E,F). When overexpressed SAD-1 protein was no longer confined to synapse-rich regions of the axon and became evident in sensory dendrites and axonal commissures, ectopic vesicle clusters appeared in the dendrite, and axons were malformed (Figures 5G,H). We suggest that overall increases in SAD-1 activity inhibit axon outgrowth, and that mislocalization of SAD-1 to dendrites causes ectopic clusters to form in dendrites.

Discussion

The SAD-1 kinase regulates presynaptic vesicle clustering

1
2
3
4
5
6
7
8
9
10
11
12
13
14
15
16
17
18
19
20
21
22
23
24
25
26
27
28
29
30
31
32
33
34
35
36
37
38
39
40
41
42
43
44
45
46
47
48
49
50
51
52
53
54
55
56
57
58
59
60
61
62
63
64
65
66
67
68
69
70
71
72
73
74
75
76
77
78
79
80
81
82
83
84
85
86
87
88
89
90
91
92
93
94
95
96
97
98
99
100

101
102
103
104
105
106
107
108
109
110
111
112
113
114
115
116
117
118
119
120
121
122
123
124
125
126
127
128
129
130
131
132
133
134
135
136
137
138
139
140
141
142
143
144
145
146
147
148
149
150
151
152
153
154
155
156
157
158
159
160
161
162
163
164
165
166
167
168
169
170
171
172
173
174
175
176
177
178
179
180
181
182
183
184
185
186
187
188
189
190
191
192
193
194
195
196
197
198
199
200

A defining feature of presynaptic differentiation is the clustering of neurotransmitter-filled vesicles near active zones and postsynaptic neurotransmitter receptor clusters. We have identified a new serine/threonine kinase, SAD-1, that affects the size, shape, position, and number of vesicle clusters. Although we set out to identify molecules specifically required for synapses between neurons, *sad-1* mutants have defects at both neuron-to-neuron and neuromuscular synapses.

In general, decreasing and increasing SAD-1 activity have reciprocal effects on vesicle clustering. In *sad-1* mutant animals vesicle clusters are smaller, more diffusely distributed, mislocalized, and irregularly spaced within the axon. SAD-1 is not absolutely required for vesicle clustering as vesicle clusters still form in null *sad-1* animals. Overexpression of SAD-1 induces the formation of well-organized SNB-1::GFP-containing vesicle clusters in the dendrite. These clusters are indistinguishable in size, shape, and spacing from those normally seen in axons. We do not know to what extent these ectopic vesicle clusters express other synaptic vesicle proteins and participate in neurotransmitter release, nor do we have any evidence for the presence of ectopic active zones in the dendrite. SAD-1 is normally localized to axons, but overexpression of SAD-1 causes some SAD-1 to be mislocalized to the dendrite, where its appearance correlates with the appearance of ectopic vesicle clusters. This result suggests that increased SAD-1 activity can induce new vesicle clusters.

SAD-1 does not appear to control all aspects of presynaptic differentiation. A protein associated with presynaptic active zone regions, SYD-2, localizes normally in *sad-1* mutants, suggesting that SAD-1 is not necessary for active zone formation. By contrast, in *syd-2* mutants active zones are wider than normal (Zhen and Jin, 1999). The additive phenotype of *syd-2 sad-1* double mutants suggests that SYD-2 and SAD-1 function in independent pathways. Thus, SAD-1 presumably acts in concert with other regulatory molecules to coordinate different facets of presynaptic development.

How might SAD-1 regulate vesicle clustering? SAD-1 partially colocalizes with the synaptic vesicle protein SNT-1 but is not dependent on synaptic vesicles for its localization. In addition, SAD-1 does not colocalize exactly with the active zone protein SYD-2. These results suggest that SAD-1 localizes to a peripheral

1. The first part of the document is a list of names and addresses of the members of the committee. The names are listed in alphabetical order, and the addresses are listed below each name. The list includes names such as Mr. J. H. Smith, Mr. J. B. Jones, and Mr. W. C. Brown.

2. The second part of the document is a list of the names and addresses of the members of the committee who were present at the meeting. The names are listed in alphabetical order, and the addresses are listed below each name. The list includes names such as Mr. J. H. Smith, Mr. J. B. Jones, and Mr. W. C. Brown.

domain near active zones that is in close proximity to vesicle clusters. One model is that the interaction between pre- and post- synaptic cells establishes active zones through pathways that are independent of SAD-1 function; subsequent signals near active zones activate the SAD-1 kinase, which recruits and shapes vesicle clusters. When overexpressed, the SAD-1 kinase is mislocalized and can be activated independent of the active zone to induce vesicle clusters in ectopic locations. Several mutations in *sad-1* map to the kinase domain, indicating that the kinase activity of SAD-1 is critical to its function. SAD-1 could phosphorylate one or more targets to regulate the interaction of vesicle clusters with active zones.

Highly conserved SAD-1 homologs are found in invertebrates and vertebrates, suggesting that SAD-1 has a conserved function in all animals. Homology in the kinase domain of SAD-1 places it in the AMPK family of serine/threonine kinases (Carling et al., 1994). Within the *C. elegans* AMPK family SAD-1 shares highest similarity with PAR-1. PAR-1 is required for asymmetric cell divisions along the anterior-posterior (A-P) axis and localizes cortically to the posterior pole of the one-cell embryo (Guo and Kemphues, 1995). In *par-1* mutants P-granules and cell fate determinants such as SKN-1 fail to segregate asymmetrically to the posterior daughters of A-P cell divisions. PAR-1 is related to a family of at least three vertebrate kinases: MARK1, MARK2/EMK1, and MARK3/C-TAK1/Kp78. MARK1 and MARK2 (MAP/microtubule affinity-regulating kinases 1 and 2) were identified biochemically in rat based on their ability to phosphorylate *tau*, an axonal MAP (microtubule associated protein). Overexpression of MARK1 or MARK2 in fibroblasts disrupts microtubules and causes a loss of polarity (Drewes et al., 1997). MARK3, which phosphorylates Cdc25C phosphatase (Peng et al., 1998), localizes to the apical domain of epithelial cells (Parsa, 1988). Thus, the PAR-1-related proteins share a polarized location and possibly the ability to regulate the cytoskeleton and cell polarity. Intriguingly, the ascidian SAD-1 homolog was identified in a search for mRNAs that localize to the posterior pole of the one cell embryo (Sasakura et al., 1998). This localization suggests that PAR-1 and SAD-1 may have related functions in cell polarity, though we have no evidence that *sad-1* is expressed in early embryos.

1. The first part of the document is a list of names and addresses of the members of the committee. The names are listed in alphabetical order, and the addresses are given in full. The list includes the names of the members of the committee, the names of the members of the sub-committee, and the names of the members of the advisory committee. The addresses are given in full, including the street name, the city, the state, and the zip code.

2. The second part of the document is a list of the names and addresses of the members of the committee. The names are listed in alphabetical order, and the addresses are given in full. The list includes the names of the members of the committee, the names of the members of the sub-committee, and the names of the members of the advisory committee. The addresses are given in full, including the street name, the city, the state, and the zip code.

SAD-1 and PAR-1 share highly conserved kinase domains, yet each contains a unique C-terminal domain that is highly conserved among homologs but unrelated between SAD-1 and PAR-1. This domain of PAR-1 mediates an interaction with the non-muscle myosin NMY-2. Disruption of *nmy-2* leads to mislocalization of PAR-1 protein and loss of asymmetry in cell divisions, suggesting that the PAR-1 C-terminal domain regulates the localization and function of the kinase domain (Guo and Kemphues, 1996). C-terminal regions of the SAD-1 protein are essential for function, as *sad-1* mutations that truncate the C-terminus but leave the kinase domain intact show the null phenotype. The unique C-terminal domain of SAD-1 may provide specific regulatory or localization information that modifies the activity of the kinase domain.

The SAD-1 kinase may regulate the transition from axon outgrowth to synapse formation

During neuronal development, the end of axon outgrowth is coupled to the initiation of synaptic differentiation. In mouse mutants in which synaptic differentiation is blocked, such as the agrin and MuSK knockouts, axons extend past their targets (Gautam et al., 1996; DeChiara et al., 1996). Similarly, in *sad-1* mutants axons often fail to terminate appropriately. In addition, overexpression of SAD-1 causes axons to terminate prematurely. The reciprocal phenotypes of *sad-1* loss-of-function and SAD-1 overexpression suggest that SAD-1 has an instructive role in regulating axon outgrowth. We propose that SAD-1 has two functions: the first is to coordinate vesicle clustering with active zones and the second is to signal axons to stop elongating. We speculate that SAD-1 activation may couple the end of axon outgrowth with the beginning of presynaptic differentiation.

It is unlikely that the axon phenotypes we see are secondary to the vesicle clustering phenotypes. First, in *unc-104* animals, which lack vesicle clusters, axons never grow past their target. Second, in *unc-13* animals, in which vesicle clusters are larger and more well defined than normal, axons never terminate prematurely (Kang Shen and C.I.B., and also M.Z. and Y.J., unpublished

THE
FIRST
PART
OF
THE
HISTORY
OF
THE
PEOPLE
OF
THE
NORTH
AMERICAN
CONTINENT
FROM
THE
FIRST
DISCOVERY
TO
THE
PRESENT
TIMES
BY
JAMES
MILL
OF
THE
UNIVERSITY
OF
EDINBURGH

LONDON
PRINTED
BY
RICHARD
BENTLEY
AND
SONS
1861

observations). These observations argue that the functions of SAD-1 in vesicle clustering do not cause axon termination.

How might SAD-1 regulate axon outgrowth? The transition from a highly motile growth cone to a strong, stable synaptic adhesion likely involves modification of the cytoskeleton and cell adhesion molecules (Suter and Froscher, 1998; Grady et al., 2000). One possibility is that SAD-1 regulates the microtubule cytoskeleton, like the related PAR-1 and the MARK kinases. *par-1* affects cell polarity and the rotation of the mitotic spindle (Kemphues et al., 1988), and MARKs phosphorylate and decrease the microtubule affinity of microtubule associated proteins (MAPs) (Drewes et al., 1995) and regulate cell polarity (Drewes et al., 1997). We speculate that signaling from the postsynaptic target to the presynaptic axon may activate SAD-1, which could inhibit further axon outgrowth and promote synaptic stabilization by affecting the cytoskeleton or cell adhesion. When overexpressed at high levels SAD-1 activity may become independent of synaptic signaling and consequently cause premature axon termination. At very high levels SAD-1 is also delocalized in the cell, potentially resulting in the premature termination of both the axon and the dendrite.

SAD-1 and PAR-1 may define a new family of kinases more generally involved in controlling cell polarity

Neuronal polarity involves the assembly of presynaptic vesicle clusters and release machinery in the axon and the localization of sensory or neurotransmitter receptors to the dendrite. SAD-1 can be viewed as one regulator of neuronal polarity. SAD-1 localizes asymmetrically in neurons to synaptic regions within the axon. SAD-1 does not seem to be required for neuronal polarity, because in *sad-1* mutants the axon, though synaptically disorganized, is still different from the dendrite. However, overexpression of SAD-1 results in dendrites acquiring characteristics of axons (such as vesicle clusters). Interestingly, Wnt signals, which promote mossy fiber presynaptic differentiation, can also regulate cell polarity (Schlesinger et al., 1999; Hall et al., 2000).

1. The first part of the document discusses the importance of maintaining accurate records of all transactions. It emphasizes that proper record-keeping is essential for the integrity of the financial system and for the ability to detect and prevent fraud. The text notes that without reliable records, it would be difficult to track the flow of funds and identify any irregularities.

2. The second part of the document outlines the specific procedures for recording transactions. It details the steps involved in entering data into the system, including the use of standardized codes and the requirement for double-checking entries. The text also mentions the importance of regular audits to ensure the accuracy of the records and to identify any potential errors or discrepancies.

PAR-1 localizes asymmetrically to the posterior pole of dividing cells and is required for the polarity of A-P divisions (Guo and Kemphues, 1995). Additionally, the vertebrate PAR-1 homolog MARK2/EMK1 localizes to the lateral domain of epithelial cells where it may regulate epithelial polarity. Introduction of a dominant negative MARK2/EMK1 into epithelial cells results in decreased adhesion and the loss of asymmetric E-cadherin localization (Bohm et al., 1997). Cells undergoing asymmetric divisions, epithelial cells, and neurons are all polarized cells with asymmetric protein localization and specialized cytoskeletons. The molecular similarities between SAD-1 and PAR-1 suggest that the mechanisms generating cell polarity in different cell types may be biochemically related. As such, there may exist a larger family of cell polarity kinases in which SAD-1 has become specialized to control presynaptic development in neurons.

Experimental Procedures

Strains and Maintenance

Wild-type animals were *C. elegans* variety Bristol, strain N2. Animals were grown at 20°C on HB101 bacteria and maintained according to standard methods (Brenner, 1974). Some strains were provided by the *Caenorhabditis* Genetic Center, which is supported by the National Institutes of Health.

Screen for SNB-1::GFP defects in ASI, VD and DD neurons

p_{str-3} SNB-1::GFP was constructed by cloning a SphI-NheI PCR product containing 3kb of *str-3* upstream sequences into pSB121.51 (Nonet, 1999); an enhanced GFP from pPD95.75 was swapped with the GFP of pSB121.51 as an AgeI-ApaI fragment to increase fluorescence intensity. *lin-15(n765ts)* mutant animals were injected with p_{str-3} SNB-1::GFP at 100 ng/ul and a *lin-15(+)* pJM23 plasmid as a coinjection marker at 50 ng/ul (Huang et al., 1994). Transformants were maintained by picking animals rescued for the *lin-15* multivulval phenotype. The transgenic array was integrated into the genome using psoralen mutagenesis. One integrant, CX3572 *kyIs105; lin-15(n765ts)*, was outcrossed four times and used for subsequent analysis. *kyIs105; lin-15(n765ts)* animals were

1. The first part of the document discusses the importance of maintaining accurate records of all transactions and activities. It emphasizes that this is essential for ensuring transparency and accountability in the organization's operations.

2. The second part of the document outlines the various methods and tools used to collect and analyze data. It highlights the need for consistent data collection procedures and the use of advanced analytical techniques to derive meaningful insights from the data.

3. The third part of the document focuses on the role of technology in data management and analysis. It discusses how modern software solutions can streamline data collection, storage, and analysis processes, thereby improving efficiency and accuracy.

4. The fourth part of the document addresses the challenges associated with data management, such as data quality, security, and privacy. It provides strategies to mitigate these risks and ensure that the data remains reliable and secure throughout its lifecycle.

5. The fifth part of the document concludes by summarizing the key findings and recommendations. It stresses the importance of ongoing monitoring and evaluation to ensure that the data management processes remain effective and aligned with the organization's goals.

6. The sixth part of the document provides a detailed overview of the data management framework, including the roles and responsibilities of various stakeholders. It also includes a list of key performance indicators (KPIs) used to measure the effectiveness of the data management processes.

7. The seventh part of the document discusses the future directions of data management, including the integration of artificial intelligence and machine learning to enhance data analysis capabilities. It also mentions the importance of staying updated with the latest industry trends and technologies.

8. The eighth part of the document provides a list of references and sources used in the document. It includes books, articles, and online resources that provide additional information on data management and analysis.

9. The ninth part of the document includes a glossary of key terms and definitions used throughout the document. This helps in ensuring that all readers have a clear understanding of the terminology used.

10. The tenth part of the document provides a list of appendices, including detailed data collection forms, sample reports, and other supporting documents. These appendices are available for reference and use by the organization's staff.

mutagenized with EMS. Approximately 100,000 F2 progeny were enriched for a lack of chemotaxis to a 1:200 point source of benzaldehyde and from this enrichment approximately 10,000 were screened visually for SNB-1::GFP defects. A screen for SNB-1::GFP defects in VD/DD neurons has been previously described (Zhen and Jin, 1999; Zhen et al., 2000).

***sad-1* mapping**

sad-1(ky332) and *sad-1(ky332)* were mapped with respect to Tc1 transposable element polymorphisms in the DP13 strain (Williams, 1995) by following the SNB-1::GFP defects. *sad-1* was localized to LGX between the stP72 and stP2 polymorphisms. Three-factor mapping was conducted to further localize *sad-1(ky332)* on LGX. 4/19 *unc-9(e101)* non *unc-3(e95)* recombinants were mutant for *sad-1*. A restriction fragment polymorphism associated with *odr-1(1933)* was used to map *sad-1(ky332)* further. *unc-9(e101) sad-1(ky332) + / + + odr-1(1933)* animals segregated 14/14 *unc-9* non-*sad-1* animals that contained the *odr-1(1933)* polymorphism. These mapping data placed *sad-1* right of *unc-9* and very close to *odr-1* on LGX.

Germline transformation rescue

Transgenic strains were created as previously described (Mello and Fire, 1995). Multiple lines from each injection were characterized for rescue of the SNB-1::GFP phenotype. Cosmids spanning the region between *unc-9* and *odr-1* were injected at 20 ng/ul in pools of 5-7 cosmids using the pJM67 P_{elt-2} -GFP plasmid at 12 ng/ul as a coinjection marker (Fukushige et al., 1998). Transformants were maintained by picking animals expressing GFP in the gut. Cosmids from the rescuing pool were injected individually or in pairs at 100 ng/ul, identifying F15A2 as the single rescuing cosmid. A version of F15A2 deleted for a SacII fragment and a subclone containing a 13.8kb SacII-AvrII fragment of F15A2 rescued the *sad-1* mutant phenotype at 50-100 ng/ul. The subclone contained 0.3 kb upstream of the start codon, the entire *sad-1* open reading frame, the *sad-1* 3'UTR, and 0.25 kb of downstream sequence.

cDNA isolation and allele sequencing

Faint, illegible text from a document on the left side of the page.

Faint, illegible text from a document on the left side of the page.

A partial cDNA yk410d1 corresponding to the predicted ORF F15A2.6 was obtained from Yuji Kohara. The 5' end of the *sad-1* coding region was identified by RT-PCR from wild-type N2 RNA prepared by Trizol extraction (gift of E. Troemel). First-strand cDNAs were reverse transcribed by the primer F15cD-3A 5'cgtacttttcaccccgaataac3'. This cDNA served as a template for PCR amplification with the SL1 and F15cD-3A primers for 30 cycles at 94°C for 30 s, 52°C for 1 min, 72°C for 1 min on an MJ Research thermal cycler. A second, hemi-nested amplification was carried out under identical conditions using 1 ul of the original reaction with the SL1 and F15cD-3B 5'cgaataacttctggacatgcataatgtggagatcc 3' primers. A 0.75 kb band was isolated and subcloned into the BamHI-BsmBI sites of yk410d1 to create a full-length *sad-1* cDNA. The *sad-1* cDNA was sequenced, and the genomic organization of *sad-1* was determined by aligning the cDNA with the reported genomic sequence from the *C. elegans* genome sequencing consortium (1998). To identify the mutations in the seven *sad-1* alleles, the open reading frame and splice junctions of the mutant alleles were PCR amplified from two separate genomic DNA preparations of the mutant strains. PCR fragments were pooled and sequenced on both strands using an ABI sequencing machine (HHMI DNA facility).

Overexpression and motor neuron-specific rescue experiments

For overexpression studies the SacII deletion version of F15A2 was injected at 240 ng/ul with p_{cht-2}GFP at 12 ng/ul into *kyIs105; lin-15(n765ts)* animals and integrated into the genome using psoralen mutagenesis. The integrant *kyIs214 kyIs105; lin-15(n765ts)* was used for further analysis.

To specifically express SAD-1 in VD and DD neurons, a mini-gene construct, c4EA, was first derived from the *sad-1* cDNA clone by replacing the EcoRI-SacII cDNA fragment with a 3.9kb genomic piece from F15A2. A 1.2 kb NotI-BglII fragment from pSC375 (M.Z. and Y.J., unpublished) that contains the *unc-25* promoter was then cloned into NotI-BamHI sites in c4EA to generate pSCM1. *sad-1(ju53)* animals were injected with PSCM1 and scored for SNB-1::GFP phenotypes in VD and DD neurons.

Microscopy

1. The first part of the document discusses the importance of maintaining accurate records of all transactions. It emphasizes that proper record-keeping is essential for ensuring the integrity and reliability of financial data. This section also highlights the role of internal controls in preventing errors and fraud.

2. The second part of the document focuses on the implementation of robust internal control systems. It outlines the key components of an effective control environment, including the establishment of clear policies and procedures, the assignment of responsibilities, and the regular monitoring and evaluation of control activities.

Vesicle clusters of ASI neurons were visualized in *kyIs105; lin-15 (n765ts)* animals, and vesicle clusters of VD and DD motor neurons were visualized with an integrated *unc-25-SNB-1::GFP* transgene (CZ333, *juIs1 X*) (Hallam and Jin, 1998). AWC axons were visualized with an integrated *p_{str-2}-GFP* transgene (strain CX3621 *kyIs136 lin-15(n765ts) X*) (Troemel et al., 1999). Living animals were mounted on 2% agarose pads containing 3 mM sodium azide. Fluorescence was visualized using a Nikon Eclipse TE300 equipped with a Biorad MRC-1024 Laser Scanning Confocal Imaging System. Images were captured at 60X magnification and processed using the NIH Image and Adobe Photoshop programs.

***sad-1* expression analysis**

A reporter *p_{sad-1}-GFP* fusion was constructed by cloning a PstI-BamHI PCR product corresponding to nucleotides 34884-26254 of F15A2 in frame into the GFP expression vector pPD95.75 (a gift from A. Fire, S. Xu, J. Ahnn, and G. Seydoux). A translational *p_{unc-115}-SAD-1::GFP* fusion was made by inserting a PCR product, corresponding to 1.6kb of upstream *unc-115* sequences, as a NotI-BamHI fragment into c4EA. Into this subclone GFP from pPD102.33 (a gift from A. Fire, S. Xu, J. Ahnn, and G. Seydoux) was inserted in frame at an EcoRI site corresponding to amino acid 566 of the SAD-1 protein. The *unc-115* promoter was used because it drove expression of SAD-1::GFP at lower levels than the endogenous *sad-1* promoter and consequently gave less overexpression artefacts. The *p_{sad-1}-GFP* and *p_{unc-115}-SAD-1::GFP* transgenes were injected at 100 and 30 ng/ul into *lin-15(n765ts)* animals using the *lin-15(+)* pJM23 plasmid at 30 ng/ul as a coinjection marker (Huang et al., 1994). The *sad-1* expression and localization patterns were assessed in variably mosaic animals that contained the transgenes as unstable extrachromosomal DNA. In *C. elegans* the first intron is often very large and is thought to contribute regulatory information; anecdotally, we note that 3.6 kb of 3' first intron sequences was able to drive expression of GFP in a subset of neurons (data not shown).

Generation of SAD-1 antibodies

A 6His-GST-SAD-1 fusion protein containing amino acids

1. The first part of the document discusses the importance of maintaining accurate records of all transactions. It emphasizes that this is crucial for ensuring the integrity of the financial statements and for providing a clear audit trail.

2. The second part of the document outlines the various methods used to collect and analyze data. It includes a detailed description of the sampling techniques employed and the statistical tests used to evaluate the results.

3. The third part of the document presents the findings of the study. It shows that there is a significant correlation between the variables being studied, and it discusses the implications of these findings for future research and practice.

4. The fourth part of the document concludes the study and provides a summary of the key points. It reiterates the importance of the findings and suggests areas for further investigation.

5. Finally, the document includes a list of references and a bibliography, providing a comprehensive overview of the sources used in the research.

422–559 (from a BglIII-SalI cDNA fragment) was expressed in bacteria using the pQE41 vector (Qiagen), purified following the manufacturer's protocol, and used to immunize rats (Covance). Crude polyclonal antisera was precleared against fixed *sad-1(ky289)* animals (methanol [5'] and acetone [5'], dry ice frozen and pulverized) and used at 1:20 dilution on whole mounts. Anti-GFP, anti-SYD-2 (Zhen and Jin, 1999) and anti-SNT-1 antibodies (Nonet et al., 1993) were used as described. Cy5-conjugated goat anti-rat (Zymed) and Cy3-conjugated goat anti-rabbit (Jackson ImmunoResearch) IgG secondary antibodies were used at 1:25 and 1:300 dilutions. Secondary antibodies were similarly precleared against fixed wild-type animals. Whole-mount immunofluorescence staining was performed as described in Finney and Ruvkun, 1990.

Protein sequence analysis

Phylogenetic analysis was performed using the ClustalW (Thompson et al., 1994) and NJplot programs. Sequences used corresponded to amino acids 47-297 of the SAD-1 kinase domain. Protein alignment was performed in MacVector. The Genbank identifier numbers for the sequences used in the alignment and/or tree are as follows: *Drosophila melanogaster* CG6114, gi|7294217, and CG8201 (*Drosophila* PAR-1), gi|7302464; *Halocynthia roretzi* HrPOPK-1, gi|3172111; *Caenorhabditis elegans* PAR-1, gi|733122, and *unc-43* CaM Kinase II, gi|1118007; *Rattus norvegicus* MARK1, gi|2052188, and MARK2, gi|2052190; *Homo sapiens* CAA07196 EST, gi|3217028, MARK3, gi|4505102, and AMP Kinase $\alpha 1$, gi|5453964; *Saccharomyces cerevisiae* Snf1p, gi|6320685.

References

Adams, M.D. et al. (2000). The genome sequence of *Drosophila melanogaster*. *Science* 287, 2185-2195.

Avery, L., Bargmann, C..I, and Horvitz, H.R. (1993). The *Caenorhabditis elegans* *unc-31* gene affects multiple nervous system-controlled functions. *Genetics* 134, 455-464.

1. The first part of the document discusses the importance of maintaining accurate records of all transactions. It emphasizes that proper record-keeping is essential for the integrity of the financial system and for the ability to detect and prevent fraud.

2. The second part of the document outlines the specific requirements for record-keeping, including the need to maintain original documents and to keep copies of all transactions. It also discusses the importance of regular audits and the need to ensure that all records are up-to-date and accurate.

3. The third part of the document discusses the consequences of failing to maintain accurate records, including the potential for financial loss and the risk of legal action. It also discusses the importance of training staff on proper record-keeping procedures and the need to ensure that all staff are aware of the importance of accurate records.

4. The fourth part of the document discusses the importance of maintaining accurate records of all transactions, including the need to maintain original documents and to keep copies of all transactions. It also discusses the importance of regular audits and the need to ensure that all records are up-to-date and accurate.

5. The fifth part of the document discusses the consequences of failing to maintain accurate records, including the potential for financial loss and the risk of legal action. It also discusses the importance of training staff on proper record-keeping procedures and the need to ensure that all staff are aware of the importance of accurate records.

- Bargmann, C.I., and Horvitz, H.R. (1991). Control of larval development by chemosensory neurons in *Caenorhabditis elegans*. *Science* 251, 1243-1246.
- Bohm, H., Brinkmann, V., Drab, M., Henske, A., and Kurzchalia, T.V. (1997). Mammalian homologues of *C. elegans* PAR-1 are asymmetrically localized in epithelial cells and may influence their polarity. *Curr. Biol.* 7, 603-606.
- Brenner, S. (1974). The genetics of *Caenorhabditis elegans*. *Genetics* 77, 71-94.
- Butz, S., Okamoto, M., and Sudhof, T.C. (1998). A tripartite protein complex with the potential to couple synaptic vesicle exocytosis to cell adhesion in brain. *Cell* 94, 773-782.
- Caceres, A., and Kosik, K.S. (1990). Inhibition of neurite polarity by tau antisense oligonucleotides in primary cerebellar neurons. *Nature* 343, 461-463.
- Carling, D., Aguan, K., Woods, A., Verhoeven, A.J., Beri, R.K., Brennan, C.H., Sidebottom, C., Davison, M.D., and Scott, J. (1994). Mammalian AMP-activated protein kinase is homologous to yeast and plant protein kinases involved in the regulation of carbon metabolism. *J. Biol. Chem.* 269, 11442-11448.
- C. elegans* Sequencing Consortium. (1998). Genome sequence of the nematode *C. elegans*: a platform for investigating biology. *Science* 282, 2012-8.
- DeChiara, T.M., Bowen, D.C., Valenzuela, D.M., Simmons, M.V., Poueymirou, W.T., Thomas, S., Kinetz, E., Compton, D.L., Rojas, E., Park, J.S., Smith, C., DiStefano, P.S., Glass, D.J., Burden, S.J., and Yancopoulos, G.D. (1996). The receptor tyrosine kinase MuSK is required for neuromuscular junction formation in vivo. *Cell* 85, 501-512.
- Drewes, G., Trinczek, B., Illenberger, S., Biernat, J., Schmitt-Ulms, G., Meyer, H.E., Mandelkow, E.M., and Mandelkow, E. (1995). Microtubule-associated protein/microtubule affinity-regulating kinase (p110mark). A novel protein

1. The first part of the document is a list of names and addresses of the members of the committee. The names are listed in alphabetical order, and the addresses are given in full. The list includes names such as Mr. J. H. Smith, Mr. W. B. Jones, and Mr. C. D. Brown, among others.

2. The second part of the document is a list of the names and addresses of the members of the committee who were present at the meeting. This list is also in alphabetical order and includes names such as Mr. J. H. Smith, Mr. W. B. Jones, and Mr. C. D. Brown, among others.

kinase that regulates tau-microtubule interactions and dynamic instability by phosphorylation at the Alzheimer-specific site serine 262. *J. Biol. Chem.* 270, 7679-7688.

Drewes, G., Ebner, A., Preuss, U., Mandelkow, E.M., and Mandelkow, E. (1997). MARK, a novel family of protein kinases that phosphorylate microtubule-associated proteins and trigger microtubule disruption. *Cell* 89, 297-308.

Drewes, G., Ebner, A., and Mandelkow, E.M. (1998). MAPs, MARKs and microtubule dynamics. *Trends. Biochem. Sci.* 23, 307-311.

Fenster, S.D., Chung, W.J., Zhai, R., Cases-Langhoff, C., Voss, B., Garner, A.M., Kaempf, U., Kindler, S., Gundelfinger, E.D., and Garner, C.C. (2000). Piccolo, a presynaptic zinc finger protein structurally related to bassoon. *Neuron* 25, 203-214.

Finney, M., and Ruvkun, G. (1990). The *unc-86* gene product couples cell lineage and cell identity in *C. elegans*. *Cell* 63, 895-905.

Fukushige T, Hawkins MG, McGhee JD. (1998). The GATA-factor *elt-2* is essential for formation of the *Caenorhabditis elegans* intestine. *Dev. Biol.* 198, 286-302.

Gautam, M., Noakes, P.G., Moscoso, L., Rupp, F., Scheller, R.H., Merlie, J.P., and Sanes, J.R. (1996). Defective neuromuscular synaptogenesis in agrin-deficient mutant mice. *Cell* 85, 525-535.

Glass, D.J., Bowen, D.C., Stitt, T.N., Radziejewski, C., Bruno, J., Ryan, T.E., Gies, D.R., Shah, S., Mattsson, K., Burden, S.J., DiStefano, P.S., Valenzuela, D.M., DeChiara, T.M., and Yancopoulos, G.D. (1996). Agrin acts via a MuSK receptor complex. *Cell* 85, 513-523.

1. The first part of the document discusses the importance of maintaining accurate records of all transactions. It emphasizes that this is essential for ensuring the integrity of the financial system and for providing a clear audit trail.

2. The second part of the document outlines the various methods used to collect and analyze data. It highlights the need for consistent data collection procedures and the importance of using appropriate statistical techniques to interpret the results.

Grady, R.M., Zhou, H., Cunningham, J.M., Henry, M.D., Campbell, K.P., and Sanes, J.R. (2000). Maturation and maintenance of the neuromuscular synapse: genetic evidence for roles of the dystrophin--glycoprotein complex. *Neuron* 25, 279-293.

Guo, S., and Kemphues, K.J. (1995). *par-1*, a gene required for establishing polarity in *C. elegans* embryos, encodes a putative Ser/Thr kinase that is asymmetrically distributed. *Cell* 81, 611-620.

Guo, S., and Kemphues, K.J. (1996). A non-muscle myosin required for embryonic polarity in *Caenorhabditis elegans*. *Nature* 382, 455-458.

Hall, A.C., Lucas, F.R., and Salinas, P.C. (2000). Axonal remodeling and synaptic differentiation in the cerebellum is regulated by WNT-7a signaling. *Cell* 100, 525-535.

Hallam, S. J., and Jin, Y. (1998) *lin-14* regulates the timing of synaptic remodeling in *Caenorhabditis elegans*. *Nature* 395, 78-82.

Hosaka, M., Hammer, R.E., and Sudhof, T.C. (1999). A phospho-switch controls the dynamic association of synapsins with synaptic vesicles. *Neuron* 24, 377-387.

Huang LS, Tzou P, Sternberg PW. (1994). The *lin-15* locus encodes two negative regulators of *Caenorhabditis elegans* vulval development. *Mol. Biol. Cell.* 5, 395-411.

Kemphues, K.J., Priess, J.R., Morton, D.G., and Cheng, N.S. (1988). Identification of genes required for cytoplasmic localization in early *C. elegans* embryos. *Cell* 52, 311-320.

Kohmura, N., Senzaki, K., Hamada, S., Kai, N., Yasuda, R., Watanabe, M., Ishii, H., Yasuda, M., Mishina, M., and Yagi, T. (1998). Diversity revealed by a novel

1. The first part of the document is a list of names and addresses of the members of the committee. The names are listed in alphabetical order, and the addresses are given in full. The list includes the names of the members of the committee, the names of the members of the sub-committee, and the names of the members of the advisory committee. The addresses are given in full, including the street, city, and state.

2. The second part of the document is a list of the names and addresses of the members of the committee. The names are listed in alphabetical order, and the addresses are given in full. The list includes the names of the members of the committee, the names of the members of the sub-committee, and the names of the members of the advisory committee. The addresses are given in full, including the street, city, and state.

family of cadherins expressed in neurons at a synaptic complex. *Neuron* 20, 1137-1151.

Kopczynski, C.C., Davis, G.W., and Goodman, C.S. (1996). A neural tetraspanin, encoded by *late bloomer*, that facilitates synapse formation. *Science* 271, 1867-1870.

Lee, S.H., and Sheng, M. (2000). Development of neuron-neuron synapses. *Curr. Opin. Neurobiol.* 10, 125-131.

Lu, B., Greengard, P., and Poo, M.M. (1992). Exogenous synapsin I promotes functional maturation of developing neuromuscular synapses. *Neuron* 8, 521-529.

Lundquist, E.A., Herman, R.K., Shaw, J.E., and Bargmann, C.I. (1998). UNC-115, a conserved protein with predicted LIM and actin-binding domains, mediates axon guidance in *C. elegans*. *Neuron* 21, 385-392.

Matsuura, A., Tsukada, M., Wada, Y., and Ohsumi, Y. (1997). Apg1p, a novel protein kinase required for the autophagic process in *Saccharomyces cerevisiae*. *Gene* 192, 245-250.

Mello, C. and Fire, A. (1995). DNA transformation. *Methods Cell Biol.* 48, 451-482.

Noakes, P.G., Gautam, M., Mudd, J., Sanes, J.R., and Merlie, J.P. (1995). Aberrant differentiation of neuromuscular junctions in mice lacking s-laminin/laminin beta 2. *Nature* 374, 258-262.

Nonet, M.L., Grundahl, K., Meyer, B.J., and Rand, J.B. (1993). Synaptic function is impaired but not eliminated in *C. elegans* mutants lacking synaptotagmin. *Cell* 73, 1291-1305.

1. The first part of the document is a list of names and addresses of the members of the committee. The names are listed in alphabetical order, and the addresses are given in full. The list includes the names of the members of the committee, the names of the members of the sub-committee, and the names of the members of the advisory committee. The addresses are given in full, including the street name, the city, the state, and the zip code.

2. The second part of the document is a list of the names and addresses of the members of the committee. The names are listed in alphabetical order, and the addresses are given in full. The list includes the names of the members of the committee, the names of the members of the sub-committee, and the names of the members of the advisory committee. The addresses are given in full, including the street name, the city, the state, and the zip code.

Nonet, M. L. (1999). Visualization of synaptic specializations in live *C. elegans* with synaptic vesicle protein-GFP fusions. *J. Neurosci. Methods* 89, 33-40.

Nonet, M.L., Holgado, A.M., Brewer, F., Serpe, C.J., Norbeck, B.A., Holleran, J., Wei, L., Hartwig, E., Jorgensen, E.M., and Alfonso, A. (1999). UNC-11, a *Caenorhabditis elegans* AP180 homologue, regulates the size and protein composition of synaptic vesicles. *Mol. Biol. Cell.* 10, 2343-2360.

Ogura, K., Wicky, C., Magnenat, L., Tobler, H., Mori, I., Muller, F., and Ohshima, Y. (1994). *Caenorhabditis elegans unc-51* gene required for axonal elongation encodes a novel serine/threonine kinase. *Genes Dev.* 8, 2389-2400.

Otsuka, A.J., Jeyaprakash, A., Garcia-Anoveros, J., Tang, L.Z., Fisk, G., Hartshorne, T., Franco, R., and Born, T. (1991). The *C. elegans unc-104* gene encodes a putative kinesin heavy chain-like protein. *Neuron* 6, 113-122.

Parsa, I. (1988). Loss of a Mr 78,000 marker in chemically induced transplantable carcinomas and primary carcinoma of human pancreas. *Cancer Res.* 48, 2265-2272.

Peckol, E.L., Zallen, J.A., Yarrow, J.C., and Bargmann, C.I. (1999). Sensory activity affects sensory axon development in *C. elegans*. *Development* 126, 1891-1902.

Peng, C.Y., Graves, P.R., Ogg, S., Thoma, R.S., Byrnes, M.J. 3rd, Wu, Z., Stephenson, M.T., and Piwnicka-Worms, H. (1998). C-TAK1 protein kinase phosphorylates human Cdc25C on serine 216 and promotes 14-3-3 protein binding. *Cell. Growth. Differ.* 9, 197-208.

Porter, B.E., Weis, J., and Sanes, J.R. (1995). A motoneuron-selective stop signal in the synaptic protein S-laminin. *Neuron* 14, 549-559.

1. The first part of the document is a list of names and addresses of the members of the committee. The names are listed in alphabetical order, and the addresses are given in full. The list includes the names of the members of the committee, the names of the members of the sub-committee, and the names of the members of the advisory committee. The addresses are given in full, including the street, city, and state.

2. The second part of the document is a list of the names and addresses of the members of the committee. The names are listed in alphabetical order, and the addresses are given in full. The list includes the names of the members of the committee, the names of the members of the sub-committee, and the names of the members of the advisory committee. The addresses are given in full, including the street, city, and state.

Pulak, R., and Anderson, P. (1993). mRNA surveillance by the *Caenorhabditis elegans smg* genes. *Genes Dev.* 7, 1885-1897.

Ren, P., Lim, C.S., Johnsen, R., Albert, P.S., Pilgrim, D., and Riddle, D.L. (1996). Control of *C. elegans* larval development by neuronal expression of a TGF-beta homolog. *Science* 274, 1389-1391.

Rosahl, T.W., Spillane, D., Missler, M., Herz, J., Selig, D.K., Wolff, J.R., Hammer, R.E., Malenka, R.C., and Sudhof, T.C. (1995). Essential functions of synapsins I and II in synaptic vesicle regulation. *Nature* 375, 488-493.

Sanes, J.R., and Lichtman, J.W. (1999). Development of the vertebrate neuromuscular junction. *Annu. Rev. Neurosci.* 22, 389-442.

Sasakura, Y., Ogasawara, M., and Makabe, K.W. (1998). Maternally localized RNA encoding a serine/threonine protein kinase in the ascidian, *Halocynthia roretzi*. *Mech. Dev.* 76, 161-163.

Schackwitz, W.S., Inoue, T., and Thomas, J.H. (1996). Chemosensory neurons function in parallel to mediate a pheromone response in *C. elegans*. *Neuron* 17, 719-728.

Schaeffer, A. M., Hadwiger, G. D. and Nonet, M. L. (2000) *rpm-1*, a conserved neuronal gene that regulates targeting and synaptogenesis in *C. elegans*. *Neuron*, *in press*.

Schlesinger, A., Shelton, C.A., Maloof, J.N., Meneghini, M., Bowerman, B. (1999). Wnt pathway components orient a mitotic spindle in the early *Caenorhabditis elegans* embryo without requiring gene transcription in the responding cell. *Genes Dev.* 13, 2028-2038.

1. The first part of the document is a list of names and addresses of the members of the committee. The names are listed in alphabetical order, and the addresses are given in full. The list includes the names of the members of the committee, the names of the members of the sub-committee, and the names of the members of the advisory committee. The addresses are given in full, including the street, city, and state.

2. The second part of the document is a list of the names and addresses of the members of the committee. The names are listed in alphabetical order, and the addresses are given in full. The list includes the names of the members of the committee, the names of the members of the sub-committee, and the names of the members of the advisory committee. The addresses are given in full, including the street, city, and state.

Serpinskaya, A.S., Feng, G., Sanes, J.R., and Craig, A.M. (1999). Synapse formation by hippocampal neurons from agrin-deficient mice. *Dev. Biol.* 205, 65-78.

Serra-Pagés, C., Medley, Q.G., Tang, M., Hart, A., and Streuli, M. (1998). Liprins, a family of LAR transmembrane protein-tyrosine phosphatase-interacting proteins. *J. Biol. Chem.* 273, 15611-15620.

Shapiro, L., and Colman, D.R. (1999). The diversity of cadherins and implications for a synaptic adhesive code in the CNS. *Neuron.* 23, 427-430.

Suter, D.M., and Forscher, P. (1998). An emerging link between cytoskeletal dynamics and cell adhesion molecules in growth cone guidance. *Curr. Opin. Neurobiol.* 8, 106-116.

Thompson, J.D., Higgins, D.G., and Gibson, T.J. (1994). CLUSTAL W: improving the sensitivity of progressive multiple sequence alignment through sequence weighting, position-specific gap penalties and weight matrix choice. *Nucleic Acid Res.* 22, 4673-4680.

Troemel, E.R., Sagasti, A., and Bargmann, C.I. (1999). Lateral signaling mediated by axon contact and calcium entry regulates asymmetric odorant receptor expression in *C. elegans*. *Cell* 99, 387-398.

Wan, H. I., DiAntonio, A., Fetter, R. D., Bergstrom, K., Strauss, R. and Goodman, C. S. (2000). Highwire regulates synaptic growth in *Drosophila*. *Neuron, in press.*

White, J.G., Albertson, D.G., and Anness, M.A. (1978). Connectivity changes in a class of motoneurone during the development of a nematode. *Nature* 271, 764-766.

1. The first part of the document discusses the importance of maintaining accurate records of all transactions and activities. It emphasizes that this is essential for ensuring transparency and accountability in the organization's operations.

2. The second part of the document outlines the various methods and tools used to collect and analyze data. It highlights the need for consistent and reliable data collection processes to support informed decision-making.

White, J.G., Southgate, E., Thomson, J.N., and Brenner, S. (1986). The structure of the nervous system of the nematode *C. elegans*. Philosophical Transactions of the Royal Society of London 314B, 1-340.

Williams, B.D. (1995). Genetic mapping with polymorphic sequence-tagged sites. Methods Cell. Biol. 48, 31-58.

Zhen, M., and Jin, Y. (1999). The liprin protein SYD-2 regulates the differentiation of presynaptic termini in *C. elegans*. Nature 401, 371-375.

Zhen, M., Xun, H., Bamber, B. and Jin, Y. (2000). Regulation of presynaptic terminal organization by *C. elegans* RPM-1, a putative GTP-GDP exchanger with a Ring-H2 finger domain, Neuron, *in press*.

1. The first part of the document discusses the importance of maintaining accurate records of all transactions. It emphasizes that proper record-keeping is essential for the integrity of the financial system and for the ability to detect and prevent fraud.

2. The second part of the document outlines the specific procedures for recording transactions. It details the steps involved in the accounting cycle, from identifying the transaction to posting it to the appropriate ledger account.

Chapter 5

Model for SAD-1 function and future directions

1. The first part of the document discusses the importance of maintaining accurate records of all transactions. It emphasizes that proper record-keeping is essential for the integrity of the financial system and for the ability to detect and prevent fraud.

2. The second part of the document outlines the specific requirements for record-keeping, including the need to maintain original documents and to keep copies of all transactions. It also discusses the importance of regular audits and the need to ensure that all records are up-to-date and accurate.

3. The third part of the document discusses the consequences of failing to maintain accurate records, including the potential for financial loss and the risk of legal action. It also discusses the importance of training staff on proper record-keeping procedures and the need to ensure that all staff are aware of the importance of accurate record-keeping.

4. The fourth part of the document discusses the importance of maintaining accurate records of all transactions, including the need to maintain original documents and to keep copies of all transactions. It also discusses the importance of regular audits and the need to ensure that all records are up-to-date and accurate.

5. The fifth part of the document discusses the consequences of failing to maintain accurate records, including the potential for financial loss and the risk of legal action. It also discusses the importance of training staff on proper record-keeping procedures and the need to ensure that all staff are aware of the importance of accurate record-keeping.

The model

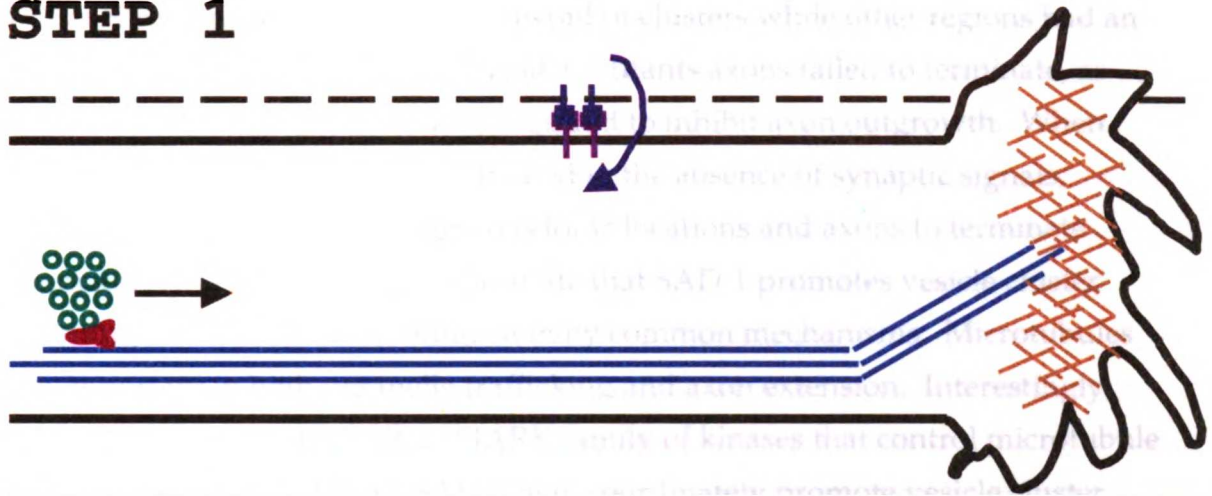
Though the following model is highly speculative, it provides a framework for addressing the mechanisms by which SAD-1 organizes presynaptic development. During Step 1 axon outgrowth is nearing completion, and the axon has a highly motile growth cone rich in actin (brown) and stabilized by penetrating microtubules (blue). Vesicle clusters (green) have formed and are being transported along microtubule tracks by a motor protein (dark brown). Perhaps, the first step of presynaptic development is the formation of an adhesion complex (purple) between the pre- and post- synaptic neurons that promotes signaling from the postsynaptic to the presynaptic neuron (purple arrow). In Step 2 signaling in the presynaptic neuron activates SAD-1 through a mechanism that is dependent on SAD-2. SAD-2 may help activate SAD-1 by localizing it to presynaptic sites or by coupling it to upstream signal transduction machinery. SAD-1 could target vesicle clusters to synaptic sites by three mechanisms: promotion of vesicle cluster attachment to synaptic components, local inhibition of the transport of vesicle clusters, or modification of the microtubule tracks along which vesicle clusters are transported. Simultaneously, SAD-1 may inhibit further axon outgrowth through the modification of microtubules, actin, or cell adhesion in the growth cone. In parallel with the recruitment of vesicle clusters by SAD-1 additional pathways may organize the active zone (orange). Step 3 shows a mature synapse that contains an active zone, a vesicle cluster, and specialized actin and microtubule cytoskeletons. Whereas synaptic microtubules may direct recycling vesicles back to the synapse, synaptic actin may stabilize vesicle clusters and other synaptic components. Additionally, SAD-1 and SAD-2 may control the size and shape of vesicle clusters by regulating the reassociation of recycling vesicles with the clustered pool.

This model explains many of the phenotypes observed in loss-of-function *sad-1* and SAD-1 overexpressing animals. In *sad-1* mutants vesicle clusters are spatially disorganized and irregular in size and shape and axons branch and fail to properly terminate. If SAD-1 were required to target vesicle clusters to synapses, as in Step 2, then in *sad-1* mutants clusters would form but would

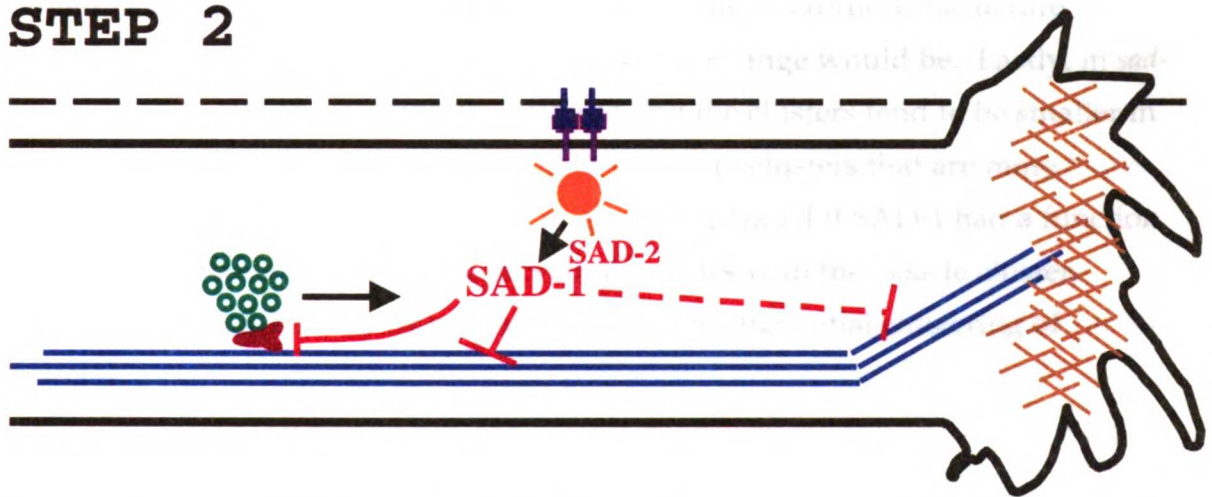
1. The first part of the document is a list of names and addresses of the members of the committee. The names are listed in alphabetical order, and the addresses are given in full. The list includes names such as Mr. J. H. Smith, Mr. W. D. Jones, and Mr. R. L. Brown, among others.

2. The second part of the document is a list of the names and addresses of the members of the committee who have been appointed to the various sub-committees. The names are listed in alphabetical order, and the addresses are given in full. The list includes names such as Mr. J. H. Smith, Mr. W. D. Jones, and Mr. R. L. Brown, among others.

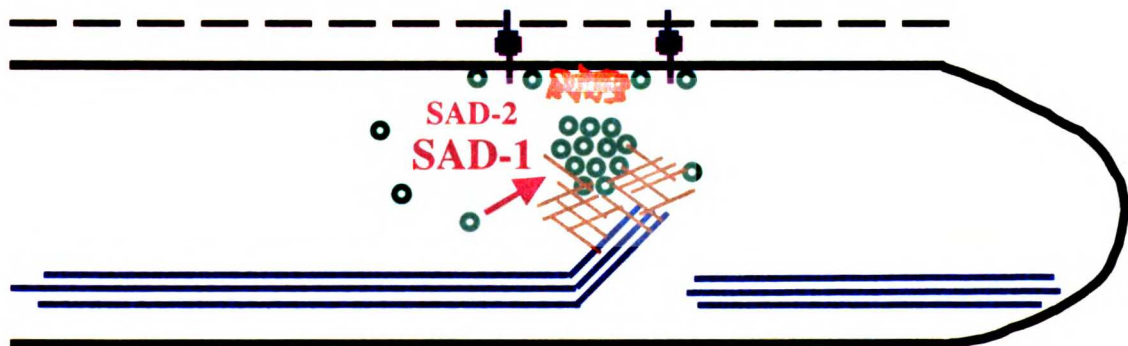
STEP 1



STEP 2



STEP 3



1. The first part of the document is a list of names and addresses of the members of the committee. The names are listed in alphabetical order, and the addresses are given in full. The list includes names such as Mr. J. H. Smith, Mr. J. B. Jones, and Mr. W. C. Brown, among others.

2. The second part of the document is a list of the names and addresses of the members of the committee who were present at the meeting. This list is also in alphabetical order and includes names such as Mr. J. H. Smith, Mr. J. B. Jones, and Mr. W. C. Brown, among others.

remain unanchored in the axon. This prediction might explain why in *sad-1* mutants regions of the axon were devoid of clusters while other regions had an overly high density of clusters. In *sad-1* mutants axons failed to terminate, as would be expected if SAD-1 were required to inhibit axon outgrowth. When overexpressed, SAD-1 may be activated in the absence of synaptic signals, causing vesicle clusters to target to ectopic locations and axons to terminate prematurely. It is tempting to speculate that SAD-1 promotes vesicle cluster targeting and inhibits axon outgrowth by common mechanisms. Microtubules are important in both organelle trafficking and axon extension. Interestingly, SAD-1 is related to the PAR-1/MARK family of kinases that control microtubule dynamics and cell polarity. SAD-1 may coordinately promote vesicle cluster targeting and inhibit axon outgrowth by modifying microtubule structure, though it is unclear what the exact nature of this change would be. Lastly, in *sad-1* mutants vesicles are less tightly clustered and the clusters tend to be smaller in size. Conversely, overexpression of SAD-1 leads to clusters that are more sharply defined. These observations might be explained if SAD-1 had a function in promoting the reassociation of recycling vesicles with the vesicle cluster. Alternatively, SAD-1 may be partially required for the initial clustering of vesicles.

Future directions

The most informative direction for exploring SAD-1 function is the identification of the upstream pathways that regulate SAD-1 activity and the downstream targets of SAD-1 that organize the synapse and control axon outgrowth. Three approaches can be taken to address the question of SAD-1 activation. The first approach is to identify the domains of SAD-1 required for activation. *sad-1* mutations that truncate the C-terminus of the protein result in the null phenotype, suggesting that C-terminal regions may be required for synaptic localization or activation. SAD-1 structure-function studies can identify regions of the protein that are necessary or sufficient for localization or activation. Additionally, it may be that the mechanism of SAD-1 activation involves its translocation to synapses. Retargeting an inactive and mislocalized

THE UNIVERSITY OF CHICAGO
DIVISION OF THE PHYSICAL SCIENCES
DEPARTMENT OF CHEMISTRY
5708 SOUTH CAMPUS DRIVE
CHICAGO, ILLINOIS 60637
TEL: 773-936-3700
FAX: 773-936-3701
WWW: WWW.CHEM.UCHICAGO.EDU

1998
2000
2002
2004
2006
2008
2010
2012
2014
2016
2018
2020

SAD-1 to synapses by another means could test the functional implications of SAD-1 localization to synapses. A second method of exploring SAD-1 regulation involves the further characterization of *sad-2*. Overexpression of SAD-1 rescues the vesicle clustering defects of *sad-2*, suggesting that *sad-2* is upstream of *sad-1*. In particular, the cloning of *sad-2* would shed light on the pathways upstream of SAD-1. Lastly, additional proteins that interact with SAD-1 could be identified biochemically or by the yeast two-hybrid system. Most interesting would be proteins that interact with domains of SAD-1 required for localization or regulation. Loss-of-function and overexpression genetics would reveal *in vivo* roles for these interacting proteins.

Both genetic and biochemical approaches may identify downstream targets of SAD-1. Overexpression of SAD-1 leads to striking and easily scorable phenotypes: paralysis, axon termination, and vesicle clusters in the dendrite. A screen for suppressors of SAD-1 overexpression would identify molecules required downstream of SAD-1 signaling. Additionally, this type of screen may isolate different classes of suppressors. For example, some mutants may suppress only the axon or synapse phenotype, whereas other mutants may suppress both phenotypes. The molecular analysis of these mutants will identify pathways that are common or unique to the control of axon and synapse structure. As SAD-1 is a kinase, potential downstream targets of SAD-1 could be identified biochemically based on their ability to be phosphorylated by SAD-1. These phosphorylation assays would be most easily done *in vitro* with purified SAD-1. Candidate targets such as synapsins and MAPs or bulk protein preparations (e.g. from purified synaptic vesicles) could be tested as SAD-1 substrates. The *in vivo* functional significance of these biochemically identified targets would then be tested.

Whereas the further characterization of SAD-1 will illuminate pathways organizing vesicle clusters and controlling axon outgrowth, additional approaches are needed in order to understand other aspects of synaptogenesis. Analogous GFP screens based on markers for active zones, postsynaptic densities, and pre- and post- synaptic alignment would identify molecules that act in parallel with SAD-1 at the synapse. Ultimately, many of the key regulators of synapse formation will be known, and a further understanding of synaptic

1. The first part of the document is a list of names and addresses of the members of the committee. The names are listed in alphabetical order, and the addresses are given in full. The list includes names such as Mr. J. H. Smith, Mr. W. D. Jones, and Mr. R. L. Brown.

2. The second part of the document is a list of the names and addresses of the members of the committee who were present at the meeting. The names are listed in alphabetical order, and the addresses are given in full. The list includes names such as Mr. J. H. Smith, Mr. W. D. Jones, and Mr. R. L. Brown.

1. The first part of the document is a list of names and addresses of the members of the committee. The names are listed in alphabetical order, and the addresses are listed below each name. The list includes names such as Mr. J. H. Smith, Mr. J. D. Jones, and Mr. W. E. Brown, among others.

2. The second part of the document is a list of the names and addresses of the members of the committee who were present at the meeting. The names are listed in alphabetical order, and the addresses are listed below each name. The list includes names such as Mr. J. H. Smith, Mr. J. D. Jones, and Mr. W. E. Brown, among others.

1. The first part of the document is a list of names and addresses of the members of the committee. The names are listed in alphabetical order, and the addresses are given in full. The list includes the names of the members of the committee, the names of the members of the sub-committee, and the names of the members of the advisory committee. The addresses are given in full, including the street, city, and state.

2. The second part of the document is a list of the names and addresses of the members of the committee. The names are listed in alphabetical order, and the addresses are given in full. The list includes the names of the members of the committee, the names of the members of the sub-committee, and the names of the members of the advisory committee. The addresses are given in full, including the street, city, and state.

THE
LIBRARY
OF THE
MICHIGAN
UNIVERSITY LIBRARY
ANN ARBOR, MICHIGAN

THE
LIBRARY
OF THE
MICHIGAN
UNIVERSITY LIBRARY
ANN ARBOR, MICHIGAN

For reference

Not to be taken
from the room.

LIBRARY

7064820



3 1378 00706 4820

